CRYSTALLOGRAPHY AND PHASE TRANSITIONS OF SOME PYROPHOSPHATES

AN INVESTIGATION OF THE CRYSTAL STRUCTURE AND PHASE TRANSFORMATIONS OF Cu AND Zn PYROPHOSPHATE

By

BEVERLY ELLIS ROBERTSON, B.Sc., M.Sc.

A Thesis
Submitted to the Faculty of Graduate Studies
in Partial Fulfilment of the Requirements
for the Degree
Doctor of Philosophy

McMaster University
October 1967

DOCTOR OF PHILOSOPHY (1967)
(Physics)

McMASTER UNIVERSITY
Hamilton, Ontario

TITLE: An Investigation of the Crystal Structure and Phase Transformations of Cu and Zn Pyrophosphate .

AUTHOR: Beverly Ellis Robertson, B.Sc. University of New Brunswick

M.Sc. McMaster University

SUPERVISOR: Professor C. Calvo

NUMBER OF PAGES: x, 194

SCOPE AND CONTENTS:

The crystal structures of the high temperature phase of $Cu_2P_2O_7$ has been refined by the method of least squares. The structure of the low temperature form was refined using both of the allowed space groups and the centric space group C2/c is preferred. Diffuse streaks which were found to be associated with the phase transformation were analyzed and used to construct a pseudo one dimensional order-disorder model for the mechanism of the phase transformation. Also the lattice parameters of α-$Zn_2P_2O_7$ have been measured and the structure has been refined using the non-centric space group Ic.

PREFACE

Some of the results presented here are an extension of the work described earlier in a Master's thesis (1965) and it has therefore been necessary in the interests of clarity to briefly review that work. Further, since this thesis will describe both the determination of crystal structures and the study of related phase transformations, some repetition has been necessary in order to ensure that each section be complete.

I wish to express my most sincere gratitude to Professor C. Calvo for his guidance and assistance over the past five years. I wish to thank the other members of the crystallography group at McMaster for their advice and discussions. In particular the Fortran least squares and Fourier programs prepared by John Stephens and John Rutherford have been most helpful. The experimental results obtained by Dr. Datars and Dr. Stager and their graduate students has been most valuable since they have complemented the study of the phase transformations by x-rays. In addition, I thank Dr. Stager for his assistance with the experimental arrangement shown in Figure 8.

I wish to express my appreciation for the tolerance and assistance given me by the staff of the Computing Center. I also thank Mrs. Barbara Nichols, Mrs. Carolyn Williams

and my wife for their assistance with the preparation of the thesis. Finally I thank my wife for her endurance and moral support over the past nine years.

I wish to acknowledge the receipt of two Ontario Government Fellowships. This research was made possible through grants-in-aid from the National Research Council to Professor C. Calvo.

I would like to thank Mrs.Kennelly for typing this thesis.

TABLE OF CONTENTS

Page

1. INTRODUCTION

2. DETERMINATION OF THE STRUCTURE OF α-$Cu_2P_2O_7$

3. DETERMINATION OF THE STRUCTURE OF β-$Cu_2P_2O_7$

4. DETERMINATION OF THE STRUCTURE OF α-$Zn_2P_2O_7$

LIST OF TABLES

LIST OF ILLUSTRATIONS

CHAPTER 1: INTRODUCTION

(A) Pyrophosphate Compounds

This study is one of a series directed towards obtaining an understanding of the crystal chemistry of those pyrocompounds involving tetrahedrally bonded anion groups. As with silicate systems, phosphates can be classified in terms of the degree of condensation of a fundamental XO_4^{-n} tetrahedron. In the orthophosphates the PO_4^{-3} groups are isolated from each other and are very nearly regular tetrahedra. They are linked together through the sharing of oxygen atoms with metal cations. The pyrophosphate anion $P_2O_7^{-4}$ is formed from two PO_4^{-3} tetrahedra by the sharing of one oxygen atom. The metaphosphates can exist as either rings of PO_4^{-3} tetrahedra such as is found in $Na_4P_4O_{12}.4H_2O$ (Anders, Fischer and Gehring, 1949) or as infinite linear chains such as in $RbPO_3$ (Corbridge, 1956). Van Wasser (1958) has discussed extensively the chemistry of phosphate systems.

The research reported here has been primarily a complete crystallographic investigation of the phases of a number of similar pyrophosphates. This thesis will describe the determination and refinement of the crystal structures of the three pyrophosphates α-$Zn_2P_2O_7$, α-$Cu_2P_2O_7$ and β-$Cu_2P_2O_7$ and the phase transformation which relates the latter two. These results will be interpreted in the light of several other parallel investigations which have been recently carried out at this university.

There had been a small number of crystallographic studies of pyrocompounds prior to the present work. Many of these compounds fall into two distinct crystallographic groups. Among the remainder are ZrP_2O_7, $Na_4P_2O_7 \cdot 10H_2O$ and $Cd_2P_2O_7$. Levi and Peyronel (1935) suggested that the $P_2O_7^{-4}$ ion in zirconium pyrophosphate possessed a threefold axis and that the shared oxygen atom and the two phosphoros atoms were colinear. Lazarev (1964c) has noted a phase transformation in this compound at 300°C and therefore this system should be restudied. The crystal structure of $Na_4P_2O_7 \cdot 10H_2O$ was originally investigated by MacArthur and Beevers (1957) and recently refined by McDonald and Cruickshank (1967). These latter results indicate that in this monoclinic compound the P-O-P groups are bent to an angle of 130° and the anion possesses a twofold axis. Similarly, in $Cd_2P_2O_7$ (Au, 1966) where the crystals are triclinic the P-O-P group is bent to an angle of 128°. In detail, the structures of these three compounds are quite dissimilar as can be anticipated from the large amount of water that is accommodated in $Na_4P_2O_7 \cdot 10H_2O$ together with the different number of cations in each formula unit.

Almost all of the divalent metal ion pyrophosphates that have been studied in the solid state fall into two distinct families, with both families exhibiting interesting polymorphic behaviour. The members of one group, which is characterized by relatively large cationic radii, are the "alkaline earth pyrophosphates", consisting of $Ba_2P_2O_7$, $Ca_2P_2O_7$ and $Sr_2P_2O_7$. Ranby, Mash and Henderson (1955) studied their phase transformations by noting changes in the luminiscent wavelengths and intensity of the emission spectra of Mn^{+2} in solid solutions formed from these alkaline earth pyrophosphates. X-ray powder patterns indicated that some of these changes corresponded to solid state phase transformations. In Figure 1 the phase relations and transformation temperatures of Ranby et al. are summarized. β-$Ca_2P_2O_7$ (Corbridge, 1957) and β-$Sr_2P_2O_7$ (Hoffmann and Mooney, 1960) have isomorphic structures and the structure of β-$Ca_2P_2O_7$ is now known.

The crystal structure of β-$Ca_2P_2O_7$ has recently been reported by Webb (1966). He finds two crystallographically independent anions with P-O-P angles of 131° and 138°. Furthermore the anions are in almost eclipsed configurations; that is, the terminal oxygen atoms overlap when the anion is viewed down the length of the P-P vector. In contrast, in $Na_4P_2O_7 \cdot 10H_2O$ the pyrophosphate ions are in the staggered configuration; that is, the terminal oxygen atoms do not overlap when the anion is viewed down the P-P vector. Single crystals of α-$Ca_2P_2O_7$ have been prepared by Hoffmann and its crystal structure is under study here (Calvo, 1967a). At the present time, very little is known of the crystalline character of the δ phase of $Ba_2P_2O_7$.

The family of pyrophosphates which particularly concern us involve cations with radii less than 1.0 A. The pyrophosphates which have been shown to fall into this category are those of Mg (Łukaszewicz, 1961), Mn (Łukaszewicz and Smajkiewicz, 1961), Zn (Calvo, 1965b) Cu (Łukaszewicz and Nagler, 1961), Co and Ni (Sarver, 1966). Each member of this group has a high temperature form isostructural to the mineral thortveitite, $(Sc,Y)_2Si_2O_7$. Recently, Cruickshank, Lynton and Barclay (1962) have refined the structure of this compound and in addition they addressed the problem of the space group ambiguity which seems indigenous to most of the "small cation" pyrocompounds. They chose the space group C2/m, as had Zachariasen (1930) in an earlier investigation. In this space group, the central oxygen atom of the $Si_2O_7^{-6}$ group appears to lie on a center of symmetry and thus the Si-O-Si angle must be 180^o. The anion is also forced to have the staggered configuration. The cations have an irregular octahedral environment. These irregular octahedra share edges to form a pseudo-hexagonal network extending in the (001) plane. Only two-thirds of the hexagonal holes, formed by a double layer of close=packed oxygen atoms, are occupied by cations. Adjacent sheets of these octahedra are joined by sharing oxygen atoms with the pyrosilicate ions.

The structure may be described alternatively by a set of layers of separation a/2 (~3.3 A) and which contain the unit cell vectors b and c. The layers contain pairs of cation octahedra which share one edge. The two remaining shared edges join adjacent layers. These cation pairs are linked together in the layer by the $Si_2O_7^{-6}$ anions. The shared oxygen atom of the pyro ion has been labelled the "O1" atom. One of the terminal oxygen atoms at each end of the ion lies in a mirror plane as do the Si atoms. These oxygen atoms are labelled the "O_2" atoms and are the oxygen atoms involved in the shared edge. The remaining four oxygen atoms which are related in pairs by that mirror plane are labelled the "O_3" atoms. Two cation pairs are connected in the b direction by the two O3 atoms at one end of an anion. This pattern is repeated since the central oxygen atom, O_1, lies at a center of symmetry. The layers are joined to one another by additional cation-oxygen bonds.

This description of the structure is entirely applicable to the high temperature forms of all the "small cation" pyrophosphates since they are isostructural to thortveitite. Systems isostructural with thortveitite occur commonly. Lazarev (1961 a and b, 1962) has studied extensively the infrared absorption spectrum of pyrocompounds of interest here. He has inferred that $Sc_2Si_2O_7$, $Er_2Si_2O_7$ and $Y_2Si_2O_7$ are similar to the mineral thortveitite which is a Sc rich solid solution of Sc and Y pyrosilicate. The pyroarsenates of Zn and Mg have been shown to be isostructural to thortveitite (Calvo and Neelakantan, 1967; Łukaszewicz, 1963) although those of Co and Ni are not (Taylor and Heyding, 1958). In addition the pyrovanadate of Cd (Au and Calvo, 1967) and the pyrogermanate of Sc (Goldschmidt 1931) show the thortveitite structure.

(B) Methods of Crystal Structure Analysis

It is not the purpose of this thesis to present a summary of crystallographic methods. It will be necessary,however, to describe the manner in which the present crystal structures were determined and thus a certain amount of the nomenclature must be defined. For this reason a brief survey of the standard methods, equations and terminology used in crystal structure analysis will be presented.

A crystal may be defined as an array of atoms whose time averaged positions can be described by the operation in three-dimensional space of translational symmetry on an array consisting of a finite number of atoms. If a parallel beam of x-rays is incident upon such a crystal it will interact with the constituent electrons and will exit coherently from the crystal only in well defined directions. If $\underline{k}'$ and $\underline{k}$ are the wave vectors of the incident and scattered or "diffracted" beams of x-rays respectively, then $\underline{K} = \underline{k}-\underline{k}'$ may be used to define the conditions under which diffraction will occur. If $\underline{a}$, $\underline{b}$ and $\underline{c}$ are the vectors describing the edges of the repetitive unit or "unit cell" of the translationally symmetric array, then the following relations must be satisfied.

$$\underline{a}.\underline{K} = 2\pi h$$

$$\underline{b}.\underline{K} = 2\pi k$$

$$\underline{c}.\underline{K} = 2\pi \ell$$

These are the Laue equations (James, 1962). The vector $\underline{K}$ is further limited by the requirement that the sum of the squares of its direction cosines relative to the cell edges be a constant. The only values of the indices h, k and ℓ which are compatible with these four conditions are integral values.

It is possible to represent the solutions of the Laue equations as points in a three dimensional space which also has translational symmetry. The basis vectors $\underline{a}^*$, $\underline{b}^*$ and $\underline{c}^*$ of this space, called reciprocal space, are defined by;

$$\underline{a}^* = \frac{\underline{b} \times \underline{c}}{V} \; ; \; \underline{b}^* = \frac{\underline{c} \times \underline{a}}{V} \; ; \; \underline{c}^* = \frac{\underline{a} \times \underline{b}}{V}$$

where V is the volume of a unit cell defined by $V = \underline{a} \cdot \underline{b} \times \underline{c}$. Each point in the reciprocal space is related to the direction of one of the diffracted x-ray beams. The Laue equations may be reduced to the familiar Bragg equation in terms of the distance H from the origin of reciprocal space to the point defined by the indices h, k and ℓ; that is

$$H = \frac{2 \sin \Theta(H)}{\lambda}$$

where λ is the wavelength of the x-rays used and $\Theta(H)$ is the Bragg angle depending on the magnitude of the vector $\underline{H}$ and $\underline{H} = h\underline{a}^* + k\underline{b}^* + l\underline{c}^{*\dagger}$. It is sometimes advantageous, particularly to elucidate some symmetry operation, to define a unit cell which is not the smallest repetitive unit of the atomic array. The indices which relate to the larger unit cell will then not be able to assume all possible integers and, as a result, certain types of systematic extinctions will occur. Other types of systematic extinctions arise from symmetry operators involving a translation of some fraction of the unit cell edges.

---

†note: $H = |\underline{H}|$

The symmetry of the intensity distribution of the diffracted x-rays constitutes the Laue symmetry which, together with the systematic extinctions, may or may not unambiguously define the space group of the unit cell. The intensity of the x-rays diffracted into each beam is determined by the arrangement of atoms in the unit cell. The observed intensity $I(\underline{H})$ of the reflection $\underline{H}$ is, however, dependent on a number of additional parameters. $I(\underline{H})$ may be written;

$$I(\underline{H}) = C\ (Lp)\ A\ \left|F(\underline{H})\right|^2$$

Each of the factors on the right hand side of the equation will be discussed separately.

C is an experimental constant which is dependent on the volume and density of the crystal which is being irradiated, the intensity of the incident beam, the scattering power of an individual electron, and the effeciency with which we can detect the diffracted x-rays. $I(\underline{H})$ is also dependent on the orientation of the incident and diffracted beam relative to the axis of rotation and the manner in which the crystal is swept through the position corresponding to the diffraction conditions. This geometrical dependence of the observed intensity is called the "Lorentz" factor and denoted "L". $I(\underline{H})$ also depends on the angle "2θ" between the incident and diffracted beams because the former contains x-rays randomly polarized in all planes perpendicular to their direction of propagation. This dependence is described by the polarization factor "p" where $p = \frac{1 + \cos^2 2\theta}{2}$. The Lorentz and polarization effects are usually combined and denoted the "Lp" factor.

As an x-ray beam passes through the crystal, its intensity is depleted because of interactions with the electrons in the crystals. The number of photons lost to the beam, per unit length of the crystal traversed, will be proportional to the number of photons in the beam. This fact gives directly the functional dependence of the beam intensity $I(x)$ on the distance x, travelled by the beam in the crystal, in terms of the absorption per unit distance "μ" and the initial intensity I_o. That is

$$I(x) = I_o \exp(-\mu x)$$

"μ" is normally calculated from the mass absorption coefficients as listed in the International Tables for Crystallography Vol. III (1962) and the density of each constituent atomic species in the crystal. For each reflection, the factor $e^{-\mu x}$ should be integrated over all paths followed by x-rays in the crystal. This is often a difficult task since the exact geometry of the crystal used is not usually known and difficult to determine for a crystal having dimensions of the order of 0.1 mm.

The intensity of the x-ray beam may be depleted by another phenomenon similar to absorption. An actual crystal may be thought of, at least for theoretical purposes, as a conglomeration of domains, each being a perfect crystal nearly aligned with all other domains. If the volume of a domain is relatively large, the energy of the incident or "primary" beam is depleted by the energy lost into the diffracted beam and the intensity of the primary beam is not uniform over the entire domain. This phenomenon is known as primary extinction. If the average domain volume is made relatively small, the probability increases that the x-rays diffracted from one domain will encounter another domain oriented so as to diffract them back into the main beam. The diffracted or "secondary" beam is then depleted and this phenomenon is known as secondary extinction. The magnitude of the errors caused by primary and secondary extinction are sufficiently small in the case of x-rays that it is usually not necessary to make corrections, although a few very strong reflections may sometimes be affected by them.

The term in the expression for $I(\underline{H})$ which is sensitive to the details of the atomic arrangement is $|F(\underline{H})|^2$ which may be written as a function of the positions of the atoms of one unit cell. Most of the scattering processes take place in the core of the atoms where the electronic density is highest. These cores are approximately spherically symmetric and have approximate Gaussian cross sections. X-rays scattered from different volume increments in an atomic core will not necessarily be in phase with those from other volume increments. The intensity of scattering from one atom is therefore dependent on the scattering angle and the wavelength of the scattered x-rays and may, in fact, be calculated as a function f of H. f(H) is called the atomic scattering factor. Each atom may then be described by a mathematical point with variable scattering power f(H) which in fact is the Fourier transform of its electron density. The phase of the scattering from one atom relative to an arbitrary origin may be defined by the term $\exp(-2\pi i\underline{H}\cdot\underline{r})$ where $\underline{r}$ is the vector from the origin of the unit cell to the atom. The calculated structure factor $F_c(\underline{H})$ may then be written;

$$F_c(\underline{H}) = \sum_{j=1}^{n} f_j(H)\exp(-2\pi i\underline{H}\cdot\underline{r}_j)$$

where the sum is over all n atoms in the unit cell. If the structure contains a center of symmetry the imaginary components of $F_c(\underline{H})$ cancel.

Since the tabulated f_j are for atoms at rest, the expression must be further modified to account for the effects of thermal vibration. If the second order tensor $\underline{\underline{U}}_j$ describes the anisotropic motion of the j'th atom, then the contribution of this atom to $F_c(\underline{H})$ is multiplied by $\exp(2\pi^2\underline{H}\cdot\underline{\underline{U}}_j\cdot\underline{H})$. The square root of the component U_{ii} of $\underline{\underline{U}}$ gives directly the average root mean square displacement of an atom in the direction i. Often the atoms are assumed to undergo isotropic motion which is described by the single parameter B_j and is usually called the Debye-Waller factor. In general, it is necessary to determine the six independent components of the tensor $\underline{\underline{U}}_j$ and the three components of $\underline{r}_j$ for all crystallographically independent atoms in the unit cell; that is, all atoms not related by symmetry. The portion of the unit cell that contains only atoms unrelated by symmetry operators is called the asymmetric unit.

Because of the form of the structure factor, it may be considered as the Fourier transform of the electron density, as defined by the vectors $\underline{r}_j$. Then the appropriate Fourier transform of the observed structure factors, $F_o(H)$ should give the electron density in the unit cell; that is,

$$\rho(r) = \frac{1}{V}\sum_{\underline{H}} F_o(\underline{H})\exp(2\pi i\underline{H}\cdot\underline{r})$$

where the sum is over all reflections $\underline{H}$. We may determine $|F_o(\underline{H})|$ from the observed intensity $I_o(\underline{H})$.

$I_o(\underline{H})$ may be recorded with a Geiger-Müller tube or scintillation counter. Each reflection will also produce a darkened area when it is incident on a photographic film. $I_o(\underline{H})$ is then proportional to the darkening of the spot on the film produced by the reflection $\underline{H}$. One normally records on a film only those reflections belonging to a plane in reciprocal space. These planes are referred to as layer lines. It is often convenient to choose layer lines with the property that one of the indices h, k and ℓ is constant throughout and if this index has the value n, then the layer line is called the n'th layer line. Layer lines containing the origin of reciprocal space are called zones.

In general $F_o(\underline{H})$ is a complex quantity and we cannot measure its phase. We do not then have sufficient information to calculate $\rho(\underline{r})$ directly. In some cases, if the structure contains a center of symmetry, probable values of the phases of the reflections may be inferred directly from the distribution of the magnitudes of $|F_o(\underline{H})|$ (Wooster, 1961) but these methods have not been used here. An alternative procedure is to use the Patterson function (Buerger, 1960); that is,

$$P(\underline{s}) = \frac{1}{V} \sum_{\underline{H}} |F_o(\underline{H})|^2 \cos(2\pi \underline{H} \cdot \underline{s})$$

$\underline{s}$ defines a vector space and P is large only when $\underline{s}$ corresponds to an interatomic vector in the real unit cell and further, when this condition is satisfied $P(\underline{s})$ is proportional to the product of the electron densities of the two atoms defining the interatomic vector.

$P(\underline{s})$ may be calculated directly from the experimental data since it uses only $|F_o(\underline{H})|^2$. We must next find a set of atomic coordinates consistent with $P(\underline{s})$. The solution to this problem is not always unique. Also $P(\underline{s})$ is usually poorly resolved and we can only find the positions of the heavier atoms. The approximate phases (or "signs" if the structure is centric) calculated for $F_c(\underline{H})$ from the heavier atom positions may be assigned to $F_o(\underline{H})$ in order to calculate $\rho(\underline{r})$. Then the positions of the lighter atoms may hopefully be found.

In order to obtain improved or "refined" atomic coordinates we may substitute $F_o(\underline{H})-F_c(\underline{H})$ for $F_o(\underline{H})$ in the equation for $\rho(\underline{r})$ to obtain a difference Fourier synthesis. Atoms are then shifted from areas where the difference synthesis is negative towards areas where it is positive. The advent of fast electronic digital computers in the past few years has made possible refinement by least squares methods. This procedure calculates small adjustments to the parameters describing the crystal structure which will minimize the quantity R_2 defined by

$$R_2^2 = \frac{\sum\limits_{\underline{H}} \omega(\underline{H}) \, \big| |F_o(\underline{H})| - |F_c(\underline{H})| \big|^2}{\sum\limits_{\underline{H}} \omega(\underline{H}) \, |F_o(\underline{H})|^2}$$

where $\omega(\underline{H})$ is a weight assigned to the reflection $\underline{H}$. Some methods of assigning $\omega(\underline{H})$ are described in Appendix A. R_2 is the "normalized residue" of the least squares analysis. It is also referred to in the literature as the "weighted R factor". In the past it has been more convenient to use the "R factor" or "unweighted R factor" or "agreement index", R_1, to indicate the quality of agreement between $F_o(\underline{H})$ and $F_c(\underline{H})$. R_1 is defined by

$$R_1 = \frac{\sum\limits_{\underline{H}} \big| |F_o(\underline{H})| - |F_c(\underline{H})| \big|}{\sum\limits_{\underline{H}} |F_o(\underline{H})|}$$

If we assume a "normal" distribution of error in $F_o(\underline{H})$, we should minimize R_2 to obtain the optimum model for the crystal structure. (Hamilton, 1964). The method of least squares is discussed further in Appendix A.

(C) Previous Structure Determinations

The first investigation of $Mg_2P_2O_7$ pertinent to this study was that of Roy, Middleswarth and Hummel (1948). They determined the differential thermal analysis (D.T.A.) curves, the thermal expansion parameters and the Debye-Scherrer patterns of $Mg_2P_2O_7$ as a function of temperature and they concluded that there was a transformation to a high temperature phase at $68^\circ \pm 2^\circ C$. In the present nomenclature this form is called the β phase. Łukaszewicz (1961) reported a preliminary structure analysis of the high temperature phase at $80^\circ C$ which confirmed that β-$Mg_2P_2O_7$ is an isostructure of thortveitite. However, better resolution was required. Further refinement of this structure was carried out by Calvo (1965c) in order to elucidate the chemical nature of the pyrophosphate ion and to gain some insight into the nature of the phase transformation. The P-O bond distances were in better agreement with the predicted nature of the $P_2O_7^{-4}$ ion. Also, the central O_1 atom appeared to have a large component of thermal vibration along the $\underline{b}$ direction.

The structure of the room temperature magnesium pyrophosphate, that is α-$Mg_2P_2O_7$, has also been reported by Łukaszewicz (1966). A more complete investigation of α-$Mg_2P_2O_7$ has been carried out by Calvo (1967d). The differences between the atomic coordinates determined by these workers are in most cases less than the combined errors as reported for the two structure determinations. Here the length of the a and c axes are roughly double those of β-$Mg_2P_2O_7$, and the space group is $B2_1/c$. This non-standard space group was chosen to facilitate a comparison of this crystal structure with that of the high temperature form. The structures are similar but the α form contains two independent Mg^{+2} cations, one with octahedral coordination as in β-$Mg_2P_2O_7$ but the other with only five ligands.

The structure of $Mn_2P_2O_7$ has been reported by Łukaszewicz and Nagler (1961). They used 72 observed structure factors and obtained an R factor of approximately 0.18. The structure is similar to that of thortveitite but the P-O bond distances are unrealistic. The two symmetry independent terminal P-O distances were 1.74 and 1.60 A. The longest possible P-O distances would have a bond order of "one" and this corresponds to a bond length of 1.71 A (Cruickshank, 1961). A study of this crystal structure is now in progress at this University for the purpose of obtaining better resolution (Calvo, 1967b). No crystallographic evidence of a phase transformation has been observed for this crystal. Also Lazarev (1962) has observed the infrared absorption at various temperatures down to -150°C and has found no major changes in the spectrum.

Sarver (1966) has investigated the D.T.A. curves of $Ni_2P_2O_7$ and $Co_2P_2O_7$ and he observed rapidly reversible phase transformations at 575 ± 5°C and 304 ± 5°C respectively. He examined the lower temperature phase of each compound by powder diffractometry and concluded that their structures were similar to that of α-$Mg_2P_2O_7$. The structure of α-$Ni_2P_2O_7$ was reported by Łukaszewicz (1966) and it is indeed almost identical to that of α-$Mg_2P_2O_7$. Any discrepancies are probably not significant since relatively small amounts of data were used . Preliminary results on the structure of α-$Co_2P_2O_7$,which is under investigation at this laboratory,indicate that its structure is also very similar to that of α-$Mg_2P_2O_7$ (Calvo, 1967c).

The first crystallographic study of $Cu_2P_2O_7$ was reported by Łukaszewicz and Nagler (1961). They found at room temperature the Laue symmetry and extinctions were consistent with either of the space groups C2/c or Cc. The unit cell dimensions were similar to those of the other pyrophosphates although the c axis was approximately double that of β-$Mg_2P_2O_7$. They did not investigate the possibility of a high temperature form although Roy et.al.had mentioned some evidence of a phase transformation from D.T.A. results. A phase transformation has since been found (Robertson, 1965) near 70°C by x-ray methods. The crystal structure of the high temperature form, β-$Cu_2P_2O_7$ and the room temperature form, α-$Cu_2P_2O_7$ were also studied with x-rays. The β form is isomorphic to β-$Mg_2P_2O_7$. This thesis will describe more accurate refinements of these structures which were necessary in order to draw conclusions about the nature of the phase transformation.

A phase transition was first reported in $Zn_2P_2O_7$ by Katnack and Hummel (1955). They found an endothermic peak in their D.T.A. results centred at 132°C. The electron paramagnetic resonance (e.p.r.) results of Chambers, Datars and Calvo (1964) on Mn^{+2} in $Zn_2P_2O_7$ indicates an additional phase transition, probably of second order, extending from 132°C to 155°C. The structure of β-$Zn_2P_2O_7$ has been resolved above 155°C by Calvo (1965b) and was found to be isomorphic to the other high temperature forms in this series. The lattice parameters of the low temperature form, α-$Zn_2P_2O_7$ have been reported by DeWolff (1958). If an I centred unit cell is chosen, the length of the a axes will be roughly three times that of the β phase and, as in all the other α phases of the series, the c axis is roughly double that of the conjugate β phase. The structure exhibits the characteristic c glide plane and the space group must be one of Ic or I2/c. The elucidation of the manner in which a pseudo-symmetric structure such as this deviates from the higher symmetry is definitely a non-trivial problem.

(D) Space Group Ambiguities

The symmetry of the pattern of diffracted x-rays permits one to determine the Laue class to which the crystal belongs. The information regarding the actual space group resides in the intensity distribution. Some components of the space group symmetry, but generally not all, can be determined from the class of those reflections having rigorously zero intensity. This class is said to be systematically extinct. Unfortunately, two or more space groups are sometimes consistent with the Laue class and the systematic extinctions.

In some cases one answers the question of the space group ambiguity by refining the structure in the lower symmetry space group (or space groups) and noting whether the final atomic positions found are consistent, within the estimated standard deviations (e.s.d.'s), with the higher symmetry space group. This method has been notably unsuccessful in the case of thortveitite and the pyrophosphates considered here. One reason for this is that the e.s.d's of the atomic coordinates obtained in the non-central space groups are probably unrealistically low because of the high degree of pseudosymmetry. Atomic coordinates which would be related by symmetry in the β phase are strongly interdependent and the e.s.d.'s given by the statistics of the least squares treatment are probably smaller than the actual errors. Beyond this, the question of the proper criteria for an adequate trial structure in the lower symmetry space group is not clear.

The Laue symmetry and systematic extinctions of thortveitite and all the β forms of the pyrophosphates (including $Mn_2P_2O_7$) allows the space group to be one of Cm, C2 or C2/m. Cruickshank et.al. refined the structure of thortveitite in all three space groups but the atomic coordinates obtained in both of the non-centric cases were significantly different from those obtained in the centric space group C2/m. However, they noted that those bond lengths that should be chemically equivalent were significantly dissimilar. Any differences in these bond lengths could be caused only by the environment of the anion and therefore should be small since the two halves of the anion see nearly identical environments. For this reason, they rejected the non-centric space groups and chose C2/m as the proper space group of thortveitite.

In any least square refinement of a set of data the discrepancy can be reduced by increasing the number of adjustable parameters. For this reason, the agreement between observed structure factors and calculated structure factors should be improved when additional parameters, permitted by a reduction in symmetry, are introduced. If the lower symmetry space group is the correct one, the improvement should be significant, and further, the deviations of the parameters from their high symmetry values should be significant. The relation between the degree of improvement and the probability that the additional parameters are proper variables can be discussed quantitatively (Hamilton, 1965). The ratio of the agreement factor R_2 obtained before the extra variables are added to the refinement, to R_2 obtained with the inclusion of the extra variables is compared with an analysis-of-variance ratio corresponding to some significance level. If the ratio is greater, the extra variables can be said to be valid at that significance level. Hamilton used thortveitite as an example of the application of his significance tables and concluded that the extra variables needed to define the structure in the space groups Cm or C2 did not provide a better model at the 25% level of significance.

The symmetry of a crystal is reflected in its physical properties including the structure. Paramagnetic ions in a crystal are subjected to internal fields and therefore the splitting of energy levels depends not only on the strength of an external field, but on internal ones as well. In an electron paramagnetic resonance (e.p.r.) experiment, electromagnetic radiation corresponding to microwave frequencies is absorbed in the process of exciting transitions in the paramagnetic ions corresponding to changes in the effective spin quantum number S_z. If two paramagnetic ions are in crystallographically independent sites they will not be subject to identical internal fields and thus their e.p.r.

absorption spectra will also not be identical. Since the energy levels are in general nonisotropic, the tensorial properties of $\underline{\underline{g}}$ which defines the relation between the magnetic moment $\underline{\mu}$ and the spin vector $\underline{S}$ ($\underline{\mu} = \beta\underline{\underline{g}}\cdot\underline{S}$) may also be determined. Using e.p.r. techniques, it is often possible to determine the maximum point group symmetry at the paramagnetic ion and, second, the number of signals, that is sites, in the crystal that are not equivalent.

This technique has been applied to Cu^{+2} and Mn^{+2} doped $Zn_2P_2O_7$ (Chambers, Datars and Calvo, 1964), Mn^{+2} doped $Mg_2P_2O_7$ (Calvo, Leung and Datars, 1967), and to thortveitite (Datars and Calvo, 1967) which occurs naturally with both Fe^{+3} and Mn^{+2} impurities. In all cases the spectra are consistent only with the C2/m space group, but as yet the sensitivity of the method has not been investigated theoretically.

$Cu_2P_2O_7$ and $Mn_2P_2O_7$ are themselves paramagnetic materials and the e.p.r. method is not applicable. The technique of anomalous dispersion has been used to determine the space group of $Mn_2P_2O_7$. If the energy of the incident x-rays is near the energy required to excite the electrons of one of the atomic species, then the phase change upon scattering can differ from the normal 180° and if the crystal is non-centrosymmetric, the scattering from planes defined by $\underline{H}$ will no longer be the same as the scattering from planes defined by $-\underline{H}$. No systematic differences between such reflections could be seen in $Mn_2P_2O_7$ with CoKα radiation (Calvo, 1967b) which implies that the space group is C2/m. It should be mentioned here that this technique and the method of e.p.r. measures the symmetry of the paramagnetic impurity which is assumed identical to that of the cations and only indirectly infers the symmetry of the other atomic species in the crystal.

(E) The Pyrophosphate Anion

Cruickshank (1961) has discussed the nature of the bonding about a tetrahedrally coordinated X atom where X can equal Si, S, Cl or P atoms. In an isolated tetrahedron four σ bonds to four oxygen atoms, for example, are constructed from the hybridized sp^3 orbitals of the X atom. The two π bonding systems are formed from the $d\gamma$ orbitals of the central atom and the oxygen $2p\pi$ orbitals. A σ lone pair is left at the back of each oxygen atom, which may be used to bond with other atoms. If we now join two tetrahedra by the sharing of one oxygen atom to form a pyro-group, the degree of π bonding becomes dependent on the hybridization of the central oxygen atom. If the angle subtended at the central O1 atom of the anion by the two X atoms is the tetrahedral angle of $109^{o}25'$, the O_1 atom would be sp^3 hybridized and unable to sufficiently overlap with the 3d orbitals of the X atom to support any significant π bonding. If the shared oxygen atom is sp^2 hybridized , the subtended angle becomes 120^{o} and one of the two π bonding systems in each tetrahedra is joined across the atom. When the subtended angle is 180^{o}, the central oxygen atom is sp hybridized and both π bonding systems are joined. As the amount of π bonding to the shared oxygen atom increases, its bond distances to the X atoms are decreased and the bond lengths to the terminal oxygen atoms are increased.

Upon assuming a linear bond distance versus bond length relationship together with a π bond order of one half for an isolated PO_4^{-3} tetrahedron and Shoemaker and Stephenson's (1941) calculated single bond length, Cruickshank has predicted bond lengths from valence bond theory for the P-O(-P) and terminal P-O bonds for each of these hybridization schemes. He obtains 1.64 A and 1.51 A for the P-O(-P) and P-O bond lengths respectively when the P-O-P angle is 120° and 1.58 A and 1.53 A when the P-O-P angle is 180°. These considerations necessarily neglect the effect of the environment. The group of pyrophoshpates under consideration here permit an observation of the manner in which the cations perturb the $P_2O_7^{-4}$ group. In particular, electrons from the anion may be attracted by the positive cation which would cause the bond lengths between the atoms in the anion to increase, and the P-O-P angle to deviate further from 180°.

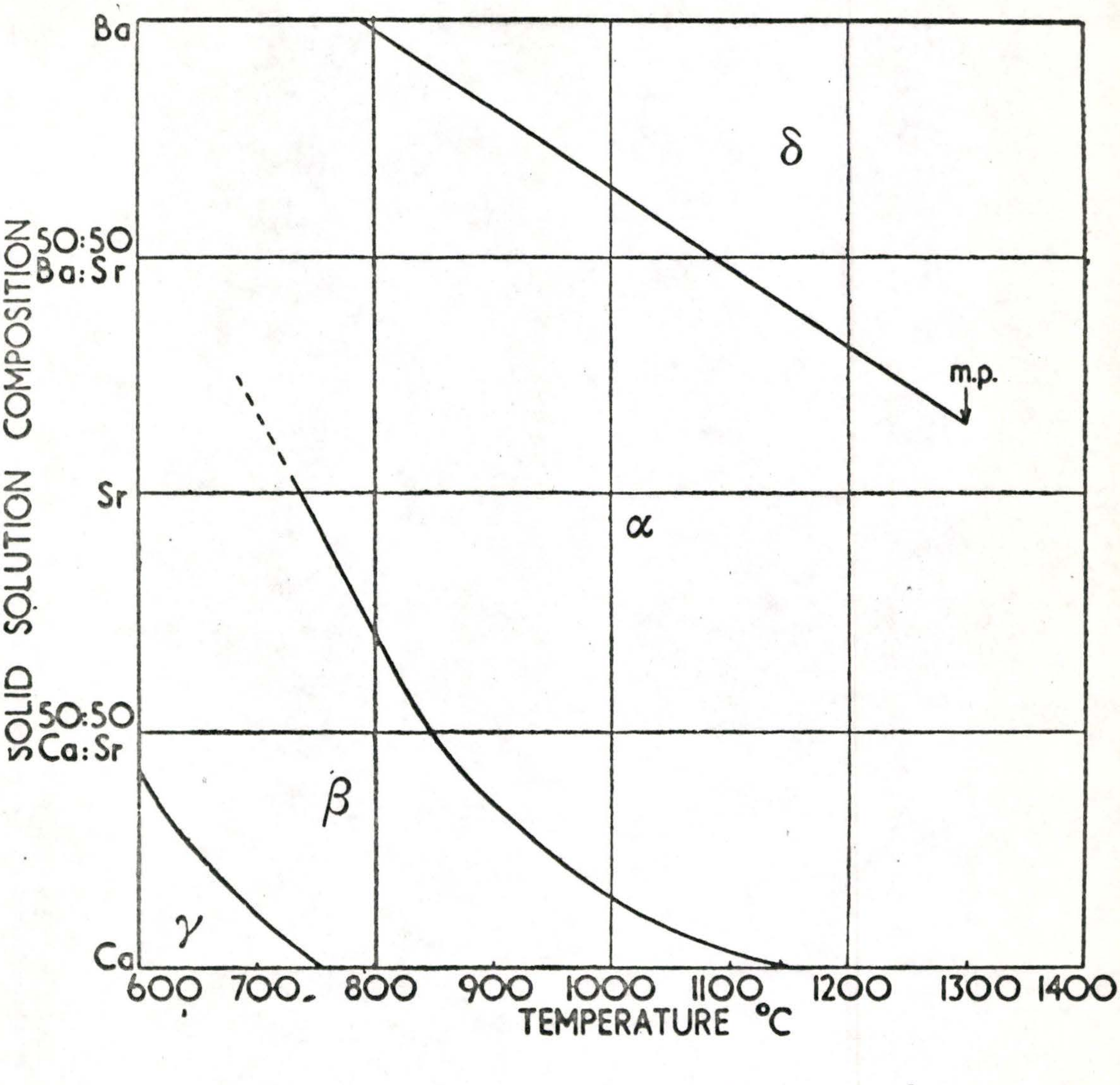

Approximate phase diagram for pure (Alkaline earth) pyrophosphates

(From Ranby, Mash and Henderson, 1955)

Figure 1

CHAPTER 2: DETERMINATION OF THE STRUCTURE OF α-$Cu_2P_2O_7$

(A) Preliminary Investigations

The first crystallographic investigation of $Cu_2P_2O_7$ was reported by Łukaszewicz and Nagler (1961). They examined its powder pattern at room temperature and concluded that the structure must be similar to thortveitite. The unit cell volume was about twice that found for thortveitite (Cruickshank, Lynton and Barclay (1962)) with similar lattice parameters except for a doubled c axis.

The systematically extinct reflections, that is, those with h + k odd in addition to those with k = 0 and ℓ odd, indicate that the space group is either C2/c or Cc. Roy, Middleswarth and Hummel (1948) had examined $Cu_2P_2O_7$ by D.T.A. and reported some evidence for a phase transformation but gave no further information.

Since $Mg_2P_2O_7$ (Łukaszewicz, 1961) and $Zn_2P_2O_7$ (Calvo, 1965b) undergo phase transformations above room temperature to a form isostructural to thortveitite, it was decided that $Cu_2P_2O_7$ should be investigated for evidence of a high temperature (β) polymorph. A phase transformation was found at about 70°C (Robertson, 1965) by x-ray examination. In this transformation the c axis halves by the disappearance of the reflections with ℓ odd and the space group is transformed to one of C2, Cm or C2/m.

The structure of α-$Cu_2P_2O_7$ had been partially refined (Robertson, 1965). In the present work, this refinement is completed. Additional data have been recorded with an accuracy sufficient for a resolution of the space group anomaly in the α phase and as a result, the geometry for the $P_2O_7^{-4}$ anion is in better agreement with predictions based on chemical considerations. Łukaszewicz (1966) has also recently refined the structure of α-$Cu_2P_2O_7$ using 230 reflections of the hk0, h0ℓ and h1ℓ type. He has obtained substantially the same structure as reported here but with much larger errors in the atomic positions. Also, he did not consider the problem of the space group ambiguity.

The crystals used here were prepared by the reaction of a slight excess of an aqueous solution of $Na_4P_2O_7$ with an aqueous solution of $CuSO_4$. The precipitate was filtered, washed and dried. The sample was then heated to 1200°C and allowed to cool slowly across the melting temperature, reported to be 1140°C by Łukaszewicz and Nagler (1961). Some of the small blue-green crystals obtained were found to be twinned on their [110] faces but single crystals could easily be selected.

Lattice parameters were determined from a Debye-Scherrer photograph obtained from a powdered portion of these crystals. Thirty-nine lines were identified and the quantity "$\sin\Theta/\lambda$" was used in a least squares fit of the lattice parameters. The computer programs used here are described in Appendix B. The reflections used, together with their measured and calculated "$\sin\theta/\lambda$" values, are shown in Table 1. These lattice parameters are compared with those of similar pyrophosphates in Table 2.

(B) Preparation of Data

A crystal having the approximate dimensions 0.08 x 0.08 x 0.40 mm^3 was glued to a fiber with its long dimension parallel to the goniometer's rotation axis. Weissenberg photographs of the type hk0, hk1 and hk2 were recorded with Cu Kα radiation. The hk0 reflections were also recorded on a Supper single crystal manual diffractometer using Mo Kα radiation. This crystal was also used to record 0kℓ data using the precession camera with Mo Kα radiation. A second crystal was used to collect data of the type hnℓ, n = 0,1,2,3,4, using a Weissenberg camera and Mo Kα radiation. The approximate dimensions of this crystal were 0.10 x 0.10 x 0.05 mm^3.

In order to measure accurate data with the diffractometer a system was designed (Figure 2) to be attached to the front of the counter so that dead time corrections could be reduced to less than 15% of the total number of counts by the insertion of filters in the path of the incident x-ray beam. For Mo radiation, zirconium filters were used. The integrated intensity was measured by rocking the crystal while holding the counter fixed. This method is usually referred to as an "ω" scan. The background was measured at approximately 3^o in ω on either side of the Bragg reflection. The integrated intensity of each reflection was corrected for background, variation in scanning rate, filter attenuation and variation in incident beam intensity as monitored by the periodic measurement of a standard reflection. In order to apply corrections for dead time, the intensity profile of each reflection was approximated by the sum of two Gaussian curves corresponding to the Kα_1 and Kα_2 spectral lines. The relative separation of the peaks is proportional to the tangent of the Bragg angle. The constant of proportionality and also the width of the two Gaussian curves were found graphically by curve fitting at high angles where the peaks were well resolved and then extrapolating to low angles. In order to apply the dead time corrections, the reflection profile was broken into 100 strips and the height of each strip was individually corrected for dead time.

The integrated intensity of the photographic data was visually estimated using the logarithmic method (Robertson, 1965). In the previous refinement, the data of type $0k\ell$; hkn, $n = 0,1,2$; and $hn\ell$, $n = 0,1$ were used. For the present refinement the data indexed as $hn\ell$, $n = 2,3,4$ were added. All of the data were corrected for the effects of Lorentz and polarization. The estimated standard deviations (e.s.d.'s) for the visually estimated data were initially assigned as 10% of the magnitude of the structure factor except for very weak or moderately strong reflections in which case the e.s.d.'s were multiplied by 1.5. The e.s.d.'s of the reflections recorded with the diffractometer were assigned as a constant times $1/\sqrt{N}$ where N is the total number of counts used to record the integrated intensity of a given reflection.

Since the linear absorption coefficients are 160 cm^{-1} for Cu Kα radiation and 100 cm^{-1} for Mo Kα radiation approximate absorption corrections were applied. The crystals were approximated by spheres or cylinders, where appropriate, whose volumes were made equal to those estimated for the crystals. In addition, the length of the cylinder was set equal to the crystal length along the rotation axis. The changes in the value of the structure factors arising from these corrections varied by a maximum of 10% over the range of θ used to record this data. Thus errors caused by the assumed idealized crystal shape should be of the order of only 2 or 3%. These corrections were not applied until the structure was partially refined.

In addition to the corrections for linear absorption, the data measured with Cu Kα radiation was approximately corrected for the effects of anomalous absorption. A constant factor of 2.0 was subtracted from the Cu^{+2} scattering curve. (International Tables, Volume III, 1962). A correction for the phase shift upon scattering must also be applied if the space group is noncentric. However, in the case of α-$Cu_2P_2O_7$, if the space group is indeed non-centric, the Cu^{+2} atoms, the only anomalous scatterers, are nearly centrically related and therefore this correction should be suitable.

(C) Refinement

The reflections indexed with an odd value of ℓ in α-$Cu_2P_2O_7$ do not occur in the β phase. The x-rays diffracted into these reflections are scattered only by electrons which are not consistent with the symmetry of the β phase. The intensities of the reflections with ℓ odd are weak which then implies that the two half unit cells of α-$Cu_2P_2O_7$, which become full unit cells above the transformation temperature, are very similar. As is generally the case with any structure having pseudo-symmetry, the Patterson function (Chapter 1(B)) showed only the average positions consistent with the more symmetric phase since it is dominated by the stronger reflections. The deviations from the structure of higher symmetry could not be easily inferred from the normal Patterson diagram. The peak broadening, however, showed the directions of the deviations from the β phase for the positions of the cations.

The partial refinement of β-$Cu_2P_2O_7$ reported previously (Robertson, 1965) was used as a starting point for the α-$Cu_2P_2O_7$ refinement. The thermal ellipsoids associated with the atoms of the β structure were considerably elongated. Cu^{+2} ions were situated on twofold rotation axes parallel to the b axis and showed high thermal motion approximately in the a direction. In addition the central oxygen atom was found from electron density maps to be elongated in the b direction. In order to infer the relationship between the thermal ellipsoids of the β phase and the coordinates of the α phase, it will be necessary to give a more complete description of the change in symmetry which occurs at the phase transformation from the β to α polymorph. This change results from the loss of translational symmetry relating two unit cells adjacent to each other in the c direction. This is manifest by the loss of the mirror plane of the β phase and its replacement by a c glide plane.

Refinement was initially done in the space group Cc. It was assumed that the displacements of the Cu^{+2} and O1 atoms were in the directions of the principal axis of thermal motion of each atom in the β phase. The origin of the unit cell is necessarily on the c glide plane. The position of the c glide plane in the structure was fixed by placing an O1 atom at $x/a = 0$ and $z/c = 1/4$. The origin was fixed by the sign of the displacements of the cations. There remains a choice as to the direction of the displacement of the aforementioned O1 atom up or down the b axis. This determines the relationship between the direction of the bending of the anion and the direction of the displacements of the cations from their positions in β-$Cu_2P_2O_7$. A displacement down the b axis was arbitrarily chosen. The displacement involves only a y coordinate and furthermore, a negative and positive displacement are superimposed in the projection on the (001) face. Therefore, only reflections from the {100} zone are sensitive to the sign of the displacement. The other phosphorus and oxygen atoms were assigned coordinates directly from their positions in the

β-$Cu_2P_2O_7$ structure. The structure was refined in the space group Cc using electron density maps with individual isotropic temperature factors assigned to the atoms. The R factors were lowered to 0.27 and 0.24 for the $\{001\}$ and $\{010\}$ zones respectively. The atoms were assigned anisotropic temperature factors and the structure was refined by the method of least squares (Appendix A). Unit weights were assigned to each reflection and the overall R factor was lowered to 0.18.

The data indexed as $0k\ell$, hk1 and hk2 were added to the refinement and further cycles of least squares lowered the R factor to 0.16. The greatest discrepancies between the observed and calculated structure factors occurred among the hkl reflections. These are all absent in the β phase and are most sensitive to the sign of the displacement of the central oxygen atom. The sign of the displacement was made positive and two more cycles of refinement lowered the R factor to 0.13. Of particular significance is the fact that the agreement between the observed and calculated structure factors of the hkl data had improved considerably.

The molecular geometry of the structure was calculated and it was found that a number of bond lengths were not chemically realistic. For example, the two P-O(-P) bond lengths were 1.80 and 1.38 A. Therefore, all the atomic positions were arranged such that the results were consistent with the space group C2/c. The Cu^{+2} ions were now related by a center of symmetry and the two halves of the $P_2O_7^{-4}$ anion were related by a twofold rotation axis. Initially the R factor was now higher than that obtained in the noncentric refinement but three cycles of refinement in this space group lowered the R factor back to 0.13. All the P-O bond lengths had improved and were consistent with chemical considerations.

The data of type $h1\ell$, $h2\ell$, $h3\ell$ and $h4\ell$ were now added to that already in use and the structure was further refined by least squares with a $(1/\sigma)^2$ weighting scheme (Appendix A). Absorption corrections and anomalous dispersion corrections were now applied to the data. Parallel refinements were then carried out in both the centric and non-centric space groups. The weighting scheme suggested by Cruickshank et. al. (1961) was used (Appendix A). The weight "ω" was set as

$$\omega^{-1}(\underline{H}) = A + B\ |F_o(\underline{H})|\ + C\ |F_o(\underline{H})|^2 + D\ |F_o(\underline{H})|^3$$

where $F_o(\underline{H})$ is the observed structure factor and the values of A, B, C and D are given in Table 3. The structures were refined until no appreciable changes occurred in the values of the R factors. Reflections which were too weak to be observed and whose calculated structure factors were less than the minimum observable value were assigned zero weight in the refinement. Otherwise, F_o for these reflections was replaced by 0.70 times the minimum observable value. The final value of the agreement factors R_1 and R_2, defined in Chapter 1(B) were 0.107 and 0.104 respectively for the space group C2/c and 0.107 and 0.100 respectively for the space group Cc. An attempt was made to assess the reliability of the higher symmetry space group using the criteria of Hamilton.

The atomic parameters obtained for both space groups are compared in Table 5. All of the eleven atoms in the lower symmetry space group have non-positive definite thermal parameters, Table 4 lists the 1112 recorded independent structure factors together with their calculated values. The column headed FC(1) are absolute values of the structure factor obtained in the space group Cc and that headed FC(2) are the structure factors obtained in the space group C2/c. The molecular geometries calculated from the atomic parameters obtained in both space groups are given in Table 6.

The results of these refinements seem to favor the space group C2/c. This choice has been supported by the nuclear magnetic resonance (n.m.r.) studies of Stager and Atkinson (1967). This technique is similar to e.p.r. except that the energy level splittings of the nuclear spin are observed and radio frequency electromagnetic radiation is used instead of microwaves. The ${}_{15}P^{31}$ nucleus has a spin of 1/2 whose levels are split in a magnetic field. Transitions between these levels are induced by bathing the nuclei in electromagnetic radiation of the proper frequency. In $Cu_2P_2O_7$, the ${}_{15}P^{31}$ nuclei are also subject to the local magnetic field generated by the paramagnetic Cu^{+2} cations and thus the environment of the ${}_{15}P^{31}$ nucleus will shift its absorption frequency. This effect is known as the chemical shift. If the space group of α-$Cu_2P_2O_7$ is Cc the unit cell must contain two independent P atoms which would give rise to two n.m.r. absorption signals. If the space group were C2/c, only one signal should be seen. Stager and Atkinson have only seen one signal. Furthermore, the shift in absorption frequency was isotropic over a wide range of temperature. It is unlikely that the chemical shifts of two independent ${}_{15}P^{31}$ atoms would accidentally superimpose over such a temperature range. Also, at low temperatures, the spectral lines are very sharp and any doubling of the ${}_{15}P^{31}$ absorption line should be observable. These experiments support the choice of the space group C2/c although the accuracy of this method has not yet been evaluated. Thus although there may be still some uncertainty as to the space group of α-$Cu_2P_2O_7$,at worse it can not differ very greatly from C2/c.

Table 1

Observed and calculated values of sin Θ/λ for the Debye-Scherrer lines used to determine the lattice parameters of α-$Cu_2P_2O_7$

h	k	ℓ	sinΘ/λ(obs)	sinΘ/λ(calc)
0	0	2	0.05406	0.05356
$\bar{1}$	1	2	0.06850	0.06850
0	2	1	0.07436	0.07424
2	0	0	0.09553	0.09470
$\bar{2}$	0	2	0.10111	0.10036
0	2	2	0.11488	0.11441
$\bar{2}$	2	1	0.14563	0.14499
2	2	0	0.15527	0.15555
1	3	0	0.15976	0.16058
$\bar{2}$	0	4	0.21362	0.21315
3	1	0	0.22990	0.22829
1	3	2	0.23798	0.23809
2	2	2	0.25748	0.25701
$\bar{2}$	2	4	0.27516	0.27400
0	4	2	0.29734	0.29695
$\bar{1}$	3	4	0.32758	0.32693
$\bar{3}$	3	2	0.33383	0.33169
3	3	0	0.35103	0.34998
1	3	4	0.42370	0.42273
$\bar{2}$	0	6	0.43425	0.43307
2	2	4	0.46688	0.46560
3	3	2	0.47684	0.47539
0	6	0	0.54664	0.54761
$\bar{1}$	3	6	0.57243	0.57080
3	5	0	0.59325	0.59336
$\bar{4}$	2	6	0.63758	0.63432
$\bar{2}$	6	2	0.64863	0.64798

(continued)

Table 1 (continued)

h k ℓ	$\sin\Theta/\lambda$(obs)	$\sin\Theta/\lambda$(calc)
$\bar{3}$ 5 4	0.66497	0.66392
5 1 1	0.68309	0.68035
1 9 4	1.51671	1.51796
3 3 8	1.49633	1.49439
1 5 8	1.35743	1.35678
5 7 0	1.33986	1.33724
$\bar{2}$ 8 4	1.18702	1.18669
2 8 2	1.16847	1.16970
1 3 8	1.11477	1.11339
1 5 6	0.95723	0.95788

TABLE 2

Refinement Data for α-$Cu_2P_2O_7$

$\mu(Mo) = 100\ cm^{-1}$ $\mu(Cu) = 160\ cm^{-1}$

Number of observed reflections	715
Total number of reflections	1112

(a) Space group C2/c

Weighting curve constants

A = 11.91319

B = -0.99401

C = 0.03397

D = -0.00018

R_1 (observed reflections only)	0.0976
R_1 (all reflections)	0.1069
R_2 (observed reflections only	0.1017
R_2 (all reflections)	0.1045

(b) Space group Cc

Weighting curve constants

A = 11.69711

B = -1.02278

C = 0.03653

D = -0.00019

TABLE 2 (continued)

R_1 (observed reflections only)	0.0946
R_1 (all reflections)	0.1075
R_2 (observed reflections only)	0.0950
R_2 (all reflections)	0.0999

Unobserved reflections whose calculated values were greater than the minimum observable value, F(min) in that area were replaced by 0.70 F(min). Otherwise their weight was set at zero.

TABLE 3

Lattice parameters of structures related to that of thortveitite (e.s.d.'s in parantheses)

	Ref.	a(A)	b(A)	c(A)	β	Z	Space Group	Range of Stability
β-$Cu_2P_2O_7$		6.827(6)	8.118(6)	4.567(6)	108.85(10)$^\circ$	2	C 2/m	above 71°C
β-$Mg_2P_2O_7$	(a)	6.494(7)	8.28 (1)	4.522(5)	103.8 (1)$^\circ$	2	C 2/m	above 68°C
β-$Zn_2P_2O_7$	(b)	6.61 (1)	8.30 (1)	4.51 (1)	105.4 (1)$^\circ$	2	C 2/m	above 155°C
$Mn_2P_2O_7$	(c)	6.63	8.58	4.54	102.66°	2	C 2/m	at least above 150°C
$Sc_2Si_2O_7$	(d)	6.542(5)	8.519(5)	4.669(5)	102.5 (2)$^\circ$	2	C 2/m	
$Mg_2As_2O_7$	(e)	6.584	8.509	4.761	103.9°	2	C 2/m	
$Zn_2As_2O_7$	(f)	6.66	8.36	4.75	104°	2	C 2/m	
$Cd_2V_2O_7$	(g)	7.088	9.091	4.963	103.3°	2	C 2/m	
α-$Cu_2P_2O_7$		6.877(4)	8.113(4)	9.162(10)	109.54(6)$^\circ$	4	C 2/c	below 71°
α-$Mg_2P_2O_7$	(h)	13.198(5)	8.295(5)	9.072(5)	104.9(1)$^\circ$	8	B 2_1/c	below 68°C
α-$Zn_2P_2O_7$		20.068(15)	8.259(6)	9.099(8)	106.35(8)$^\circ$	12	I c	below 132°C
α-$Ni_2P_2O_7$	(i)	13.093(7)	8.275(5)	8.974(5)	104.9(1)$^\circ$	8	B 2_1/c	below 575°C
α-$Co_2P_2O_7$	(j)	13.23 (1)	8,318(8)	8.983(8)	104.3(1)$^\circ$	8	B 2_1/c	below 304°C

References for Table 3

(a) Calvo (1965a)

(b) Calvo (1965b)

(c) Łukaszewicz and Smajkiewicz (1961)

(d) Cruickshank, Lynton and Barclay (1962)

(e) Łukaszewicz (1963)

(f) Calvo and Neelakantan (1967)

(g) Au (1966)

(h) Calvo (1967d)

(i) Calvo (1967c)

(j) Łukaszewicz (1967a)

TABLE 4

Observed and calculated structure factors of α-$Cu_2P_2O_7$. The columns headed FC(1) are the absolute values of the structure factors obtained in the space group Cc. The columns headed FC(2) are the structure factors obtained in the space group C2/c. Reflections which were too weak to be observed are marked with an asterisk. The structure factors divided by ten refer to one unit cell.

```
             IF0I  FC(1)  FC(2)
  H    L                  K = 0
  0    4     687    535    538
  0    6     656    603    620
  0    8     608    582    608
  0   10     777    563    577
  0   12    • 68     20     12
  0   14     302    267    277
  0   16     197    175    176
  0   18     120    118    114
  0   20     144    141    125
  0   22    • 60     61     -4
  2  -22     178    126     96
  2  -20      87     67     60
  2  -18    • 54     61     30
  2  -16     118    186    194
  2  -14    • 54     57      8
  2  -12     478    451    461
  2  -10     274    228    226
  2   -8     348    358    369
  2   -6     538    526    535
  2   -4     955    809    798
  2   -2    1690   1720   1720
  2    0     378    313    308
  2    2     409    450    440
  2    4    1271   1094   1105
  2    6     593    616    627
  2    8     635    607    617
  2   10    • 53     38     19
  2   12     529    453    467
  2   14     315    285    292
  2   16     121    110    123
  2   18     152    151    153
  2   20      75     70     63
  2   22     132    162    160
  4  -22    • 69     35     -5
  4  -20    • 79     94    -25
  4  -18     168    154    146
  4  -16    • 80     35     -5
  4  -14     220    210    214
  4  -12     128     98     65
  4  -10     170    167    177
  4   -8     503    555    558
  4   -6     206    214    186
  4   -4    1077    956    965
  4   -2     127    135    126
  4    0     804    768    758
  4    2     987    876    886
  4    4     508    474    481
  4    6     576    540    529
  4    8     178    175    163
  4   10     580    526    544
  4   12     365    319    331
  4   14      87     85     93
  4   16     242    231    234
  4   18     118    149    145
  4   20     179    200    208
  6  -22    • 70     85    -35
  6  -20     123    113    104
  6  -18      90     67    -79
  6  -16    • 80     80     87
  6  -14    • 75    108     -8
  6  -12     126    124    128
  6  -10     276    272    271
  6   -8      89     86    -60
  6   -6     477    448    463
  6   -4     285    252    243
 -6    2     409    405    398
  6    0     651    578    586
  6    2     202    175    164
  6    4     700    588    583
  6    6     184    178    161
  6    8     556    477    497
  6   10     302    280    275
  6   12     131    132    119
  6   14     338    295    303
  6   16     204    175    184
  6   18     206    197    212
  8  -22    • 68     43     43
  8  -20     103     99    -94
  8  -18    • 82     47     31
  8  -16    • 82     74      3
  8  -14    • 78      9     -5
  8  -12     127    140    138
  8  -10     217    205   -197
  8   -8     354    334    348
  8   -6      69     76     42
  8   -4     215    175    174
  8   -2     277    237    232
  8    0     128    121    113
  8    2     508    452    449
  8    4     134    135    101
  8    6     300    303    302
  8    8     268    274    271
  8   10     135    145    122
  8   12     374    296    311
  8   14     150    144    151
  8   16     201    200    214
 10  -22      75     96    -77
 10  -20    • 75     18     24
 10  -18    • 81     53    -34
 10  -16    • 82     49    -53
 10  -14    • 81     49     47
 10  -12     152    142   -137
 10  -10     138    141    155
 10   -8    • 73     49    -13
 10   -6    • 71     43    -43
 10   -4     213    187    178
 10   -2    • 77     31    -24
 10    0     294    316    333
 10    2     101     89    -61
 10    4     267    209    206
 10    6     275    228    223
 10    8     117    121     94
 10   10     285    224    226
```

```
             IF0I  FC(1)  FC(2)
 10   12     106    109    112
 10   14     201    199    208
 12  -18    • 76     78    -72
 12  -16    • 81     51     58
 12  -14     142    145   -145
 12  -12    • 82     72     76
 12  -10    • 81     94    -86
 12   -8    • 80     38    -36
 12   -6    • 80     74     61
 12   -4    • 80     75    -63
 12   -2     160    133    141
 12    0      75     79    -74
 12    2    • 82     98     85
 12    4     187    169    179
 12    6    • 79     66     -1
 12    8     168    160    156
 12   10    • 64     65     64
 12   12     181    170    182
 14  -18    • 67     23     30
 14  -16      97    106   -116
 14  -14    • 78     19      3
 14  -12    • 80     47    -37
 14  -10    • 82     83    -78
 14   -8    • 82     47     38
 14   -6     131    145   -145
 14   -4    • 82    105    107
 14   -2    • 81    100   -114
 14    0    • 71     34     26
 14    2    • 77     75     74
 14    4    • 72     58    -43
 14    6    • 65     95     84
 14    8    • 54     24     20
 16   -6    • 82     58     44
 16   -4    • 72     86    -88
 16   -2    • 70     57    -63
 16    0    • 58     52     48
 16    2    • 59     79    -83

  H    L                  K = 1

  1  -19    •117    123   -124
  1  -18     127     93   -101
  1  -16    •118     56      2
  1  -17     142    134   -123
  1  -15     135    132   -124
  1  -14     165    179   -178
  1  -13     130    141   -140
  1  -12    • 98     38    -45
  1  -11     178    196   -197
  1  -10    • 86     61     52
  1   -9     167    222   -227
  1   -8     414    500   -497
  1   -7     186    197   -193
  1   -6     109     99    -98
  1   -5     170    172   -170
  1   -4     334    340   -335
  1   -3     265    261   -260
  1    2     921    877   -872
  1    3      90     82     89
  1    4      97     90     87
  1    5      53     41     36
  1    6     634    568   -559
  1    7      98    115    113
  1    8    • 80     41     27
  1    9     119    104     94
  1   10     150    141   -152
  1   11     118    121    112
  1   12     206    232   -227
  1   13     119    118    112
  1   14    •114     46      8
  1   15    •118    111    105
  3  -17    •120    100   -105
  3  -16    •117     69    -70
  3  -15     161    167   -173
  3  -14    •107     31    -36
  3  -13     224    209   -214
  3  -12     105     97     85
  3  -11     207    219   -225
  3  -10     396    451   -455
  3   -9     165    191   -184
  3   -8      94    123    115
  3   -7     335    339   -336
  3   -6     230    247   -240
  3   -5     412    409   -412
  3   -4      87    111   -106
  3   -3     424    362   -363
  3   -2     530    525   -524
  3   -1     155    158   -146
  3    0     522    559   -559
  3    1     175    198   -203
  3    2     184    159    151
  3    3     190    194   -202
  3    4     375    468   -453
  3    5      71     98    -92
  3    6     137    168   -171
  3    7    • 83     42     18
  3    8     120    130   -138
  3    9    • 94     40     26
  3   10     222    246   -245
  3   11    •106     46     36
  3   12    •111     39     37
  3   13    •115     64     33
  3   14     156    182   -192
  3   15    •120     87     70
  5  -18    •121     24    -29
  5  -17     149    161   -159
  5  -16    •117     36    -29
  5  -15     148    157   -159
  5  -14    •108     63     63
  5  -13     136    145   -150
  5  -12     264    255   -262
  5  -11     213    207   -209
  5  -10     123    126    125
  5   -9     359    337   -338
```

```
             IF0I  FC(1)  FC(2)
  5   -8      74     95    -95
  5   -7     357    367   -375
  5   -6     245    232   -224
  5   -5     270    249   -247
  5   -4     164    136   -137
  5   -3     382    321   -314
 -5    2     476    448   -446
  5   -1     427    371   -373
  5    0     329    312    322
  5    1     410    372   -373
  5    2     530    535   -539
  5    3     158    157   -145
  5    4     185    164   -162
  5    5      91    103   -100
  5    6     104    103   -100
  5    7     101    106   -109
  5    8     194    193   -184
  5    9    •105     88    -88
  5   10    •110     12     -9
  5   11    •115     67    -21
  5   12     228    232   -237
  5   13    •120     54     27
  5   14    •120      1    -13
  7  -17    •120     78    -80
  7  -16    •118     96    103
  7  -15     129    118   -123
  7  -14     178    162   -172
  7  -13     172    188   -192
  7  -12     144    148    140
  7  -11     260    257   -261
  7  -10     107    111   -110
  7   -9     247    204   -209
  7   -8    • 89     94    -73
  7   -7     238    223   -221
  7   -6    • 84     29    -27
  7   -5     504    341   -337
  7   -4     272    229   -224
  7   -3     496    394   -398
  7   -2     238    179    177
 -7    1     261    293    293
  7    0     336    349   -355
  7    1     187    202   -198
  7    2     193    153   -157
  7    3     264    208   -211
  7    4    • 96     43     33
  7    5     270    242   -246
  7    6     225    209   -209
  7    7     121    142   -137
  7    8    •113     16    -13
  7    9    •116     81    -70
  7   10     286    245   -251
  7   11    •120     51    -49
  7   12    •120     33     22
  9  -13    •114    130   -132
  9  -12    •111     26    -19
  9  -11     134    132   -136
  9  -10    •105     75    -51
  9   -9     159    185   -186
  9   -8     103    100     96
  9   -7     304    299   -299
  9   -6     255    233   -233
  9   -5     274    243   -245
  9   -4     232    212    213
  9   -3     233    220   -214
  9   -2     277    247   -255
  9   -1     225    217   -213
  9    0    • 61     48    -43
  9    1     283    285   -290
  9    2    •105     41     26
  9    3     275    253   -246
  9    4     163    162   -157
  9    5     134    152   -145
  9    6    •117     17    -16
  9    7     125    124   -125
  9    8     186    196   -188
  9    9     127    143   -150
  9   10    •119     46     27
 11  -12    •118     45      1
 11  -11     171    152   -155
 11  -10    •115     56     55
 11   -9     167    173   -172
 11   -8    •112    125   -131
 11   -7     139    142   -143
 11   -6     154    156    156
 11   -5     154    163   -156
 11   -4    •111     92    -93
 11   -3     268    230   -230
 11   -2    •112     69    -69
 11   -1     258    232   -232
 11    0      78     73     79
 11    1     191    203   -194
 11    2     164    137   -138
 11    3     122    144   -140
 11    4    •120     49     51
 11    5     167    187   -192
 11    6     158    168   -165
 11    7     156    186   -189
 11    8    •116     51     38
 11    9    •112    147   -144
 13  -11    •120     90    -88
 13  -10     134    105   -108
 13   -9    •120     79    -79
 13   -8     158    161    168
 13   -7     127    145   -142
 13   -6    •120     79    -78
 13   -5     158    160   -160
 13   -4    •120     26    -24
 13   -3     138    151   -152
 13   -2    •120     68     63
 13   -1     127    143   -133
 13    0    • 73     61    -56
 13    1     149    157   -158
 13    2    •119     51     50
 13    3     154    190   -190
 13    4    •115    125   -114
```

```
             IF0I  FC(1)  FC(2)
 13    5     139    173   -170
 13    6    •107     51     29
 15   -2    •113     58    -56
 15   -1    •111    129   -128
 15    0    •109     64     75
 15    1    •106    147   -146

  H    L                  K = 2

  0    0      61     27    -22
  0    1     135    135   -138
  0    2     907   1180  -1210
  0    3      24     39     -8
  0    4     371    377   -373
  0    5     213    171   -186
  0    6     382    386   -378
  0    7     108    102   -100
  0    8     477    458   -464
  0    9      93    116    -96
  0   10     129    121   -128
  0   11     127    122   -130
  0   12     315    330   -341
  0   13    •117    111   -116
  0   14    •123      1     -1
  0   15    •128     94    -95
  0   16    •131    154   -140
  0   17    •132     87    -68
  0   18     167    154   -141
  0   19    •103     96    -75
  2  -18    •132     92    -85
  2  -17     139    135    131
  2  -16    •129     75     57
  2  -15     131    120    124
  2  -14     288    270   -282
  2  -13     120    131    132
  2  -12    •107     59    -52
  2  -11     106    105     97
  2  -10     290    317   -310
  2   -9     203    228    229
  2   -8     143    166   -169
  2   -7     417    251    263
  2   -6     333    358   -359
  2   -5     190    193    195
  2   -4     893    924   -919
  2   -3      80     70     70
  2   -2     150    142   -140
  2   -1     240    220    226
  2    0     646    713   -715
  2    1     198    188    178
  2    2     663    635   -618
  2    3      77     92     82
  2    4     375    438   -418
  2    5      71     78    -74
  2    6     539    576   -581
  2    7    • 70     48      3
  2    8     103     82    -89
  2    9    • 99     60    -68
  2   10     478    442   -447
  2   11    •112     48    -35
  2   12    •118     75    -69
  2   13    •124     85    -77
  2   14     179    200   -192
  2   15    •131     84    -61
  2   16     174    185   -178
  2   17    •130     77    -66
  4  -18    •132     78     59
  4  -17    •131     91     84
  4  -16     188    184   -186
  4  -15    •124     86     86
  4  -14    •119     20      2
  4  -13     148    149    152
  4  -12     133    126   -128
  4  -11     207    223    227
  4  -10     140    145   -144
  4   -9     213    238    250
  4   -8     116    133   -128
  4   -7      90    104    101
  4   -6     610    689   -691
  4   -5     282    288    290
  4   -4     164    148    141
  4   -3     372    330    332
  4   -2     603    625   -616
  4   -1     368    360    356
  4    0     474    495   -476
  4    1      57     69     59
  4    2     400    444   -438
  4    3      83     80     89
  4    4     410    440   -445
  4    5     121    140    136
  4    6     109    101   -100
  4    7     104     81     70
  4    8     513    494   -488
  4    9    •110     41     -3
  4   10     137    144   -142
  4   11    •122     44    -31
  4   12     176    182   -172
  4   13    •130     39    -17
  4   14     194    219   -219
  4   15    •131     44    -10
  6  -16    •129     72     61
  6  -15     148    145    147
  6  -14    •121     65    -72
  6  -13     153    166    172
  6  -12    •111     87    -68
  6  -11     125    116    123
  6  -10    •101     40    -23
  6   -9     158    145    148
  6   -8     365    341   -355
  6   -7     332    302    298
  6   -6     133    124    122
  6   -5     422    336    342
  6   -4     403    345   -335
  6   -3     243    185    182
 -6    2     382    387   -386
```

```
             IF0I  FC(1)  FC(2)
  6   -1     167    175    173
  6    0     156    154   -156
  6    1     202    191    204
  6    2     419    386   -386
  6    3     282    285    283
  6    4    • 98     51    -23
  6    5    •103     94     81
  6    6     501    503   -503
  6    7    •113     57     52
  6    8    •118    113   -111
  6    9    •123     50     47
  6   10     158    163   -144
  6   11    •130     78     76
  6   12     229    242   -240
  6   13    •132     68     27
  8  -13    •122     97    100
  8  -12    •118     97     94
  8  -11     135    137    142
  8  -10     214    231   -244
  8   -9     258    264    267
  8   -8     181    173    171
  8   -7     150    150    158
  8   -6     222    229   -223
  8   -5     162    155    156
  8   -4     133    137   -140
  8   -3     201    205    202
 -8    2    • 72     55    -59
  8   -1     301    277    286
  8    0     232    253   -246
  8    1     252    224    217
  8    2    •108     71     -7
  8    3     124    106     99
  8    4     384    371   -371
  8    5     132    110    110
  8    6    •122     89    -88
  8    7     157    160    163
  8    8    •129    118    -80
  8    9    •131    111    109
  8   10     242    249   -256
  8   11    •131     73     49
 10  -10    •122    120    121
 10   -9    •120     88     95
 10   -8    •118     53    -52
 10   -7     123    125    123
 10   -6     121     87    -86
 10   -5     247    241    239
 10   -4    •115     59     55
 10   -3     189    175    179
 10   -2     224    205   -200
 10   -1     173    170    165
 10    0      90    109    100
 10    1     128    103    100
 10    2     298    266   -272
 10    3     196    192    197
 10    4    •129     36    -31
 10    5     172    177    175
 10    6    •113    100    -45
 10    7     140    107    106
 10    8     183    201   -206
 10    9    •129     80     70
 12   -7    •129    146    139
 12   -6    •128     54     49
 12   -5    •128    100    106
 12   -4    •128     87    -85
 12   -3    •129    110    102
 12   -2    •130    117    110
 12   -1     138    150    150
 12    0     163    152   -146
 12    1     155    172    170
 12    2    •132     29    -30
 12    3     140    149    145
 12    4    •131     73     31
 12    5    •130     83     84
 12    6     158    147   -154
 12    7    •123    127    125
 14   -2    •130    103   -105
 14   -1    •129    123    124
 14    0    • 71     21     14
 14    1    •126     94     89

  H    L                  K = 3

  1  -19    •129     70     17
  1  -18    •133     86    -17
  1  -17    •134     60     62
  1  -16     217    226    227
  1  -15    •128     53     51
  1  -14     181    170    161
  1  -13    •117     83     65
  1  -12     239    219    217
  1  -11    •104     70     56
  1  -10     292    305    318
  1   -9      96     75     57
  1   -8     118    145    141
  1   -7     103    100    103
  1   -6    1051   1043   1055
  1   -5      99    107     95
  1   -4     672    650    659
  1   -3    • 39     33     13
  1    0     724    749    744
  1    2    1102    942    953
  1    3     102    108    102
  1    4    1300   1224   1241
  1    5     122    115    -99
  1    6      69     36     23
  1    7    • 68     23     27
  1    8     550    448    460
  1    9     102     70    -63
  1   10     431    440    438
  1   11    •110     37    -34
  1   12     251    252    257
  1   13    •122     39    -35
  1   14     247    228    239
  1   15    •132     44    -41
```

```
          IF0I  FC(1)  FC(2)
  H   L                K = 3
  ( CONTINUED )

  1  16 •133     37     12
  1  17 •133     84    -19
  1  18  212    217    213
  1  19 •123     48    -43
  3 -17 •133     71     56
  3 -16 •131     64     40
  3 -15 •126     72     36
  3 -14  128     94     54
  3 -13 •115     92     85
  3 -12  308    290    303
  3 -11 •102     68     56
  3 -10 • 96     97     63
  3  -9  142    160    169
  3  -8  551    651    659
  3  -7   67     73     40
  3  -6  187    188    188
  3  -5  155    150    148
  3  -4  457    440    436
  3  -3  103     94     87
  3  -2  801    808    806
  3  -1  159    167    157
  3   0  746    755    766
  3   1   76     97     76
  3   2  878    873    880
  3   3 • 58     59     40
  3   4   91     89     84
  3   5 • 67     25     27
  3   6  670    580    587
  3   7 • 94     40     23
  3   8  649    577    587
  3   9 •107     21    -17
  3  10  212    200    205
  3  11 •119     15     14
  3  12  262    252    269
  3  13 •129     35    -37
  3  14 •132     98     96
  3  15 •134     66     -2
  3  16  319    326    322
  3  17 •128     28    -33
  5 -16 •130     81     22
  5 -15 •126     75     74
  5 -14  223    220    223
  5 -13 •116     93     79
  5 -12 •111     66    -54
  5 -11 •105     98     98
  5 -10  268    279    287
  5  -9  118     98     80
  5  -8  102    127    109
  5  -7   92     94     93
  5  -6  293    312    312
  5  -5  203    220    213
  5  -4  528    588    585
  5  -3   80     82     72
 -5   2  183    180    180
 -5   1  177    181   -178
  5   0  659    698    699
  5   1 • 39     30     23
  5   2  124    146    131
  5   3  138    141    140
  5   4  595    579    587
  5   5 • 97     60     47
  5   6  450    474    478
  5   7 •108     48     41
  5   8  120    150    154
  5   9 •119     27     30
  5  10  315    314    326
  5  11 •129     18      1
  5  12  173    179    182
  5  13 •134     40     18
  5  14  358    345    341
  5  15 •130      2     -3
  7 -15 •129     59     34
  7 -14  148    157   -151
  7 -13 •121     85     81
  7 -12  130    158    166
  7 -11 •112     54     45
  7 -10 •108     86     43
  7  -9  133    130    127
  7  -8  178    162    162
  7  -7  128    132    124
  7  -6  255    228    225
  7  -5  116     99     98
  7  -4 • 92     53    -15
  7  -3  120    113    105
 -7   2  521    505    504
  7  -1  126    120    122
  7   0  134    165    134
  7   1  129    123    116
  7   2  320    323    324
  7   3  117    115    107
  7   4  364    349    353
  7   5 •113     52     30
  7   6  135    123    118
  7   7 •122     89     86
  7   8  321    358    373
  7   9 •130     36     26
  7  10  156    152    152
  7  11 •134     45     55
  7  12  303    305    301
  7  13 •130     20     12
  9 -13 •128     68     65
  9 -12 •124     61      9
  9 -11 •121     67     60
  9 -10 •118     25    -19
  9  -9 •115    114    110
  9  -8  120    125    116
  9  -7 •111     29     26
  9  -6  130    113   -110
  9  -5  143    141    141
  9  -4  363    366    377
  9  -3  115     83     78
  9  -2 •110     67    -26

          IF0I  FC(1)  FC(2)
  9  -1  146    137    132
  9   0  141    147    140
  9   1 •116     83     68
  9   2  242    245    237
  9   3 •121     64     73
  9   4  139    109    106
  9   5 •128    103     96
  9   6  297    279    288
  9   7 •132     65     64
  9   8 •133     90     75
  9   9 •133     57     55
  9  10  241    255    245
  9  11 •128     51     39
  9  12  144    148    168
  9  13 •115     45     33
 11  -9 •127     60     50
 11  -8 •126    115   -107
 11  -7 •125     88     80
 11  -6 •124    164    177
 11  -5 •124     89     86
 11  -4 •124     84    -73
 11  -3 •125     65     59
 11  -2 •126     22     10
 11  -1 •127     93     92
 11   0  174    186    186
 11   1 •130     47     54
 11   2 •131     25     11
 11   3 •133    124    118
 11   4  166    181    189
 11   5 •134     51     48
 11   6 •133     40     -5
 11   7 •131     76     69
 11   8  172    207    205
 11   9 •122     65     53
 13  -7 •133     20     26
 13  -6 •133     90    -94
 13  -5 •133     61     63
 13  -4 •134     20    -16
 13  -3 •134     61     57
 13  -2 •134     79     79
 13  -1 •134     61     67
 13   0 • 73     61    -48
 13   1 •133     87     75
 13   2 •131     97     96
 13   3 •129     53     55
 13   4 •126     53    -33
 13   5 •123     67     58
 13   6  131    128    127
 13   7 •111     79     72
 15  -5 •127     67     63
 15  -4 •126     31     32
 15  -3 •125     15     22
 15  -2 •124     93    -91
 15  -1 •122     75     69
 15   0 •119     67     67
 15   1 •115     30     33

  H   L                K = 4

  0   0  312    275    262
  0   2  382    384   -391
  0   3  228    224    221
  0   4  217    210    216
  0   5   94     91     75
  0   6  110    114     98
  0   7  176    158    156
  0   8  185    194   -179
  0   9  161    145    166
  0  10   95    112     87
  0  11  150    137    136
  0  12  155    141   -131
  0  13  173    169    161
  0  14  191    181    160
  0  15  135    141    109
  0  16 •130     49    -37
  2 -18 •130     21     -8
  2 -17  149    142   -123
  2 -16  160    162    142
  2 -15  194    204   -202
  2 -14  167    167   -165
  2 -13  138    142   -136
  2 -12  114    100     66
  2 -11  219    204   -216
  2 -10  100     81    -74
  2  -9  184    214   -216
  2  -8  137    145    141
  2  -7  258    296   -300
  2  -6   77     96     74
  2  -5  215    265   -267
  2  -4  397    459   -476
  2  -3  157    196   -196
  2  -2  325    332    331
  2  -1  184    183   -190
  2   0   63     79    -67
  2   1  196    188   -206
  2   2  110     88     81
  2   3   53     67    -39
  2   4 • 56     71    -16
  2   5 • 61     76    -32
  2   6  209    231   -221
  2   7  115     94    108
  2   8  225    204    210
  2   9 •100     34     -2
  2  10  144    145   -138
  2  11  119    118    104
  2  12  148    140    113
  2  13 •124    120     69
  4 -18 •130     93     86
  4 -17  149    148   -152
  4 -16  151    135   -136
  4 -15  146    128   -121
  4 -14  126    102     85
  4 -13  208    199   -198
  4 -12 •108     14     -5

          IF0I  FC(1)  FC(2)
  4 -11  306    281   -290
  4 -10 • 96     51     30
  4  -9  272    230   -237
  4  -8 • 85     84     44
  4  -7  316    321   -329
  4  -6  287    358   -367
  4  -5  206    214   -218
  4  -4  369    424    440
  4  -3  398    468   -486
  4  -2   91    109   -101
 -4   1  257    253    262
  4   0   64     70    -71
  4   1  213    227   -225
  4   2 • 60     55    -56
  4   3  138    155   -134
  4   4  111    123   -102
  4   5  153    120   -118
  4   6  281    250    256
  4   7  124    103   -108
  4   8  215    218   -203
  4   9 •111     67      6
  4  10 •117     95     48
  4  11 •122     64     25
  4  12 •126     53    -10
  6 -16 •128    107     87
  6 -15  205    207   -195
  6 -14 •121     22    -26
  6 -13  213    201   -211
  6 -12 •112     35    -19
  6 -11  195    184   -183
  6 -10 •102     88     70
  6  -9  229    249   -246
  6  -8  191    205   -211
  6  -7  301    307   -322
  6  -6  325    293    309
  6  -5  372    373   -383
  6  -4  136    132   -132
  6  -3  352    307   -311
  6  -2  159    115   -119
 -6   1  199    203    205
  6   0   78     64     71
  6   1  355    358   -350
  6   2 • 91     76    -72
  6   3  229    193   -203
  6   4  245    217    219
  6   5  243    203   -210
  6   6  276    272   -267
  6   7 •113     72    -49
  6   8 •118     89     59
  6   9 •122    100    -98
  6  10 •126     44     53
  8 -14 •125     27    -21
  8 -13 •122     96    -97
  8 -12  140    117    111
  8 -11  255    258   -251
  8 -10  155    177   -178
  8  -9  233    204   -225
  8  -8  203    194    201
  8  -7  292    294   -299
  8  -6  126    120   -119
  8  -5  215    195   -195
  8  -4 • 99     42    -39
  8  -3  332    282   -289
  8  -2  111     86     92
  8  -1  378    349   -342
  8   0   71     96    -89
  8   1  254    237   -248
  8   2  168    152    147
  8   3  216    190   -193
  8   4  223    233   -219
  8   5  165    171   -168
  8   6 •123     75     72
  8   7  175    177   -182
  8   8 •128     75     79
  8   9  162    165   -155
  8  10  138    120    -98
  8  11 •129     72    -52
 10 -14 •130     88     83
 10 -13  151    183   -168
 10 -12  149    143   -147
 10 -11  138    141   -156
 10 -10 •122    123    126
 10  -9  126    153   -146
 10  -8 •118     39    -37
 10  -7  171    205   -206
 10  -6 •129     54    -36
 10  -5  249    211   -222
 10  -4 •115     77     79
 10  -3  409    316   -312
 10  -2  134    122   -121
 10  -1  188    147   -152
 10   0  132    151    150
 10   1  235    232   -232
 10   2  167    168   -166
 10   3  224    210   -210
 10   4 •128     69     58
 10   5  237    223   -230
 10   6 •130     75     60
 10   7  145    170   -156
 10   8 •129    124   -105
 12  -9 •129    135   -140
 12  -8 •128     46    -38
 12  -7  168    162   -174
 12  -6 •128     46     45
 12  -5  159    177   -170
 12  -4 •128     81    -80
 12  -3  151    146   -146
 12  -2 •129    142    134
 12  -1  230    201   -198
 12   0  137    133   -122
 12   1  252    225   -227
 12   2 •130     20     11
 12   3  171    168   -173
 12   4 •128     82     69
 12   5  166    183   -171

          IF0I  FC(1)  FC(2)
 12   6 •123     95    -89
 12   7  140    128   -141
 12   8 •113     56     41
 12   9  173    184   -192
 14  -8 •129     70     61
 14  -7 •129    145   -130
 14  -6 •129     68    -68
 14  -5 •129     86    -93
 14  -4 •128    105    114
 14  -3 •128    184   -180
 14  -2  167    111   -109
 14  -1 •126    139   -142
 14   0 • 69     16      4
 14   1 •122    142   -143
 14   2 •119     96     73
 14   3 •115    164   -154
 14   4 •111     79    -69
 14   5 •105    147   -160
 14   6 • 98     39     28
 14   7  117    173   -173
 14   8 • 78     44    -49

  H   K                L = 0

  0   6 1028   1050   1073
  0   8  240    216   -210
  0  10  367    316    311
  0  12  245    215    224
  0  14   30     30    -22
  0  16  135    145    149
  0  18   25     23    -28
  0  20 • 85     68     64
  1   1  223    196   -195
  1   5  681    648   -646
  1   7  296    245    251
  1   9  165    157    151
  1  11  349    290   -297
  1  13  297    240    256
  1  15   53     70    -60
  1  17   60     79    -79
  1  19   78    125    136
  1  21   45     86    -80
  2   6   86     67     57
  2   8  696    616   -635
  2  10  223    188    194
  2  12  149    131   -129
  2  14  298    243   -250
  2  16  222    186    191
  2  18   79    123   -125
  2  20 • 85     74    -66
  3   5  708    712   -725
  3   7   78     90    -97
  3   9  111    112    105
  3  11  363    315   -326
  3  13  133     90     70
  3  15   51     57    -65
  3  17 • 78     58    -54
  3  19   53     63     52
  3  21   57     78    -84
  4   6  370    374    360
  4   8  440    383   -379
  4  10  171    144    147
  4  12 • 66     55     40
  4  14   91    117   -125
  4  16   81    103    115
  4  18   50     69    -56
  4  20 • 86     17      9
  5   5   79     66    -58
  5   7  476    423    433
  5   9  257    230    227
  5  11  111    113    -97
  5  13  375    301    315
  5  15 • 73     60     -6
  5  17   76     67    -42
  5  19  100    142    160
  6   6  320    302    308
  6   8  198    189   -201
  6  10  110    154    163
  6  12 • 70     32     39
  6  14 • 73     80    -81
  6  16 • 70    128    125
  6  18 • 62     68    -54
  7   5  441    448   -443
  7   7  135    137   -129
  7   9   20     45     -7
  7  11  268    254   -244
  7  13 • 73     15      7
  7  15 • 71     69    -52
  7  17 • 64     62    -59
  8   6 • 62     28     20
  8   8  251    253   -247
  8  10 • 70     76     43
  8  12 • 73     31    -43
  8  14   70    119   -112
  8  16 • 65     90     70
  8  18 • 54     25    -54
  9   5   68    123   -135
  9   7 • 67     48     44
  9   9 • 71     56     26
  9  11   51     68    -96
  9  13   72     85     91
  9  15 • 66     31    -29
  9  17 • 55     26    -32
 10   6  197    213    221
 10   8 • 72     61     10
 10  10  111    113    123
 10  12 • 71     95     85
 10  14 • 66     60     -0
 10  16 • 56     81     74
 11   5 • 71     23     15
 11   7 • 72     75     74
 11   9 • 73     87     87
 11  11 • 71     52    -12
 11  13 • 65     71     53

          IF0I  FC(1)  FC(2)
 11  15 • 56     62     20
 12   6   61     97    -83
 12   8   80    130   -131
 12  10 • 69     92    -56
 12  12 • 63    100    -59
 12  14 • 54     40    -63
 12  16 • 40     45     -4
 13   5 • 72     80    -75
 13   7 • 71     52    -42
 13   9 • 67     57    -41
 13  11 • 61     67    -55
 13  13 • 52     44     -7
 14   6 • 67     38     14
 14   8 • 64     29      0
 14  10 • 57     33     -3
 14  12 • 48     33     18
 15   5 • 62     67     73
 15   7 • 59     23     32
 15   9 • 52     40     47
 16   2 • 58     94    101
 16   4 • 55     75     73
 16   6 • 52     37     33
 17   1 • 48     53    -45
 17   5 • 42     62    -31

  H   K                L = 1

  0   6  134    124   -136
  0   8   91     98    -97
  0  10   58     63    -49
 -1   9   83     75    -57
 -1   7   75     68     67
 -1   5  176    159   -151
  1   5  109     88    -98
  1   7  130    139   -124
  1   9 • 40     41    -26
 -2  10  134    107    123
 -2   8   80     76     55
 -2   6   60     73    -65
  2   6   67     80     71
  2   8  107    107     82
 -3   9  130    117   -108
 -3   7  198    197    188
 -3   5 • 37     37     14
  3   5   84     69     72
  3   7   53     58    -55
  3   9  180    175    178
 -4   8  111     93    -94
 -4   6  202    207   -217
  4   6  134    169    146
  4   8   75     71    -60
 -5   7  150    140    149
 -5   5  329    272   -276
  5   5   92    106     90
  5   7  294    269   -286
 -6   6  260    275   -250
  6   6   74     75     80
 -7   5   83     85    -84

  H   K                L = 2

  0   6  236    254    247
  0   8  616    635   -646
  0  10  111     97     95
 -1   9  108     86     83
 -1   7  376    349    371
 -1   5  571    596   -599
  1   5  609    809   -800
  1   7  119     74    -69
  1   9  227    188    190
 -2  10  399    372    369
 -2   8  118    154   -148
 -2   6  658    842    865
  2   6  265    313    309
  2   8  398    427   -426
 -3   9  301    261    257
 -3   7  164    123    113
 -3   5  486    533   -518
  3   5  162    172   -177
  3   7  526    472    485
  3   9  384    305    305
 -4   8  544    459   -459
 -4   6 • 90     56     48
  4   6  521    521    522
  4   8  283    287   -280
 -5   7 • 87     15     -8
 -5   5  593    511   -528
  5   5  646    636   -624
  5   7  123     74    -60
 -6   6  336    275    265
 -7   5  121     85     40

  K   L                H = 0

  6   3   21     45     44
  6   4  277    257    252
  6   5  109    107   -103
  6   6  378    351    351
  6   7   87     92    -82
  6   8  314    315    299
  6   9   84     94    -75
  6  10  393    396    391
  8   3   63     78     54
  8   4  427    410   -420
  8   5   33     41    -52
  8   6  343    331   -335
  8   7 • 20     32     -8
  8   8  380    392   -380
 10   3  111    100    108
 10   4  333    351    359
 10   5   22     27     15
```

TABLE 5

Atomic coordinates of α-$Cu_2P_2O_7$
(e.s.d.'s in parantheses)

(a) Space group C2/c

Configuration coordinates

	x/a	y/b	z/c
Cu	-0.0178(2)	0.3133(2)	0.5068(1)
P	0.1977(3)	0.0076(4)	0.2059(2)
O1	0	0.0484(22)	1/4
O2	0.3767(8)	-0.0027(11)	0.3630(7)
O3(C)	0.2218(8)	0.1562(9)	0.1134(6)
O3(T)	0.1783(11)	-0.1530(10)	0.1187(8)

Thermal coordinates (A^2 x 10^4)

	U_{11}	U_{22}	U_{33}	U_{12}	U_{13}	U_{23}	
Cu	56(3)	68(5)	59(2)	4(4)	-34(18)	9(6)	
P	10(4)	81(11)	35(5)	-13(7)	3(3)	13(9)	
O1	72(26)	439(91)	255(46)	0	76(29)	0	
O2	33(13)	188(35)	112(18)	1(24)	-32(13)	5(33)	
O3(C)	114(16)	9(22)	75(15)	-10(21)	15(14)	67(29)	*
O3(T)	190(23)	65(31)	109(4)	-23(17)	-42(28)	3(35)	

* non positive definite.

TABLE 5 (continued)

(a) Space group Cc

Configuration coordinates

	x/a	y/b	z/c
Cu(I)	-0.0178	0.3120(5)	0.2520
Cu(II)	0.0175(4)	-0.3146(5)	0.2386(3)
P(I)	0.1921(11)	0.0085(11)	-0.0489(8)
P(II)	-0.2029(10)	0.0067(10)	0.0395(7)
O1	0.0000(42)	0.0471(26)	0.0000(42)
O2(I)	-0.3873(29)	-0.0037(33)	-0.1236(27)
O2(II)	0.3674(23)	-0.0032(24)	0.1042(17)
O3(CI)	-0.2206(29)	0.1634(23)	0.1315(12)
O3(CII)	0.2229(29)	0.1509(23)	-0.1418(23)
O3(TI)	-0.1750(24)	-0.1530(20)	0.1257(21)
O3(TII)	0.1840(38)	-0.1540(33)	-0.1369(22)

TABLE 5 (continued)

Thermal coordinates (x 10^4) *

	U_{11}	U_{22}	U_{33}	U_{12}	U_{13}	U_{23}
Cu(I)	57(9)	80(17)	129(13)	-11(20)	-34(10)	-96(26)
Cu(II)	55(8)	64(15)	26(6)	25(17)	-33(7)	85(22)
P(I)	14(18)	86(32)	33(13)	88(28)	-34(13)	-92(38)
P(II)	12(17)	112(38)	56(15)	32(35)	29(14)	-82(38)
O1	105(30)	549(109)	267(60)	-235(114)	114(35)	-107(177)
O2(I)	54(45)	320(131)	170(67)	14(125)	-105(43)	73(170)
O2(II)	1(31)	76(65)	23(270)	-31(76)	-61(25)	17(104)
O3(CI)	164(53)	-7(41)	-27(23)	101(54)	18(29)	-50(66)
O3(CII)	73(42)	-23(43)	247(74)	81(58)	33(47)	44(99)
O3(TI)	134(42)	-11(42)	114(52)	-93(48)	-67(38)	-193(77)
O3(TII)	425(61)	525(87)	116(52)	-586(56)	137(53)	-470(87)

* All thermal ellipsoids are non-positive definite in this space group.

TABLE 6

Molecular geometry of α-$Cu_2P_2O_7$. (e.s.d's in parantheses)

(a) Space group C2/c

Bond distances (A)

P-O1	1.577(5)	O1-O2	2.482(15)
P-O2	1.552(10)	O1-O3(C)	2.436(15)
P-O3(C)	1.515(10)	O1-O3(T)	2.570(15)
P-O3(T)	1.511(10)	O2-O3(C)	2.530(20)
		O2-O3(T)	2.513(20)
		O3(C)-O3(T)	2.529(20)
Cu-O2	1.962(10)		
Cu-O2'	1.988(10)		
Cu-O3(C)	1.942(10)		
Cu-O3' (C)	2.322(10)		
Cu-O3(T)	1.907(10)		
Cu-O3'(T)	2.940(10)		

Angles

P-O1-P	155.8°	O2-P-O3(C)	111.2°
O1-P-O2	105.0°	O2-P-O3(T)	110.3°
O1-P-O3(C)	104.0°	O3(C)-P-O3(T)	113.4°
O1-P-O3(T)	112.6°		

TABLE 6 (continued)

(b) Space group Cc

Bond distances (A)

P(I)-O1	1.59(3)	O1-O2(I)	2.55(4)
P(II)-O1	1.57(3)	O1-O2(II)	2.42(4)
P(I)-O2(I)	1.61(3)	O1-O3(CI)	2.42(4)
P(II)-O2(II)	1.52(3)	O1-O3(CII)	2.47(4)
P(I)-O3(CI)	1.55(3)	O1-O3(TI)	2.51(4)
P(II)-O3(CII)	1.49(3)	O1-O3(TII)	2.63(4)
P(I)-O3(TI)	1.50(3)	O2(I)-O3(CI)	2.61(4)
P(II)-O3(TII)	1.54(3)	O2(II)-O3(CII)	2.48(4)
		O2(I)-O3(TI)	2.57(4)
		O2(II)-O3(TII)	2.47(4)
		O3(CI)-O3(TI)	2.59(4)
		O3(CII)-O3(TII)	2.49(4)

Cu(I)-O2(I)	1.96(2)	Cu(II)-O2(I)	1.91(2)
Cu(I)-O2(II)	2.00(2)	Cu(II)-O2(II)	2.02(2)
Cu(I)-O3(CI)	1.89(2)	Cu(II)-O3(CI)	1.90(2)
Cu(I)-O3(CII)	2.32(2)	Cu(II)-O3(CII)	2.33(2)
Cu(I)-O3(TI)	2.97(3)	Cu(II)-O3(TI)	2.89(3)
Cu(I)-O3(TII)	1.91(2)	Cu(II)-O3(TII)	1.98(2)

Angles

P(I)-O1-P(II)	156°
O1-P(I)-O2(I)	106°
O1-P(II)-O2(II)	103°
O1-P(I)-O3(CI)	101°
O1-P(II)-O3(CII)	108°
O1-P(I)-O3(TI)	109°
O1-P(II)-O3(TII)	116°
O2(I)-P(I)-O3(CI)	112°
O2(II)-P(II)-O3(CII)	111°
O2(I)-P(I)-O3(TI)	112°
O2(II)-P(II)-O3(TII)	108°
O3(CI)-P(I)-O3(TI)	116°
O3(CII)-P(II)-O3(TII)	111°

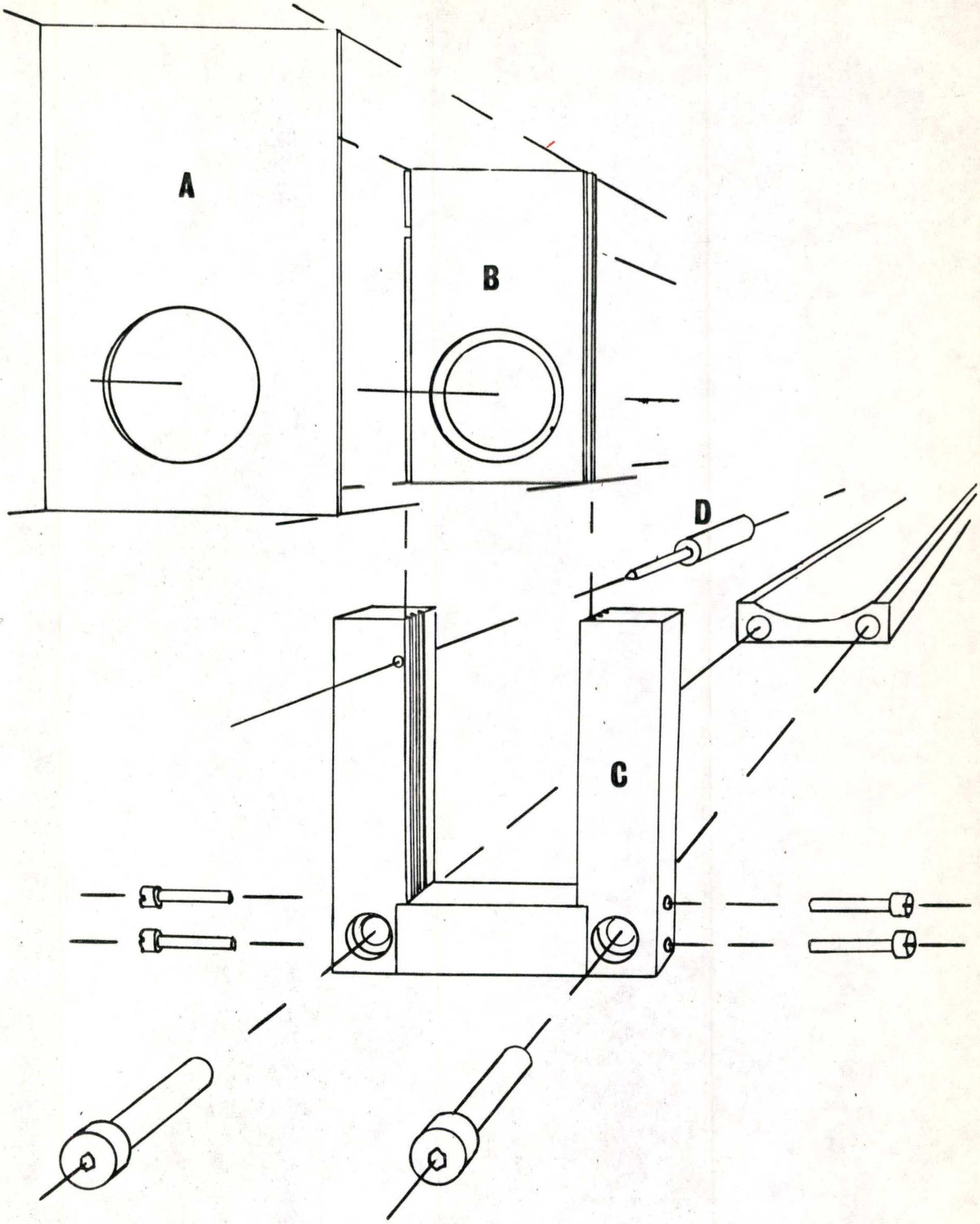

Figure 2

The filter system designed for use with the manual diffractometer

CHAPTER 3: DETERMINATION OF THE STRUCTURE OF β-$Cu_2P_2O_7$

(A) Preliminary Investigations

A comparison of x-ray photographs of β-$Cu_2P_2O_7$ with those of β-$Zn_2P_2O_7$ and β-$Mg_2P_2O_7$ suggested that their structures were similar. However, in order to gain some insight into the changes in the atomic positions and molecular geometries during the phase transformation, the detailed structure of the high temperature phase must be resolved. In the earlier refinement of the β-$Cu_2P_2O_7$ structure (Robertson, 1965), the degree of resolution was not sufficient for these proposed purposes.

As is the case for the other high temperature phases of this group of crystals, the Laue symmetry and extinctions limit the space group to one of C2, Cm or C2/m. The space group was assumed to be C2/m for this refinement. This assumption will be explored in the discussion. The lattice parameters were taken from an earlier determination (Robertson, 1965). These were measured at 100°C by comparison with the room temperature lattice parameters of α-$Cu_2P_2O_7$.

(B) Preparation of Data

The same crystals were used to collect data for the study of β-$Cu_2P_2O_7$ as for the study of α-$Cu_2P_2O_7$. The first crystal ($0.08 \times 0.08 \times 0.40$ mm^3) was used to collect data of the type hk0 with Mo Kα radiation and the manual diffractometer. A pair of hair dryers was used to heat the crystal while the diffractometer data were recorded. The temperature was monitored by a Chromel-Alumel thermocouple placed within a few millimeters of the crystal and supported by the collimator. The temperature was maintained at $100 \pm 8^\circ C$. Because of the difficulty in maintaining a constant temperature with the "open" geometry of the precession camera, no precession photographs of the β phase were taken.

The second crystal ($0.10 \times 0.10 \times 0.05$ mm^3) was used to collect additional data of the type $hn\ell$, $n=0,1,2,3,4,5$ with a Nonius Weissenberg camera using Mo Kα radiation. The crystal was heated with a high temperature attachment supplied with the camera. The crystal was maintained at $100 \pm 3^\circ C$ and the temperature was monitored by a thermocouple on the collimator.

The integrated intensities recorded with the diffractometer were corrected for background, sweep rate, incident beam intensity, dead time and filter attenuation in the same manner as described in Chapter 2.

All of the data were corrected for the effects of Lorentz and polarization. The same absorption corrections were applied as in the case of α-$Cu_2P_2O_7$.

(C) Refinement

Since the intensities of the reflections of the (010) zone were similar to those of β-$Zn_2P_2O_7$, the atomic coordinates of β-$Zn_2P_2O_7$ (Calvo,1965b) were used as trial parameters to calculate the structure factors of this zone. The R factor obtained in this manner was 0.30. Changes in atomic positional coordinates and individual isotropic temperature factors were estimated from an electron density map and were used to determine a new trial structure whose calculated structure factors led to an R value of 0.26. Difference synthesis maps suggested that the Cu^{+2} and O1 atoms should be assigned large thermal parameters. This caused a drop in the R factor to 0.20. The x coordinates obtained for the atoms in this way were used with the y atomic coordinates from β-$Zn_2P_2O_7$ to calculate an R factor of 0.51 for the data from the (001) zone. Using new coordinates derived from two successive electron density maps the agreement for this zone was lowered to 0.21. All the data were then entered into a full matrix least squares calculation using a $(1/\sigma)^2$ weighting scheme. When anisotropic temperature factors were varied the R value was lowered to 0.135. Absorption corrections were now applied. The details of these corrections are presented in Chapter 2. The structure was again refined by the method of least squares until a minimum value of R_2 (as defined in Chapter 1) was obtained. It was found that the convergence of the refinement was improved by applying only half the calculated shifts to the atomic coordinates. The weighting scheme proposed by Cruickshank et. al. (1961) was now applied. This weighting scheme endeavors to account for the effects of systematic errors inherent in the method of measurement of the integrated intensities. It is reasonable to expect that these systematic errors in the case of data recorded with a diffractometer would not necessarily be the same as those associated with data recorded on film and measured visually. For this reason the data were separated into two groups such that the coefficients in the expression (Appendix A)

$$\omega^{-1}(\underline{H}) = A + B\ |F_o(\underline{H})| + C\ |F_o(\underline{H})|^2 + D\ |F_o(\underline{H})|^3$$

could be calculated separately for the film and diffractometer data. The two sets of coefficients are listed in Table 7. The refinement was now continued using weights calculated from the above coefficients. The final values of R_1 and R_2 were 0.149 and 0.130 respectively. Unobserved reflections were treated as described in Chapter 2(C) . The final atomic positional and thermal parameters are listed in Table 9. The magnitude of the observed structure factors FO($=F_o(\underline{H})$) and the calculated structure factors FC(A)($=F_c(\underline{H})$) based on these final least squares parameters are given in Table 8. The bond lengths and interatomic angles were calculated from the atomic coordinates and are listed in Table 10.

(D) Disordered Model

During the investigation of the phase transformation in $Cu_2P_2O_7$ it was observed that some diffuse scattering occurred in the temperature region of the transformation. The detailed nature of this phenomenon will be discussed in Chapter 6. However, this diffuse scattering suggests that the high temperature form of $Cu_2P_2O_7$ might be disordered. A comparison of the atomic coordinates of α-$Cu_2P_2O_7$ and β-$Cu_2P_2O_7$ indicates that the disordering could be caused by very small atomic displacements. In a completely disordered crystal, the mathematical model used to describe the β-$Cu_2P_2O_7$ unit cell would consist of the superposition of two halves of an α-$Cu_2P_2O_7$ unit cell when one half has the normal origin and the other has its origin shifted by $\underline{c}/2$. If this description of the high temperature phase is correct, then it should be possible to describe the structure of β-$Cu_2P_2O_7$ by replacing each atom by two half atoms whose atomic positions are derived from those of α-$Cu_2P_2O_7$.

The structure factors can be calculated by the general expression given in Chapter 1. By the use of the symmetry of the unit cell this can be reduced to an expression which is summed over only the asymmetric zone. If $F_c(\underline{H})$ is the calculated structure factor then

$$F_c(\underline{H}) = \sum_j m_j f_j(H)\cos 2\pi(hx_j + \ell z_j)\cos 2\pi k y_j$$

where m_j is the number of equivalent atoms. Now we may modify this expression to describe two half atoms in each atomic position by replacing the vector $\underline{r}$ whose components are $x_j\underline{a}$, $y_j\underline{b}$ and $z_j\underline{c}$ by the vectors $\underline{r}_j + \underline{\delta}_j$ where the components of $\underline{\delta}_j$ are $\delta x_j\underline{a}$, $\delta y_j\underline{b}$ and $\delta z_j\underline{c}$. Then

$$F_o(\underline{H}) = \Sigma\ m_j f_j(H)\ \{\cos 2\pi(hx_j+\ell z_j)\cos 2\pi(h\delta x_j+\ell\delta z_j)\cos 2\pi k y_j \cos 2\pi k\delta y_j+\sin 2\pi(hx_j+\ell z_j)\sin 2\pi(h\delta x_j+\ell\delta z_j)\sin 2\pi k y_j \sin 2\pi k\delta y_j\}$$

Effectively each atom is now described by the three components of the vector $\underline{r}_j$; the three components of the vector $\underline{\delta}_j$ and one isotropic temperature factor. In contrast, the atoms were formerly described by the components of $\underline{r}_j$ and six anisotropic thermal parameters.

Each atom was modified in the above manner and the components of $\underline{r}_j$ and $\underline{\delta}_j$ and the individual isotropic temperature factors were varied by the method of least squares. The components of the vector describing the terminal oxygen atoms, that is O2 and O3, were found to vary randomly. Attempts were made to find a least squares minimum corresponding to these parameters by applying only a small fraction of the calculated changes to those coordinates but to no avail. Apparently we do not have sufficient and precise enough data to describe these vectors. The oxygen atoms are the weakest scatterers in the structure and the $\underline{\delta}$ vectors for the terminal oxygen atoms would be expected to be rather short in comparison, for example, to those of the O1 atom. It was necessary to revert back to the original description of the terminal oxygen atoms in terms of whole atoms with anisotropic thermal parameters. As indicated previously, two sets of coefficients were used in a "Cruickshank" weighting scheme. The components of the vectors $\underline{r}_j$ and $\underline{\delta}_j$ describing the O1, P and Cu^{+2} atoms and their isotropic temperature factors were varied together with the positional and anisotropic thermal parameters describing the terminal oxygen atoms. This model was then refined until a least squares minimum was obtained. The coordinates of the half-atoms representing the Cu and P atoms corresponded, within their e.s.d.'s, with the equivalent positions of the α-$Cu_2P_2O_7$ structure. However, the y coordinate of the O1 atom was approximately one-half the corresponding value in α-$Cu_2P_2O_7$. Attempts were made to fix this atom at the desired position. Small fractions of the calculated changes were applied to the y coordinate and its thermal parameters were varied anisotropically but the only least squares minimum that was found was at y/a = 0.0256.

The final values of R_1 and R_2 for this model were 0.150 and 0.121 respectively. The atomic coordinates, based on this disordered model of β-$Cu_2P_2O_7$ are listed in Table 11. In order to facilitate a comparison with α-$Cu_2P_2O_7$, the low temperature structure was refined in the space group C2/c with isotropic thermal parameters assigned to the Cu^{+2}, P and O1 atoms. These results are also presented in Table 11. It should be noted that the anisotropic thermal parameters of the terminal oxygen atoms in the disordered model of β-$Cu_2P_2O_7$ should not necessarily be identical to those of α-$Cu_2P_2O_7$ since the former may be averaged over two displaced half atoms. The calculated structure factors based on the disordered model of β-$Cu_2P_2O_7$ are listed in Table 8 under the heading FC(D).

TABLE 7

Refinement data for β-$Cu_2P_2O_7$

$\mu(Mo) = 100\ cm^{-1}$ Space group C2/m

Number of observed reflections	371
Total number of reflections	613

(a) Fully anistropic model

Weighting curve coefficients

Diffractometer data	Visually estimated data
A = 3.70778	A = 32.75002
B = 0.31990	B =-2.94330
C =-0.03560	C = 0.06882
D = 0.00065	D = 0.00013

R1 (observed reflections only)	0.1352
R1 (all reflections)	0.1493
R2 (observed reflections only)	0.1393
R2 (all reflections)	0.1202

(b) Disordered model

Diffractometer data	Visually measured data
A = 4.99565	A = 28.14925
B = 0.03330	B = -2.38407
C =-0.02077	C = 0.05130
D = 0.00041	D = 0.00027

TABLE 7 (continued)

Rl (observed reflections only)	0.1363
Rl (all reflections)	0.1505
R2 (observed reflections only)	0.1432
R2 (all reflections	0.1215

Unobserved reflections whose calculated values were greater than the minimum of observable value F(min), in that area were replaced by 0.70 x F(min). Otherwise their weight was set at zero.

TABLE 8

Observed and calculated structure factors for β-$Cu_2P_2O_7$. The columns headed FC(A) are the structure factors based on the disordered model. The reflections which were too weak to be observed are marked with an asterisk. The structure factors divided by ten refer to the contents of one unit cell.

```
          IF0I  FC(A)  FC(D)
  H   L                K = 0
  0   2   545    550    555
  0   3   647   -626   -625
  0   4   587    583    590
  0   5   600   -556   -558
  0   6  •118     57     60
  0  -7   267   -285   -283
  0  -8   156    163    164
  0  -9  •119   -111   -103
  0 -10  •108    141    142
  0 -11  • 87    -28    -22
  2 -11  • 96   -115   -109
  2 -10  •113     70     60
  2  -9  •120    -42    -34
  2  -8   226    212    218
  2  -7  •108    -65    -64
  2  -6   623    454    467
  2  -5   219   -228   -232
  2  -4   480    411    429
  2  -3   564   -564   -585
  2  -2  1058    823    843
  2  -1  1277  -1706  -1727
  2   0   284    288    286
  2   1   427   -458   -458
  2   2  1124   1102   1107
  2   3   554   -615   -607
  2   4   532    582    582
  2   5   100    -53    -38
  2   6   481    447    446
  2   7   264   -256   -249
 -2  -8  •120    121    113
 -2  -9   135   -162   -155
 -2 -10  • 99     79     75
 -2 -11    95   -119   -111
  4 -10  •115     -3    -19
  4  -9   196   -166   -159
  4  -8  •116     64     56
  4  -7   199   -221   -221
  4  -6  • 79     79     77
  4  -5   262   -241   -258
  4  -4   623    601    625
  4  -3   242   -227   -249
  4  -2  1014    948    966
  4  -1   120   -139   -161
  4   0   754    796    815
  4   1   784   -871   -887
  4   2   388    472    466
  4   3   464   -488   -481
  4   4   125    176    164
  4   5   604   -507   -496
  4   6   260    284    278
  4   7  •120    -99    -78
 -4  -8   203    215    206
 -4  -9   105   -135   -124
 -4 -10   161    155    145
  6 -10  •115    130    108
  6  -9  •120     -1     30
  6  -8  •117     99     80
  6  -7  •110     -7      9
  6  -6   214    216    212
  6  -5   295   -317   -330
  6  -4  • 68     -0    -14
  6  -3   483   -453   -487
  6  -2   266    295    303
  6  -1   432   -460   -501
  6   0   504    563    544
  6   1   150   -181   -182
  6   2   466    528    539
  6   3   187   -178   -171
  6   4   520    457    455
  6   5   221   -231   -219
 -6  -6  •119    117     99
 -6  -7   269   -255   -241
 -6  -8   142    162    150
 -6  -9   170   -158   -143
  8 -10  •113    -17    -73
  8  -9  •119    -37      2
  8  -8  •119     30    -12
  8  -7   114    -96    -69
  8  -6   169    183    155
  8  -5   158    139    166
  8  -4   379    357    354
  8  -3   135   -128   -136
  8  -2   242    255    253
  8  -1   185   -211   -232
  8   0   153    154    144
  8   1   561   -414   -446
  8   2   122    134    129
  8   3   313   -283   -285
  8   4   225    217    214
  8   5  •120   -121   -107
 -8  -6   298    250    244
 -8  -7   119   -137   -121
 -8  -8   171    156    142
 10  -9  •116     -1     59
 10  -8  •120     49    -17
 10  -7  •118    -67    -24
 10  -6  •115    -72   -143
 10  -5   184   -183   -175
 10  -4  • 87     92     42
 10  -3  • 85    -35    -26
 10  -2   163    157    141
 10  -1  •105    -59    -56
 10   0   323    321    316
 10   1  •112     -1      2
 10   2   201    195    195
 10   3   218   -178   -184
 10   4  •119    109    102
 10   5   233   -181   -180
-10  -6  •102    106     94
-10  -7   181   -145   -135
 12  -8  •116     65     -9
 12  -7  •120     74    149
 12  -6  •120    124     64
 12  -5  •118      0     57
 12  -4  •117     31    -31
 12  -3  •116    -58    -44
 12  -2  •116     55      5
 12  -1   163   -155   -163
 12   0    24    -12    -42
 12   1   123   -103   -106
 12   2   195    154    155
 12   3  •116    -49    -43
 12   4   123    122    123
 12   5  • 94    -72    -63
-12  -6   134    126    125
 14  -6  •116     22    -76
```

```
          IF0I  FC(A)  FC(D)
 14  -5  •118     14     74
 14  -4  •119     59     -2
 14  -3  •119     17     71
 14  -2  •119    114     76
 14  -1  •118     44     78
 14   0  •116     73     50
 14   1  •112    -86    -80
 14   2  •105     23      2
 16  -4  •106     -0    -95
 16  -3  •106    -48     -8
 16  -2  •105    -12    -80
 16  -1  •101    -16     15
 16   0  • 46     61     27

  H   L                K = 1
  1  -8  •169    -18    -15
  1  -7   168    193    195
  1  -6  •115    -34    -26
  1  -5  •101    -54    -45
  1  -4   591   -517   -509
  1  -3   147    130    130
  1  -2   491   -303   -296
  1   0   193   -196   -187
  1   1   997    862    845
  1   2    85     63     70
  1   3   454    571    565
  1   4   116     47     50
  1   5   134    137    132
 -1  -6   246   -237   -228
 -1  -7  •163     14     17
 -1  -8  •172    -92    -85
  3  -8  •136    -95    -92
  3  -7  •126     31     30
  3  -6  •112     71     69
  3  -5   546    473    473
  3  -4   114     86     86
  3  -3   329    224    227
  3  -2    90    -86    -97
  3  -1   959    576    566
  3   0   470   -533   -516
  3   1   153   -139   -141
  3   2   384   -450   -438
  3   3   119    140    139
  3   4   103   -132   -118
 -3  -5   251    244    241
 -3  -6  •129     13     20
 -3  -7   138    146    142
 -3  -8  •140     -8      0
  5  -7  •127    -35    -39
  5  -6   262   -268   -270
  5  -5   106    -87    -95
  5  -4   104    -90   -104
  5  -3   267    226    224
  5  -2   236   -193   -203
  5  -1   525    415    411
  5   0   290    301    286
  5   1   497    522    517
  5   2   132   -140   -138
  5   3  •129    105     98
  5   4   143   -174   -166
  5   5  •157     23     18
  5   6  •168   -181   -171
  7  -7  •131    171    164
  7  -6   121    101    112
  7  -5   118    126    123
  7  -4  •104    -75    -83
  7  -3  • 98     92     75
  7  -2   206   -187   -207
  7  -1   133   -139   -151
  7   0   362   -346   -352
  7   1   135    141    136
  7   2  •137     11     14
  7   3   157    178    177
  7   4  •160    -32    -24
  9  -6  •159    -43    -44
  9  -5  •151     57     36
  9  -4  •144     39     46
  9  -3   187    201    195
  9  -2   119    153    151
  9  -1   233    258    257
  9   0  • 48    -33    -36
  9   1  •150     -0     -8
 11  -5  •165      2    -37
 11  -4  •162   -108   -119
 11  -3  •159    -78   -113
 11  -2  •159    -96   -108
 11  -1  •161     57     37
 11   0  •164     32     31

  H   L                K = 2
  0   2   471   -384   -373
  0   3   380    383    382
  0   4   453   -464   -457
  0   5   113    157    163
  0  -6   378   -320   -315
  0  -7  •132     13     12
  0  -8  •141   -156   -149
  2  -8  •139     41     48
  2  -7   293    265    272
  2  -6   115    -95    -95
  2  -5   327    346    353
  2  -4   146   -159   -158
  2  -3   574    388    401
  2  -2   589   -945   -949
  2  -1   212    163    172
  2   0   692   -729   -716
  2   1   513    643    641
  2   2   425   -417   -405
  2   3   564    571    569
  2   4   111   -113   -101
 -2  -5   500    428    423
 -2  -6  •127    -70    -58
 -2  -7   172    195    190
 -2  -8   177   -170   -166
 -2  -9  •136     32     27
  4  -8   172   -176   -173
  4  -7  •128     57     53
  4  -6   189   -165   -165
  4  -5   146    137    143
  4  -4   170   -164   -178
  4  -3   698    732    745
  4  -2   143    114    105
  4  -1   928    641    648
  4   0   455   -479   -468
```

```
          IF0I  FC(A)  FC(D)
  4   1   436    446    448
  4   2   354   -420   -414
  4   3   105    134    125
  4   4   397   -461   -449
  4   5  •125    126    119
 -4  -6   144   -172   -156
 -4  -7   187    203    198
  6  -8  •140      4     24
  6  -7  •131    111    102
  6  -6  •120    -60    -58
  6  -5   110     90     84
  6  -4   381   -380   -393
  6  -3    80    -68    -75
  6  -2   356   -346   -374
  6  -1   394    395    400
  6   0   178   -186   -187
  6   1   428    364    368
  6   2  •106    -67    -60
  6   3   510    463    466
  6   4  •127    -92    -82
  6   5   136    150    138
  6   6   233   -216   -206
  8  -7  •136     54     29
  8  -6   128     25     46
  8  -5   235    266    254
  8  -4   109    114    124
  8  -3   225    251    253
  8  -2   114   -156   -165
  8  -1   113    120    110
  8   0   231   -218   -230
  8   1  •116     63     55
  8   2   391   -333   -345
  8   3  •132     77     71
  8   4  •139   -101    -91
  8   5   275    218    217
 10  -5  •132    -45    -92
 10  -4  •127    -83    -83
 10  -3  •125    113     85
 10  -2  •124    -15     -9
 10  -1   194    184    188
 10   0    60     23     27
 10   1   288    246    251
 10   2  •138    -35    -33
 10   3  •142     77     73
 10   4   197   -169   -173
 12  -4  •140    -28     -3
 12  -3  •139     34     -9
 12  -2  •139    -79    -86
 12  -1  •140    -23    -57
 12   0   149   -135   -142
 12   1  •142     42     31

  H   L                K = 3
  1  -8   209    225    229
  1  -7   195   -150   -143
  1  -6   320    233    241
  1  -5   338   -335   -334
  1  -4   198    158    173
  1  -3  1335  -1021  -1020
  1  -2   725    672    681
  1   0   645    760    740
  1   1  1396   -930   -916
  1   2  1838   1211   1217
  1   3  • 93    -14     -4
 -1  -4   539    474    472
 -1  -5   546   -421   -413
 -1  -6   242    235    235
 -1  -7   213   -227   -220
 -1  -8  •200     55     54
  3  -8  •196     48     41
  3  -7  •181    -83    -83
  3  -6   414    332    345
  3  -5  •144    -96   -102
  3  -4   784    656    673
  3  -3   225   -192   -197
  3  -2   552    484    508
  3  -1   733   -783   -798
  3   0   666    778    754
  3   1  1113   -826   -818
  3   2  • 93     87     86
  3   3   499   -578   -562
  3   4   625    546    545
  3   5   169   -183   -168
 -3  -6   322    249    241
 -3  -7  •198   -117   -104
 -3  -8   325    272    266
  5  -8  •196     60     53
  5  -7   240   -258   -257
  5  -6  •166     12      5
  5  -5   312   -279   -285
  5  -4   145    145    151
  5  -3   395   -367   -393
  5  -2   638    596    619
  5  -1   207   -192   -198
  5   0   689    672    685
  5   1   107   -132   -135
  5   2   494    580    585
  5   3   433   -426   -419
  5   4  •169    147    135
  5   5   243   -284   -269
 -5  -6  •197    182    170
 -5  -7   262   -280   -268
  7  -7  •188     83    115
  7  -6   175    165    154
  7  -5  •162    -85    -78
  7  -4   252    262    263
  7  -3   225   -225   -240
  7  -2  •113     36     26
  7  -1   498   -477   -505
  7   0   172    173    173
  7   1   345   -328   -338
  7   2   297    309    310
  7   3  •175   -120   -110
  7   4   309    316    317
  7   5  •198   -151   -137
  7   6   210    245    236
  9  -5  •178    -81    -60
  9  -4  •170    120    100
  9  -3  •165     53     69
  9  -2   393    386    396
  9  -1  •165    -36    -38
  9   0   170    170    170
  9   1   192   -195   -203
  9   2  •186    130    127
  9   3   218   -240   -250
  9   4  •200     91     82
```

```
          IF0I  FC(A)  FC(D)
 11  -5  •194    -38    -10
 11  -4  •190    -16    -69
 11  -3   198   -206   -206
 11  -2  •187      8    -27
 11  -1  •189    -42    -38
 11   0   165    165    155
 11   1  •197    -71    -67

  H   L                K = 4
  0   0   332    325    331
  0  -2   300    242    240
  0  -3   148   -139   -128
  0  -4   197   -147   -134
  0  -5  •104    -44    -38
  0  -6   155   -113   -110
  0  -7   162   -168   -161
  0  -8  •137    -30    -24
  2  -8   151    139    139
  2  -7   149    156    158
  2  -6  •114     39     46
  2  -5  • 82     60     63
  2  -4   212    193    193
  2  -3    63    -42    -29
  2  -2   688   -465   -442
  2  -1   429   -342   -328
  2   0    17    -21    -11
  2   1    83    -87    -70
  2   2  • 58     33     44
  2   3   142    210    210
  2   4   147    177    177
 -2  -5   147    112    118
 -2  -6   132    139    142
 -2  -7  •135     62     60
  4  -7  •126    -57    -58
  4  -6  •114      9      9
  4  -5    83    -51    -46
  4  -4  • 74     20     23
  4  -3   446    373    369
  4  -2   624    480    480
  4  -1    87     89     97
  4   0  • 58    -39    -33
  4   1    63     61     63
  4   2  • 71    -67    -62
  4   3   183   -222   -214
  4   4   117   -153   -149
  4   5  •123    -69    -65
  6  -7  •128     29     33
  6  -6  •118      3      2
  6  -5  •108    -25    -28
  6  -4   195   -176   -177
  6  -3   331   -303   -305
  6  -2    95   -103   -110
  6  -1    93    126    123
  6   0  • 74     69     73
  6   1  • 78     35     40
  6   2   174    200    204
  6   3   197    222    226
  6   4  •124     73     76
  8  -6   125     85     89
  8  -5   155    146    148
  8  -4   204    193    196
  8  -3   119    125    131
  8  -2  •105    -25    -24
  8  -1  •105    -68    -76
  8   0    24    -24    -32
  8   1   114   -103   -109
  8   2   160   -175   -180
  8   3  •129    -76    -77
 10  -5  •129    -80    -92
 10  -4  •125    -33    -47
 10  -3  •123     23     13
 10  -2  •122     70     72
 10  -1  •123     76     84
 10   0   111    100    102

  H   L                K = 5
  1  -7  •346    263    267
  1  -6   314   -215   -204
  1  -5  •277    141    147
  1  -4   619   -595   -587
  1  -3   268    247    265
  1  -2   677   -665   -648
  1   0   912   -643   -604
  1   1   753    819    824
  1   2   266   -219   -211
  1   3   782    740    728
  1   4   275   -258   -244
  1   5   309    290    284
  1   6   338   -301   -294
  3  -7  •341    127    124
  3  -6  •309    -26    -29
  3  -5   432    478    490
  3  -4  •196   -135   -139
  3  -3   508    485    494
  3  -2   489   -422   -420
  3  -1   520    566    583
  3   0   699   -684   -677
  3   1   170    202    206
  3   2   779   -735   -708
  3   3   353    351    348
  3   4   300   -268   -252
  3   5   356    338    329
  3   6  •349   -152   -137
  5  -7  •343     -4     -7
  5  -6  •315   -322   -320
  5  -5  •285     62     61
  5  -4   235   -252   -257
  5  -3   297    289    305
  5  -2   308   -310   -320
  5  -1   467    549    561
  5   0    80    -76    -73
  5   1   614    647    650
  5   2   238   -291   -286
  5   3   298    227    221
  5   4   337   -336   -318
  5   5  •348    196    184
  7  -6  •331      9     32
  7  -5  •307    149    147
  7  -4  •287   -140   -140
  7  -3  •272    174    172
  7  -2   283   -338   -347
  7  -1  •215     22     28
  7   0   424   -429   -429
  7   1   287    229    234
```

```
          IF0I  FC(A)  FC(D)
  7   2  •308   -150   -145
  7   3  •331    309    307
  9  -4  •322    -52    -29
  9  -3  •313    235    232
  9  -2  •310     52     57
  9  -1   330    280    286
  9   0   134   -138   -134
  9   1  •334    104    104

  H   K                L = 0
  0   6   857   1084   1052
  0   8    80   -155   -167
  0  10   384    385    376
  0  12   212    213    201
  0  14    37     17     -9
  0  16   229    213    214
  0  18    23    -33    -47
  0  20    42     80     70
  1   7   286    288    284
  1   9   141    143    141
  1  11   316   -293   -296
  1  13   270    255    253
  1  15    92    -80    -91
  1  17    44    -68    -75
  1  19    70    118    128
  1  21    59    -91   -108
  2   6    77     65     75
  2   8   612   -633   -607
  2  10   217    203    203
  2  12   149   -143   -143
  2  14   253   -244   -243
  2  16   185    161    172
  2  18    77   -135   -148
  2  20    11    -41    -35
  3   7    45    -39    -25
  3   9    97     88     93
  3  11   323   -302   -310
  3  13   117    101    110
  3  15   100    -99   -100
  3  17  • 56    -43    -51
  3  19    32     70     83
  3  21    51   -101   -110
  4   6   356    373    376
  4   8   383   -369   -367
  4  10   179    169    171
  4  12    14     10      8
  4  14    74   -127   -140
  4  16    70    118    126
  4  18    55    -86    -97
  4  20  • 42      3      0
  5   7   436    468    460
  5   9   233    235    228
  5  11    46    -86    -96
  5  13   345    331    330
  5  15  • 58      9     -7
  5  17    73    -10    -18
  5  19    87    152    160
  6   6   296    294    294
  6   8   208   -198   -201
  6  10   178    179    183
  6  12    36     18     14
  6  14  • 58    -65    -76
  7   7   109   -101    -96
  7   9  • 52    -11     -4
  7  11   249   -236   -245
  7  13  • 58     19     26
  7  15  • 56    -89    -91
  7  17  • 50    -59    -65
  8   6  • 49     58     55
  8   8   242   -232   -238
  8  10    98     98     99
  8  12  • 58    -33    -38
  8  14   103   -105   -114
  8  16  • 52     90     98
  8  18  • 42    -53    -62
  9   7    40     76     80
  9   9  • 56     31     31
  9  11    55   -102   -105
  9  13  • 57     97    102
  9  15  • 52    -46    -51
  9  17  • 44    -28    -32
 10   6   223    212    217
 10   8  • 57    -21    -15
 10  10    59    115    117
 10  12  • 57     59     62
 10  14  • 52      1     -0
 10  16  • 44     78     80
 11   5  • 56    -38    -32
 11   7  • 57     87     85
 11   9  • 57     72     72
 11  11  • 56    -38    -37
 11  13  • 51     85     83
 11  15  • 44      4      4
 12   4    14    -70    -77
 12   6    12    -36    -51
 12   8    71   -137   -130
 12  10  • 55     -5    -12
 12  12  • 50    -55    -59
 12  14  • 43    -73    -72
 12  16  • 31     14     11
 13   1    29    -44    -53
 13   3  • 57     43     14
 13   5  • 57    -72    -66
 13   7  • 56     -2    -16
 13   9  • 53      4     -5
 13  11  • 48    -48    -42
 13  13  • 41     22      9
 14   2  • 56    -13     -1
 14   4  • 55     15     13
 14   6  • 53     46     34
 14   8  • 50    -29    -10
 14  10  • 45     30     18
 14  12  • 38      8     10
 15   1  • 52     23     38
 15   3  • 51     58     37
 15   5  • 49     -3     27
 15   7  • 46     36     35
 15   9  • 41     25     23
 16   2  • 34     18     38
 16   4  • 44     32     31
 16   6  • 40     43     24
 17   1  • 38    -35    -32
 17   3  • 37    -10    -49
 17   5  • 34    -43    -19
 18   0  • 24      0    -46
```

TABLE 9

Atomic coordinates of β-$Cu_2P_2O_7$ (anisotropic model) (e.s.d's in parantheses)

	x/a	y/b	z/c
Cu	0	0.3122(2)	1/2
P	0.1998(4)	0	-0.0883(6)
O1	0	0	0
O2	0.3759(9)	0	0.2161(17)
O3	0.2035(10)	0.1533(7)	-0.2708(15)

Thermal coordinates ($A^2 \times 10^4$)

	U_{11}	U_{22}	U_{33}	U_{12}	U_{13}	U_{23}
Cu	188(5)	65(4)	92(6)	0	-73(4)	0
P	84(7)	92(7)	62(8)	0	18(7)	0
O1	104(35)	1197(226)	292(78)	0	126(50)	0
O2	75(15)	87(16)	71(20)	0	10(18)	0
O3	296(24)	91(12)	121(19)	45(17)	23(20)	126(36)

TABLE 10

Molecular geometry of β-$Cu_2P_2O_7$ (e.s.d's in parentheses)

Bond lengths (A)

P-O1	1.542(4)	O1-O2	2.43(3)
P-O2	1.516(15)	O1-O3	2.47(3)
P-O3	1.503(15)	O2-O3	2.49(3)
		O3-O3'	2.49(3)
Cu-O2	2.003(15)		
Cu-O3	1.937(15)		
Cu-O3'	2.577(15)		

Angles

P-O-P	180°
O1-P-O2	105.5°
O1-P- O3	108.7°
O2-P-O3	111.0°
O3-P-O3'	111.8°

TABLE 11

Comparison of disordered model of β-$Cu_2P_2O_7$ with the structure of α-$Cu_2P_2O_7$.

(a) Configurational coordinates. The coordinates of α-$Cu_2P_2O_7$ are referred to the β-$Cu_2P_2O_7$ unit cell (e.s.d's in parantheses)

		x/a	y/b	z/c	B
Cu	β	0.0162(2)	0.3122(1)	-0.0144(5)	0.40(2)
	α	0.0183(2)	0.3134(2)	-0.0138(3)	0.39(2)
P	β	0.1997(3)	0.0073(8)	-0.0886(6)	0.48(4)
	α	0.1979(4)	0.0086(4)	-0.0878(5)	0.13(3)
O1	β	0	0.0256(23)	0	1.69(24)
	α	0	0.0480(24)	0	1.19(19)
O2	β	0.3760(8)	0	0.2165(17)	-
	α	0.3768(10)	-0.0019(15)	0.2254(18)	-
O3	β	0.2043(10)	0.1544(7)	-0.2714(15)	-
	α	0.2223(11)	0.1556(12)	-0.2714(18)	-
		0.1782(15)	0.1530(14)	-0.2834(10)	-

(b) Anisotropic thermal coordinates (A^2 x 10^4)

		U_{11}	U_{22}	U_{33}	U_{12}	U_{13}	U_{23}	
O2	β	75(16)	86(17)	60(20)	0	4(18)	0	
	α	12(16)	180(47)	86(22)	-1(32)	-52(16)	41(45)	*
O_3	β	268(22)	92(12)	120(20)	47(17)	24(20)	121(36)	*
	α	84(21)	-2(29)	72(20)	-6(27)	3(18)	64(41)	*
		164(30)	41(38)	84(24)	-3(38)	-45(23)	7(46)	

* non-positive definite

CHAPTER 4: DETERMINATION OF THE CRYSTAL STRUCTURE OF α-$Zn_2P_2O_7$

(A) Preliminary Investigation

α-$Zn_2P_2O_7$ shows the c glide plane and doubled c axis with respect to the β phase which are characteristic of the other phases of the family of "small cation" pyrophosphates. It is unique however in that the length of its a axis is triple that of the corresponding β phase. Studies of the phase transformation have shown that it is probably the most complex of the series. (Chambers, Datars and Calvo, 1964).

Crystals of $Zn_2P_2O_7$ were prepared by the crystallization from the melt obtained from the decomposition of precipitated zinc ammonium phosphate. These crystals had their (110), (001) and ($10\bar{1}$) faces (based on the β unit cell) sufficiently developed to permit optical alignment. Preliminary single crystal photographs showed the extinction conditions $h + k + \ell = 2n$ and for $k = 0$, $\ell = 2n$ and thus the space group must be one of Ic or I2/c. All refinements reported here have been carried out in the noncentrosymmetric space group Ic. This non-primitive cell is chosen to preserve the same approximate unit cell axial directions as in the β phase.

Lattice parameters obtained from powder diffractometry have been reported by DeWolff (1958) for α-$Zn_2P_2O_7$ for the C centered cell. These were converted to the the body centred unit cell and used in the early stages of refinement. Since the accuracy of DeWolff's unit cell parameters was not known, they have been redetermined. The unit cell of α-$Zn_2P_2O_7$ is relatively large and it was therefore necessary to obtain well resolved powder lines if lattice parameters were to be obtained from Debye-Scherrer photographs. Some crystals were ground to a very fine powder and mixed with a solution of acetone and fingernail polish. When the mixture had partially dried it could be pulled into the shape of thin fibers. One of these fibers was used to obtain a four day Debye-Scherrer photograph. Sixteen powder lines were identified by comparing their Θ values and intensities with Θ values calculated from the lattice parameters of DeWolff and the intensities calculated from the partially resolved crystal structure. New lattice parameters were obtained from a least squares fit of the observed and calculated Θ values. The observed and calculated values of Θ and their indices are listed in Table 12. The lattice parameters obtained in this way are, $a = 20.068 \pm .015A$; $b = 8.259A \pm .006A$; $c = 9.099A \pm .008A$, and $\beta = 106.35^{\circ}$. These results differ by as much as 2% from those reported by DeWolff.

(B) Preparation of Data

A crystal of dimensions 0.13 x 0.13 x 0.35 mm^3 was used to obtain photographs of the type hk0, hk1, hk2, 0kℓ and h, k, k-h/3 with Mo Kα radiation and an integrating precession camera (Buerger, 1960). The intensities of the integrated reflections recorded in this manner were measured with a Leeds and Northrup G1 microdensitometer. Where possible, all equivalent reflections were measured and the averaged intensity used.

A second crystal of approximate dimensions 0.06 x 0.06 x 0.11 mm^3 was glued to the end of a glass fibre and used to obtain Weissenberg photographs of the type hnℓ, n = 1,2,3,4,5 with Mo Kα radiation. Because of the wide variation in the intensities of the reflections, exposures of 27 hours were normally used and an additional photograph was taken of the (010) zone for 81 hours. The intensities of these reflections were measured by visual comparison using the logarithmic method (Robertson, 1965).

All of the data were corrected for the effects of Lorentz and polarization. Also, approximate corrections were made for the effects of absorption. The absorption coefficient for Mo Kα radiation in $Zn_2P_2O_7$ is 110 cm^{-1}. In order to apply the absorption corrections, the first crystal was approximated by a sphere and the second crystal by a cylinder. No corrections were made for the effects of anomalous absorption. The standard errors of those reflections measured with the densitometer were assigned as a constant fraction of the intensity divided by the square root of the number of times it was observed. The standard errors of the reflections measured visually were also assigned as a constant fraction of the intensity except that the errors of weak or very strong reflections was made between 50% and 100% larger depending on the accuracy with which the intensity could be observed.

(C) Refinement

The unit cell of α-$Zn_2P_2O_7$ contains twelve formula units but the asymmetric unit contains three if the space group is Ic. Each of the three crystallographically independent formula units can be taken as defining one "layer" of the type described in Chapter 1(A). For convenience the three layers have been labelled successively A, B and C. Those reflections which were characteristic of the α-$Zn_2P_2O_7$ unit cell in contrast to that of β-$Zn_2P_2O_7$ were weak. This implies, as was the case in $Cu_2P_2O_7$, that the α and β phases differ by modest atomic displacements. It should be possible then to generate the structure of α-$Zn_2P_2O_7$ by making small perturbations to the structure of β-$Zn_2P_2O_7$. For the same reasons as discussed in Chapter 3, these perturbations could not easily be found by direct interpretation of the normal Patterson function.

It is to be noted that the anisotropic thermal parameters of the atoms in β-$Zn_2P_2O_7$ are qualitatively similar to those of β-$Cu_2P_2O_7$. The only notable exceptions are the U_{33} components of the O1 atom. It was then assumed that the perturbation of the α-$Zn_2P_2O_7$ structure from the high symmetry form were similar in nature to the perturbations found in α-$Cu_2P_2O_7$. It was observed of the crystal structure of α-$Cu_2P_2O_7$ and α-$Mg_2P_2O_7$ which were partially resolved when this refinement was started, that the P-O-P group bends and both the cations in the same layer are displaced so as to relieve the distortions introduced. That is, the cation that would now be nearest to the central oxygen atom is found to be moved from its β phase position such as to enlarge its Zn-O1 distance while the other cation in the layer moves so as to reduce its Zn-O1 distance. The displacement of the cations was found to be in the a,c plane and that of the central oxygen atom primarily along the b axis.

Crystallographically the cation displacements were easier to find and these were investigated first. Thus we must decide the relative sense of the displacement of the pair of Zn^{+2} ions in each layer since this determines the direction of the displacement of the central oxygen atoms in that layer. It was clear from the cationic thermal parameters in β-$Zn_2P_2O_7$ that this major displacement component should be in the a,c plane. Since the direction of the displacement from their β phase positions of the pair of cations in one layer, if assumed equal and opposite, suffices to fix the origin, there remain four possible models involving the relative sense of the displacements of the cations in the two additional layers. In order to obtain a trial structure the pair of cations in layer A was displaced in the a,c plane from colinearity with the b axis the same distance as had been found in α-$Cu_2P_2O_7$ and the remaining cations were split into half atoms and these positioned so as to generate in superposition all four models. The weight attributed to the split cations at each of these positions were varied by the method of least squares using data of the type hk0, hk1, hk2 and h0ℓ. Where this weight or multiplicity was found to increase for one of the half atoms it was taken to mean that the cation should be placed there and the conjugate split cation in the same a,c plane representing the other option for this cationic displacement should be eliminated. The positions of the cations in layer C were found in this manner. Those in layer B could not be found by this method, probably because the magnitude of their displacements was wrong.

The displacements from the β structure imposed upon the cations, and in addition the remainder of the structure, had to satisfy a constraint derived from the fact that in addition to the 0kℓ reflections with k + ℓ odd, absent due to space group requirements, almost all reflections with k odd and ℓ odd were also absent. This means that the unit cell when viewed in projection down the a axis appears to be halved in both the b and c directions. The structure in this projection,assumed closely related to that of the β phase, consists of three molecules superimposed near y = 0, z = 0; y = 0, z = 1/2; y = 1/2, z = 0 and y = 1/2, z = 1/2. Thus the results of the body centering and the c glide plane operations on one of these groups of three molecules must result, or nearly so, in groups which in projection are related by a translation of b/2. An easy way to satisfy this constraint is for two of the pyrophosphate anions to be bent equal and opposite along the b direction and the third to have its entire bending within the a,c plane in such a fashion that the projected group itself has a mirror plane. The sign of the displacement of the first two was made consistent with the displacement of the cations as indicated above. The cations in layer B were left at the positions in which they are found in β-$Zn_2P_2O_7$. The appearance of the cations when viewed down the a axis of this trial structure is shown in Figure 3.

The 0kℓ data were added to that already in use and full matrix least squares refinement was attempted. The calculations diverged; that is, the agreement factors increased rather than decreased as would be expected if the proper trial structure had been chosen. An electron density map was prepared using data from the h0ℓ zone and small corrections were estimated for the x and z atomic coordinates of most of the atoms. The agreement factors with all the data measured to this point could now be lowered by successive cycles of least squares to about 0.20.

The h k k-h/3 and h1ℓ layer lines were added and the data now numbered about 1800 reflections. Further refinement lowered the agreement index R_1 to about 0.085. However, the molecular geometry calculated with the atomic coordinates at this point was not satisfactory. In particular, the P-O bond lengths varied from 1.45 to 1.65 A. The largest e.s.d's were those associated with the y coordinates. Also the effects of pseudosymmetry probably made all the e.s.d's unrealistically small. The hnℓ data contain information about the nature of the deviations from the symmetry of the β phase and are most useful in reducing the effect of pseudosymmetry on the e.s.d's. The data of type hnℓ, n = 2,3,4,5 were measured and added to the refinement. The molecular geometry was improved but still was not completely satisfactory. The data now numbered 3740 independent reflections. The twelve Zn^{+2} and P atoms were described by anisotropic thermal parameters and the twenty-one oxygen atoms were described by individual anisotropic temperature parameters. The structure was refined through several cycles of least squares calculations and after each cycle some atoms were moved so as to improve the molecular geometry.

The structure still displayed the pseudo mirror plane in projection down the a axis but the manner in which atoms had been related by this operation in the model used to start the refinement was now completely changed. The Zn^{+2} and P atoms were still related in pairs, but the atoms contributing to these pairs were not those initially used in the trial structure. The relationship between the cations in the final structure is shown in Figure 3. The lighter oxygen atoms formed an approximate sphere of low electron density in projection down the a axis, with no obvious relation between individual pairs of atoms. Only four Zn^{+2} atoms were significantly displaced from the twofold rotation axis which passes through them in the β phase but all the $P_2O_7^{-4}$ groups were bent out of the plane of the c glide operation.

The possibility that the space group was I2/c now had to be considered. In this space group there are two sets of centers of symmetry. One set is at the origin and the positions generated from the origin by symmetry operators of the space group and the other set is displaced by $\frac{1}{4}\,\frac{1}{4}\,0$ from these. A twofold screw axis passes through the point x = 0 and z = 1/4 and a two fold rotation axis passes through the point x = 1/4 and z = 1/4. In the β phase structure, referred to the α phase cell, centers of symmetry in a z = 0 plane are related by the translation 1/12, 1/4, 0. An additional set is generated by adding z = 1/4. The central oxygen atoms of the anion lie on alternate centers which are related by the C centering of the β phase. In α-$Mg_2P_2O_7$ (Calvo, 1967d), some of the centers relating adjacent anions remain but none of those within a given anion do. In the structure of α-$Zn_2P_2O_7$ with the space group I2/c, since its centers of symmetry are not commensurate with those of β-$Zn_2P_2O_7$ some of these centers would have to relate different anions while some would lie within an anion. In fact this would mean that one-third of the anions would be constrained by symmetry to have linear P-O-P bonds. Further, one pair of cations would then lie on a twofold axis. Since this is contrary to the e.s.r. results reported by Chambers et.al. (1964), in that no principal axis is found to lie along the b axis at room temperature, this model can be rejected.

In α-$Cu_2P_2O_7$ the cations were found to be related by a center of symmetry whereas the anion possesses a twofold axis. In the analogous model for α-$Zn_2P_2O_7$ one-third of the cations pairs that lie on the same twofold axis and are mirror plane related in the β phase, would now be related by a center of symmetry and one-third of the anions would have their central oxygen atom lying on a twofold axis. The model, together with the near absences of reflections with k or ℓ odd in the (100) zone would suggest that the two remaining anions should be bent in the a,c plane. However this result is not consistent with the directions of apparent thermal motion found for the central oxygen atom in the high temperature phase, since the components U_{22} and U_{33} of the tensor $\underline{U}$ are nearly equal.

The possibility that some of the pyrophosphate groups might be disordered was also considered. This would produce an effective statistical center of symmetry. It was noted that all the terminal oxygen atoms had moved such that the four oxygen atoms surrounding one phosphorous atom retained nearly tetrahedral symmetry. This also occurred in both α-$Cu_2P_2O_7$ and α-$Mg_2P_2O_7$. If the central O1 atom were disordered then the terminal oxygen atoms would also be disordered since their positions are constrained by the efforts of each half of the $P_2O_7^{-4}$ ion to retain tetrahedral symmetry. The manner in which the structure was refined could have possibly given coordinates corresponding to only one of the two disordered positions. However, if this is the case, then the isotropic temperature factors of these disordered atoms should be large since their atomic positional coordinates only represent "half" an atom. This was not found to be true. Further, if the terminal oxygen atoms are assigned anisotropic temperature factors and refined by least squares, an ellipsoid of thermal vibration with a large principal axis should be generated. The thermal ellipsoid would encompass both "half" atoms, of the disordered atom if they are as close together as the halves of the disordered terminal oxygen atoms would be expected to be. This type of refinement was carried out but no such thermal ellipsoids were generated. It appears most unlikely then that the space group of α-$Zn_2P_2O_7$ could be I2/c.

Subsequent refinements were carried out for the trial structure in space group Ic. The weighting scheme described by Cruickshank et. al.(1961) was now adopted. Separate coefficients in the expression

$$\omega^{-1}(\underline{H}) = A + B\ |F_o(\underline{H})| + C\ |F_o(\underline{H})|^2 + D\ |F_o(\underline{H})|^3$$

were used to describe the data measured visually and that measured with the aid of the microdensitometer. These coefficients are given in Table 13. The structure was refined until the corrections calculated for the least square variables were less than the estimated standard deviations. The magnitude of the observed and calculated structure factors are given in Table 14. The final values of R_1 and R_2 defined in Chapter 1 were 0.082 and 0.098 respectively. Unobserved reflections were treated as described in Chapter 2(C). The final atomic configurational and thermal coordinates are given in Table 15. The bond length and bond angles calculated from these coordinates are given in Table 16 with the estimated errors obtained from the least squares analysis.

(D) The Correlation Problem

3740 reflections of which 1945 were recorded as observable have been used in this refinement, and the agreement factors are as low as would be expected from the accuracy with which the data was recorded. However, a number of bond lengths still do not appear satisfactory. In particular some of the phosphorus oxygen bond lengths, which should be similar since they would be chemically identical in an isolated $P_2O_7^{-4}$ ion , are widely divergent. Furthermore, the changes in the atomic positions which would be necessary to bring these bond lengths within reasonable agreement with each other are up to twice the combined e.s.d's of the atoms involved.

The relatively inferior results of this refinement may arise from the pseudosymmetry which was mentioned earlier. Each atom of the α-$Zn_2P_2O_7$ crystal structure (except the O1 atoms) is related to six other atoms in the assymetric unit by a pseudosymmetric operator which becomes a proper symmetry operator in the β phase. In particular, the three layers labelled A, B and C are all quite similar. A more quantitative understanding of this effect may be gained by the investigation of the correlation matrix defined in Appendix A. The off diagonal terms of the correlation matrix indicate the extent to which the i'th least square variables is dependent on the value of the j'th least square variable. The diagonal terms which describe the self correlation of a variable is 1.0. If the coordinates of an atom are related by pseudosymmetry to the coordinates of other atoms, their off diagonal elements may be nearly as large. In α-$Zn_2P_2O_7$, the off diagonal components of the correlation matrix showed that the position of each atom was highly correlated with the position of one other atom. Some of these non-diagonal elements were as high as 0.90. The coordinates of each atom in layer A was correlated to coordinates of the atom in the same layer to which it would be related by the symmetry operators of the β phase. The atoms in layer B were correlated to the corresponding atom in layer C. There was no apparent relation between the high correlations and the aforementioned pseudo mirror plane in projection down the a axis.

One might expect that the least squares procedure would be inapplicable to this problem. In the derivation of the normal equations of the least squares analysis, we have assumed that these correlations are zero. Scheringer (1965) has discussed the problem and proposes that in a case such as this it may be necessary to use least squares variables which are only functionally dependent on the coordinates of the atoms describing the structure and such that they are independent of each other. One reason that the present analysis has apparently converged, may be that we have applied only one half of the calculated change to the coordinates after each least square cycle. The e.s.d's obtained from an analysis such as this are not realistic and thus the discrepancies in the molecular geometry are more likely to arise from this circumstance than from a gross error in the location of individual atoms. The possibility of such a mistake was explored by calculating electron density and difference Fourier synthesis in projection down the b and c axis. No evidence was found for such a mistake. As will be discussed later, the accuracy of this structure analysis has been sufficient to determine information concerning the nature of the phase transformation in $Zn_2P_2O_7$.

It is to be noted that the occurrence of the correlation problem is not dependent on the absence of a center of symmetry in the structure since a similar effect has been found by Calvo (1967c) in α-$Co_2P_2O_7$, in which case the centric space group is unique.

TABLE 12

Observed and calculated Bragg angles used to determine the lattice parameters of α-$Zn_2P_2O_7$

h k ℓ	θ(obs)	θ(calc)
$\bar{2}$ 1 1	7.8887	7.9100
3 1 0	8.7405	8.7490
4 0 0	9.1889	9.2144
2 1 1	9.4594	9.4395
0 0 2	10.1684	10.1705
$\bar{4}$ 1 1	10.6494	10.6557
$\bar{3}$ 1 2	11.8819	11.8797
1 2 1	12.4205	12.4174
6 0 0	13.9011	13.8981
$\bar{4}$ 0 2	11.6590	11.6683
$\bar{2}$ 1 3	15.7198	15.7126
3 3 0	17.7365	17.7399
$\bar{8}$ 1 1	18.7485	18.7343
$\bar{7}$ 2 1	19.1268	19.1161
6 0 2	19.6178	19.6202
6 2 2	22.5889	22.5935

TABLE 13

Refinement data for α-$Zn_2P_2O_7$

$\mu = 110\ cm^{-1}$ Space Group Ic

Number of observed reflections	1945
Total number of reflections	3740

Weighting curve coefficients

Densitometer data	Visually measured data
A = -47.13304	A = 56.57090
B = 4.03539	B = -1.36986
C = -0.04548	C = 0.01498
D = 0.00016	D = -0.00001

R_1 (observed reflections only)	0.0750
R_1 (all reflections)	0.0816
R_2 (observed reflections only)	0.0954
R_2 (all reflections)	0.0977

Unobserved reflections whose calculated values were greater than the minimum observable value, F(min), in that area were replaced by 0.70 x F(min). Otherwise their weight was set as zero.

TABLE 14

Magnitudes of the observed and calculated structure factor for α-$Zn_2P_2O_7$. The reflections which were too weak to be observed are marked with an asterisk. The structure factors divided by ten refer to the contents of one unit cell.

			IFØI	IFCI
H	L			K = 0
4	0		594	610
6	0		1617	1609
8	0		244	155
10	0		285	345
12	0		3324	3689
14	0		1737	1673
16	0		843	843
18	0		1393	1414
20	0		365	324
22	0		420	416
24	0		294	262
26	0		471	528
28	0		417	417
30	0	•	377	179
32	0	•	393	317
34	0		670	707
36	0		975	920
38	0	•	417	251
40	0		921	961
42	0	•	402	284
44	0	•	382	99
46	0		512	510
48	0	•	321	339
48	-2	•	339	206
46	-2		893	947
44	-2	•	393	103
42	-2		674	670
40	-2		650	687
38	-2	•	416	410
36	-2	•	411	110
34	-2		845	804
32	-2	•	386	157
-30	2		1011	928
-28	2		1015	1093
26	-2	•	334	240
-24	2		457	428
22	-2	•	296	199
20	-2		1348	1330
18	-2	•	213	218
16	-2	•	198	188
14	-2		709	733
12	-2		438	370
10	-2		475	449
8	-2		1310	1246
6	-2		9104	9053
0	2		2717	2752
4	2	•	126	123
6	2		2909	3268
8	2		910	985
10	2		1115	1066
12	2		4216	4238
14	2		728	767
16	2		305	343
18	2		651	656
20	2		750	703
22	2		502	498
24	2		963	976
26	2		540	544
28	2		455	349
30	2		1440	1339
32	2	•	402	212
34	2	•	412	449
36	2	•	417	445
38	2	•	415	245
40	2		618	578
42	2	•	389	227
44	2	•	365	440
46	2		565	660
48	2	•	293	372
50	-4	•	313	96
48	-4	•	349	126
46	-4		674	648
44	-4	•	397	278
42	-4		378	372
40	-4		509	474
38	-4	•	416	76
36	-4	•	409	291
34	-4		1559	1590
32	-4	•	384	213
30	-4	•	368	248
28	-4	•	351	365
26	-4		596	638
24	-4		740	806
22	-4		1161	1168
20	-4		457	503
18	-4		664	713
16	-4	•	203	167
14	-4		1080	1235
12	-4		3369	3505
10	-4		1082	1096
8	-4		2246	2241
6	-4		3299	3102
4	-4		1007	881
2	-4		1241	1186
0	4		3117	2968
2	4		926	905
4	4		688	710
6	4		5889	6795
8	4	•	182	15
10	4		264	294
12	4		2836	2818
14	4	•	221	234
16	4		381	397
18	4		3291	2918
20	4		392	437
22	4	•	339	237
24	4		638	670
26	4		410	372
28	4	•	389	205
30	4		721	690
32	4	•	412	272
34	4	•	417	185
36	4	•	415	229
38	4		354	345
40	4		740	748
42	4		515	540
44	4	•	338	242
46	4	•	300	371
48	-6	•	351	326
46	-6	•	378	175
44	-6	•	398	176
42	-6	•	411	276
40	-6		1462	1407
38	-6		432	423
36	-6	•	410	152
34	-6		516	509
32	-6	•	386	222
30	-6		630	594
28	-6		1642	1627
26	-6		353	350
24	-6		1371	1418
22	-6		1075	1043
20	-6		765	777
18	-6		946	961
16	-6		328	405
14	-6		845	976
12	-6		1393	1465
10	-6		430	423
8	-6		1653	1506
6	-6		1571	1699
4	-6		535	584
2	-6		1324	1197
0	6		3329	3118
2	6		239	260
4	6		463	466
6	6		4267	3900
8	6	•	211	242
10	6	•	222	152
12	6		3029	3337
14	6	•	246	314
16	6		429	456
18	6		698	580
20	6		695	669
22	6	•	364	147
24	6		1690	1487
26	6		481	445
28	6		470	489
30	6	•	414	365
32	6	•	417	84
34	6	•	415	413
36	6		617	603
38	6	•	389	361
40	6	•	365	200
42	6	•	335	316
50	-8	•	314	36
48	-8		414	344
46	-8		617	668
44	-8		410	375
42	-8		500	378
40	-8		456	420
38	-8	•	416	201
36	-8	•	413	170
34	-8		1142	991
32	-8		508	490
30	-8		594	534
28	-8		1323	1209
26	-8		522	524
24	-8		695	691
22	-8		580	573
20	-8		323	308
18	-8		2191	1968
16	-8		1082	1253
14	-8		989	1110
12	-8		472	473
10	-8		563	664
8	-8		1242	1333
6	-8		491	535
4	-8		242	260
2	-8		1139	1189
0	8		2451	2505
2	8		830	841
6	8		3606	3156
8	8		886	757
10	8		319	284
12	8		977	1032
14	8	•	334	104
16	8	•	348	64
18	8		2891	2695
20	8	•	376	69
22	8		405	407
24	8		1164	1095
26	8	•	411	160
28	8	•	416	131
30	8	•	416	147
32	8	•	411	385
34	8	•	400	179
36	8	•	382	207
38	8	•	357	127
40	8	•	325	190
42	8		370	460
50	-10	•	301	312
48	-10		423	422
46	-10	•	364	224
44	-10	•	386	22
42	-10	•	403	315
40	-10		719	757
38	-10		433	426
36	-10	•	416	460
34	-10		1081	933
32	-10	•	404	368
30	-10		481	510
28	-10		1077	993
26	-10	•	371	297
24	-10		1191	1125
22	-10		1887	1761
20	-10	•	336	189
18	-10		469	478
16	-10		482	505
14	-10		825	907
12	-10		351	320
10	-10		1113	1080
8	-10		410	483
6	-10		333	346
4	-10	•	296	141
2	-10		2016	1581
0	10		2072	2175
2	10		398	395
4	10		535	580
6	10		397	364
8	10	•	335	100
10	10		690	703
12	10		3357	3296
14	10	•	369	183
16	10	•	380	83
18	10		1452	1358
20	10	•	402	89
22	10	•	410	116
24	10		705	719
26	10		457	501
28	10	•	414	144
30	10		766	746
32	10	•	389	147
34	10	•	368	173
36	10	•	341	138
38	10	•	307	315
40	10	•	266	209
50	-12	•	279	87
48	-12		598	545
46	-12		380	433
44	-12	•	371	229
42	-12	•	390	389
40	-12	•	405	106
38	-12	•	413	400
36	-12		706	739
34	-12		548	713
32	-12	•	413	218
30	-12	•	407	343
28	-12		1223	1089
26	-12	•	391	317
24	-12	•	382	42
22	-12		615	546
20	-12		471	391
18	-12	•	357	313
16	-12		1297	1209
14	-12	•	345	91
12	-12		1161	991
10	-12		370	332
8	-12		1313	1188
6	-12		601	609
4	-12		436	309
2	-12		555	519
0	12		1044	1166
2	12	•	350	120
4	12		1063	1054
6	12		2468	2166
8	12		679	617
10	12		396	361
12	12		1298	1222
14	12	•	399	332
16	12	•	407	248
18	12		740	788
20	12	•	416	41
22	12	•	416	51
24	12		1299	1311
26	12	•	404	107
28	12	•	390	185
30	12		386	399
32	12	•	347	137
34	12	•	316	299
36	12		499	534
38	12	•	232	51
46	-14	•	320	141
44	-14	•	348	244
42	-14		662	635
40	-14	•	388	413
38	-14	•	401	161
36	-14	•	410	184
34	-14		876	892
32	-14	•	417	193
30	-14		469	511
28	-14	•	413	324
26	-14	•	409	76
24	-14	•	404	150
22	-14		1601	1533
20	-14	•	392	142
18	-14		413	351
16	-14		723	742
14	-14		427	481
12	-14	•	376	233
10	-14		671	673
8	-14		483	453
6	-14		1116	1055
4	-14		674	679
2	-14		933	834
0	14		705	682
2	14	•	388	296
4	14		843	806
6	14		842	763
8	14	•	404	217
10	14		501	512
12	14	•	414	309
14	14	•	416	147
16	14		538	553
18	14		1669	1588
20	14	•	409	123
22	14	•	399	198
24	14		653	665
26	14	•	366	199
28	14	•	343	172
30	14		1071	1103
32	14	•	280	74
42	-16	•	338	343
40	-16		465	497
38	-16	•	378	233
36	-16		479	439
34	-16		492	385
32	-16	•	410	197
30	-16		535	526
28	-16		1007	1077
26	-16	•	417	275
24	-16	•	416	79
22	-16	•	414	400
20	-16	•	411	69
18	-16	•	410	239
16	-16		817	790
14	-16	•	407	240
12	-16		904	865
10	-16		810	847
8	-16	•	405	376
6	-16	•	406	121
4	-16	•	408	131
2	-16		487	460
0	16	•	411	299
2	16	•	413	277
4	16	•	415	406
6	16	•	416	296
8	16	•	417	281
10	16		686	699
12	16		884	836
14	16	•	406	302
16	16	•	399	242
18	16		597	631
20	16	•	367	241
22	16	•	353	295
24	16		948	1087
26	16	•	283	196
28	16	•	267	238
44	-18	•	259	257
42	-18		407	462
40	-18	•	317	223
38	-18	•	339	26
36	-18		574	585
34	-18		566	553
32	-18	•	385	249
30	-18	•	395	391
28	-18		466	384
26	-18	•	408	187
24	-18		503	497
22	-18		534	521
20	-18	•	415	351
18	-18	•	415	251
16	-18		1036	980
14	-18	•	417	327
12	-18	•	417	406
10	-18	•	415	269
8	-18	•	417	160
6	-18		746	631
4	-18		855	788
2	-18		456	460
0	18		387	327
2	18	•	413	162
4	18		658	664
6	18	•	401	170
8	18	•	399	32
10	18	•	390	521
12	18	•	379	292
14	18	•	365	287
16	18		502	538
18	18		751	778
20	18	•	304	250
22	18	•	275	225
38	-20	•	281	236
36	-20		342	378
34	-20	•	323	189
32	-20	•	339	84
30	-20		409	407
28	-20	•	364	313
26	-20		421	415
24	-20	•	380	305
22	-20		638	673
20	-20	•	391	127
18	-20		538	461
16	-20	•	397	231
14	-20	•	398	241
12	-20	•	399	290
10	-20		938	911
8	-20	•	397	193
6	-20		411	425
4	-20	•	392	272
2	-20	•	388	381
0	20	•	383	33
2	20	•	376	273
4	20	•	367	232
6	20	•	357	407
8	20	•	344	239
10	20		500	468
12	20		447	465
14	20	•	289	265
32	-22	•	268	155
30	-22		359	380
28	-22	•	300	204
26	-22	•	312	273
24	-22		490	574
22	-22	•	330	152
20	-22	•	336	161
18	-22	•	341	226
16	-22		568	625
14	-22	•	346	216
12	-22	•	346	105
10	-22	•	345	247
8	-22		375	324
6	-22	•	337	236
4	-22		394	392
2	-22	•	324	78
0	22		452	508
2	22		350	445
4	22		372	490
6	22	•	271	98
H	L			K = 1
3	0		1535	1371
5	0		618	600
7	0		820	823
9	0		2565	2663
11	0		301	268
13	0	•	141	80
15	0		1837	1820
17	0		256	315
19	0	•	167	146
21	0		1312	1312
23	0		603	605
25	0	•	155	167
27	0		504	453
29	0	•	392	302
31	0		524	467
33	0		515	461
35	0		474	313
37	0	•	443	117
39	0	•	442	109
40	-1	•	441	366
38	-1		481	490
36	-1	•	439	115
34	-1		519	522
32	-1		1075	1015
30	-1	•	379	80
28	-1		483	436
26	-1		1894	1539
24	-1	•	277	118
22	-1	•	260	187
20	-1		2347	2538
-18	1		311	333
16	-1		758	777
14	-1		3234	3405
-12	1		374	362
10	-1		802	798
-8	1		1591	1673
-6	1		378	335
-4	1		1488	1614
0	1	•	86	70
2	1		565	595
4	1		560	607
6	1		296	237
8	1		1212	1202
10	1		1368	1373
12	1		617	644
14	1		3214	3335
16	1		1258	1236
18	1		339	311
20	1		1662	1712
22	1		429	443
24	1		334	211
26	1		2268	2046
28	1	•	369	147
30	1	•	407	85
32	1		1160	1049
34	1	•	435	138
36	1	•	442	128
38	1		565	638
40	1	•	436	343
39	-2	•	443	141
37	-2		781	710
35	-2	•	433	306
33	-2	•	419	83
31	-2	•	403	139
-29	2	•	446	389
-27	2		863	753
25	-2		417	449
23	-2	•	325	332
-21	2		1325	1289
-19	2		395	371
17	-2	•	218	159
15	-2		1647	1552
13	-2		830	805
11	-2		1112	1118
-9	2		2406	2689
7	-2	•	139	94
5	-2	•	123	225
3	-2		1400	1312
-1	2		397	332
-1	-2		496	481
3	2		5238	5273

			IF0I	IFCI
5	2	•	141	53
7	2	•	158	79
9	2		902	831
11	2	•	190	184
13	2	•	205	176
15	2		3002	3063
17	2		493	506
19	2		290	308
21	2	•	328	78
23	2	•	349	220
25	2	•	369	333
27	2	•	388	123
29	2		464	405
31	2	•	421	49
33	2	•	434	119
35	2	•	442	297
37	2	•	443	497
40	-3	•	443	331
38	-3	•	442	291
36	-3	•	436	178
34	-3		773	681
32	-3		927	935
30	-3	•	392	66
28	-3	•	373	294
26	-3		1384	1321
24	-3	•	334	148
22	-3	•	315	278
20	-3		3238	3191
18	-3		233	199
16	-3		354	463
14	-3		2769	2908
12	-3		305	323
10	-3		1221	1304
8	-3		4181	3707
6	-3		523	496
4	-3		2201	1865
2	-3		2659	2291
0	3	•	118	121
2	3		988	982
4	3		883	778
6	3		351	328
8	3		1411	1186
10	3		1194	1162
12	3		432	457
14	3		1383	1327
16	3		569	627
18	3		375	398
20	3		2107	1688
22	3		554	469
24	3	•	369	244
26	3		2287	1851
28	3	•	405	154
30	3	•	421	114
32	3		1190	960
34	3	•	441	116
36	3	•	443	52
38	3		798	775
40	3	•	425	363
41	-4	•	441	353
39	-4	•	443	123
37	-4	•	440	159
35	-4	•	430	272
33	-4	•	416	305
31	-4		671	558
29	-4	•	363	152
27	-4		1634	1429
25	-4		760	745
23	-4	•	326	244
21	-4		445	485
19	-4		295	387
17	-4		516	559
15	-4	•	209	182
13	-4		428	452
11	-4	•	183	280
9	-4	•	172	241
7	-4	•	162	219
5	-4		598	558
3	-4		1998	1715
1	-4	•	152	103
1	4	•	157	90
3	4		350	345
5	4		223	253
7	4		192	185
9	4		3137	3104
11	4		245	318
13	4		425	447
15	4		477	405
17	4	•	314	187
19	4	•	332	119
21	4	•	351	91
23	4		500	469
25	4	•	389	306
27	4		491	430
29	4	•	421	230
31	4		446	376
33	4		454	484
35	4	•	443	194
37	4	•	438	198
40	-5	•	443	490
38	-5		454	235
36	-5	•	436	169
34	-5		572	612
32	-5		469	511
30	-5	•	393	160
28	-5		565	621
26	-5		1267	1139
24	-5	•	339	94
22	-5		610	692
20	-5		1921	2498

			IF0I	IFCI
18	-5	•	235	161
16	-5	•	222	160
14	-5		2951	2349
12	-5		253	280
10	-5		837	956
8	-5		4366	4109
6	-5		341	296
4	-5		1237	1234
2	-5		2519	1936
0	-5	•	173	97
2	5		888	924
4	5		483	489
6	5		226	249
8	5		226	266
10	5		459	426
12	5		241	303
14	5		307	350
16	5		641	697
18	5		408	435
20	5		1987	1827
22	5		563	633
24	5	•	392	218
26	5		1183	1027
28	5		459	407
30	5	•	435	168
32	5		1353	1225
34	5	•	443	78
36	5	•	438	21
38	5		573	688
40	5	•	403	134
37	-6	•	440	272
35	-6	•	432	162
33	-6		703	737
31	-6		940	818
29	-6	•	388	225
27	-6		528	556
25	-6		476	420
23	-6		384	317
21	-6		365	368
19	-6		716	789
17	-6	•	236	310
15	-6	•	225	125
13	-6		288	364
11	-6		864	847
9	-6		633	601
7	-6		338	303
5	-6		486	444
3	-6		227	185
1	-6		416	434
1	6		819	752
3	6		3154	3287
5	6		637	612/
7	6		225	191
9	6		720	738
11	6	•	242	60
13	6	•	255	91
15	6		675	673
17	6	•	345	210
19	6	•	362	125
21	6		1040	1042
23	6	•	396	248
25	6	•	412	178
27	6	•	426	269
29	6	•	437	227
31	6	•	442	207
33	6		480	531
35	6	•	437	113
37	6	•	423	105
39	6		485	486
40	-7	•	456	474
38	-7	•	456	190
36	-7	•	438	280
34	-7	•	428	432
32	-7	•	415	258
30	-7	•	400	144
28	-7		1054	947
26	-7		1563	1330
24	-7	•	329	64
22	-7		699	673
20	-7		1358	1299
18	-7	•	306	101
16	-7		473	432
14	-7		3075	3283
12	-7	•	222	158
10	-7		498	519
8	-7		3480	3700
6	-7	•	207	126
4	-7		697	685
2	-7		2037	2330
0	-7	•	210	71
2	7		886	1043
4	7		1191	1329
6	7		251	217
8	7		559	603
10	7		392	338
12	7		368	340
14	7		430	450
16	7		427	426
18	7		423	384
20	7		898	897
22	7		513	516
24	7		428	337
26	7		895	872
28	7	•	438	366
30	7	•	443	197
32	7		1088	1125
34	7	•	435	132
36	7	•	420	134
38	7		598	718

			IF0I	IFCI
40	7	•	369	30
39	-8	•	443	483
37	-8		741	706
35	-8	•	436	336
33	-8	•	425	327
31	-8	•	413	152
29	-8	•	398	135
27	-8	•	383	232
25	-8		1168	1083
23	-8	•	353	283
21	-8		456	478
19	-8	•	325	246
17	-8		651	613
15	-8	•	301	11
13	-8		554	559
11	-8	•	232	215
9	-8		1072	1211
7	-8		271	268
5	-8		844	840
3	-8		2825	2606
-1	8		378	343
1	8		250	243
3	8		441	504
5	8		323	313
7	8	•	309	164
9	8		1034	1062
11	8	•	334	227
13	8	•	348	69
15	8		1051	1167
17	8	•	378	176
19	8	•	394	145
21	8	•	408	122
23	8	•	421	408
25	8	•	433	124
27	8		919	794
29	8	•	443	153
31	8	•	441	235
33	8	•	432	390
35	8	•	416	167
37	8	•	393	327
39	8	•	363	141
40	-9	•	441	313
38	-9	•	443	231
36	-9	•	441	294
34	-9	•	434	515
32	-9	•	424	225
30	-9	•	412	242
28	-9		928	891
26	-9		548	459
24	-9	•	371	116
22	-9		831	736
20	-9		943	969
18	-9	•	286	91
16	-9		645	637
14	-9		2147	2574
12	-9	•	250	134
10	-9	•	245	260
8	-9		1769	1807
6	-9	•	240	174
4	-9		589	560
-2	9		2464	2486
0	9	•	192	161
2	9		850	842
4	9		1254	1186
6	9	•	324	60
8	9		661	630
10	9		522	507
12	9	•	361	226
14	9	•	375	162
16	9	•	388	332
18	9	•	402	236
20	9	•	415	197
22	9	•	427	403
24	9	•	436	312
26	9		923	834
28	9	•	443	317
30	9	•	439	170
32	9		801	772
34	9	•	410	280
36	9	•	386	108
38	9		629	770
40	9	•	316	112
39	-10		534	451
37	-10	•	443	110
35	-10	•	441	131
33	-10	•	434	252
31	-10		674	634
29	-10	•	413	285
27	-10	•	401	205
25	-10	•	388	129
23	-10		480	484
21	-10	•	364	128
19	-10		362	453
17	-10		392	353
15	-10		1020	1079
13	-10		335	321
11	-10		832	754
9	-10		1767	1663
7	-10		557	589
5	-10		360	334
-3	10		1236	1055
-1	10		329	261
1	10		393	353
3	10		693	645
5	10		350	438
7	10		361	368
9	10		1305	1208
11	10	•	374	386
13	10	•	386	73

			IF0I	IFCI
15	10	•	399	118
17	10	•	411	94
19	10	•	423	163
21	10		1094	1106
23	10	•	440	120
25	10	•	443	215
27	10	•	442	308
29	10	•	436	103
31	10	•	423	101
33	10	•	403	269
35	10	•	377	110
38	-11	•	442	246
36	-11	•	443	337
34	-11		628	598
32	-11	•	435	123
30	-11	•	426	235
28	-11		698	614
26	-11	•	405	107
24	-11	•	405	98
22	-11		995	906
20	-11		1081	1155
18	-11	•	364	82
16	-11		826	808
14	-11		1255	1205
12	-11	•	343	184
10	-11		457	494
8	-11		1878	2024
6	-11	•	336	86
-4	11	•	337	298
-2	11		1899	1962
0	11	•	345	170
2	11		402	393
4	11		1565	1425
6	11	•	368	57
8	11		538	578
10	11		523	583
12	11	•	399	239
14	11	•	410	167
16	11	•	421	114
18	11	•	430	267
20	11	•	438	93
22	11	•	442	160
24	11	•	443	341
26	11		661	649
28	11	•	430	370
30	11	•	415	251
32	11		516	529
34	11	•	366	305
36	11	•	332	166
38	11		604	675
37	-12		595	654
35	-12	•	443	174
33	-12	•	442	156
31	-12	•	437	118
29	-12	•	429	179
27	-12	•	421	47
25	-12		586	726
23	-12	•	402	371
21	-12		559	499
19	-12		547	573
17	-12	•	377	350
15	-12		861	861
13	-12	•	365	54
11	-12	•	361	325
9	-12		881	929
7	-12		879	872
-5	12	•	359	130
-3	12	•	361	250
-1	12	•	365	197
1	12		692	620
3	12		1217	1097
5	12	•	384	65
7	12	•	393	106
9	12	•	402	227
11	12	•	411	191
13	12	•	421	368
15	12		1389	1297
17	12	•	437	48
19	12	•	442	154
21	12	•	443	227
23	12	•	441	146
25	12	•	435	155
27	12	•	423	662
29	12	•	405	166
36	-13		478	400
34	-13	•	443	427
32	-13	•	442	109
30	-13	•	439	247
28	-13	•	434	439
26	-13	•	426	129
24	-13	•	419	272
22	-13		930	926
20	-13		515	520
18	-13	•	396	123
16	-13		771	747
14	-13		549	664
12	-13	•	382	161
10	-13		459	526
-8	13		1700	1630
-6	13	•	379	178
-4	13	•	381	151
-2	13		1632	1370
0	13	•	389	129
2	13	•	394	310
4	13		1160	1261
6	13	•	408	86
8	13		427	337
10	13		636	628
12	13	•	431	126

			IF0I	IFCI
14	13		474	510
16	13	•	441	421
18	13	•	443	223
20	13	•	442	95
22	13	•	437	176
33	-14	•	443	163
31	-14		593	464
29	-14	•	441	290
27	-14	•	437	191
25	-14	•	433	292
23	-14	•	426	239
21	-14		633	620
19	-14	•	415	82
17	-14	•	410	140
15	-14		801	784
13	-14		835	799
11	-14	•	400	86
-9	14	•	399	377
-7	14	•	393	271
-5	14	•	400	427
-3	14		486	499
-1	14	•	406	181
1	14	•	410	22
3	14		427	434
5	14	•	421	116
7	14		517	463
9	14		652	756
11	14	•	438	268
13	14	•	442	146
15	14	•	443	263
17	14	•	442	109
19	14	•	439	215
21	14		762	674
23	14	•	417	113
30	-15	•	443	307
28	-15		507	532
26	-15	•	441	154
24	-15	•	438	166
22	-15		687	687
20	-15	•	430	78
18	-15	•	426	105
16	-15		635	732
14	-15		481	546
-12	15	•	429	26
-10	15		593	616
-8	15		1143	1066
-6	15	•	417	206
-4	15		431	387
-2	15		1096	1021
0	15	•	425	48
2	15	•	429	76
4	15		1066	1085
6	15	•	437	213
8	15	•	440	287
10	15		924	871
12	15	•	443	74
14	15	•	442	414
16	15	•	438	350
18	15	•	430	221
20	15	•	419	69
29	-16	•	442	187
27	-16		598	599
25	-16	•	443	75
23	-16	•	442	123
21	-16	•	440	415
19	-16		866	936
17	-16	•	436	73
-15	16	•	434	147
-13	16	•	432	116
-11	16	•	431	242
-9	16	•	431	270
-7	16	•	432	390
-5	16	•	433	112
-3	16	•	434	269
-1	16	•	436	272
1	16		476	477
3	16	•	441	258
5	16	•	442	72
7	16	•	443	225
9	16	•	443	251
11	16	•	441	170
13	16	•	436	355
15	16		519	599
17	16	•	418	167
-18	17	•	443	198
-16	17		783	763
-14	17		564	537
-12	17	•	441	128
-10	17		594	594
-8	17		453	410
-6	17	•	441	142
-4	17		535	500
-2	17		1089	927
0	17	•	443	209
2	17	•	443	94
4	17		925	949
6	17	•	441	108
8	17	•	438	176
10	17		727	766
12	17	•	425	114
14	17	•	415	186
-21	18	•	441	208
-19	18	•	442	250
-17	18	•	443	37
-15	18	•	443	294
-13	18	•	443	442
-11	18	•	443	198
-9	18	•	443	310
-7	18	•	443	223

```
           IFOI  IFCI               IFOI  IFCI               IFOI  IFCI               IFOI  IFCI               IFOI  IFCI
 -5   18 •  443   248    -12    2   2831  2824     29   -5   1191  1093     32   -8 •  424   180     -5   11   1043  1023
 -3   18 •  442    46     10   -2    381   394     27   -5 •  371    30     30   -8 •  410   177     -3   11 •  343   178
 -1   18 •  441    54      8   -2    890   843     25   -5 •  353   281     28   -8   1028  1033     -1   11    347   272
  1   18 •  440   199     -6    2 •  186   122     23   -5   1022   964     26   -8 •  381   308      1   11   1497  1443
  3   18 •  437   550      4   -2    493   625     21   -5 •  259   156     24   -8   1510  1376      3   11 •  360   137
  5   18 •  433   229     -2    2    826   619     19   -5 •  245   294     22   -8   1195  1053      5   11    399   397
  7   18 •  427   239      0   -2   7466  7212     17   -5   2774  2858     20   -8 •  336   311      7   11    537   547
  9   18 •  419   483     -2   -2    344   358     15   -5 •  219   140     18   -8    521   569      9   11 •  366   112
 11   18 •  408   240      4    2 •  198   126     13   -5    407   398     16   -8 •  255    55     11   11    567   491
-18   19 •  434   161      6    2   4363  3833     11   -5   2607  2658     14   -8    710   753     13   11    469   438
-16   19    527   557      8    2 •  168   185      9   -5    187   179     12   -8    497   576     15   11 •  420   161
-14   19 •  438    55     10    2    343   338      7   -5    514   525     10   -8    672   718     17   11 •  430   181
-12   19 •  471    89     12    2   2223  2179      5   -5   2376  2242      8   -8    476   500     19   11    439   265
-10   19    583   598     14    2    691   731      3   -5    220   145      6   -8 •  260   239     21   11 •  445   111
 -8   19 •  434   266     16    2    512   530      1   -5   1133   980      4   -8    305   342     23   11 •  447   199
 -6   19 •  437    95     18    2   1577  1475      1    5   2245  1874      2   -8   1135  1116     25   11 •  445   257
 -4   19 •  435   420     20    2 •  323   265      3    5 •  186   131      0    8   2061  1974     38  -12 •  442   305
 -2   19    766   754     22    2 •  343    86      5    5    917   886      2    8    237   328     36  -12 •  446   306
  0   19 •  429   174     24    2    688   619      7    5    593   590      4    8    244   299     34  -12    602   735
  2   19 •  424   269     26    2    383   394      9    5    270   328      6    8    600   691     32  -12 •  444   246
  4   19    563   611     28    2 •  433   210     11    5    923   946      8    8 •  261   148     30  -12    530   643
  6   19 •  409    44     30    2    741   675     13    5    508   545     10    8    294   384     28  -12 •  430   174
  8   19 •  399    39     32    2 •  433   206     15    5 •  258   296     12    8   3160  3063     26  -12 •  421   103
 10   19    520   679     34    2 •  443   281     17    5    912   804     14    8 •  360   158     24  -12 •  411   398
-14   20 •  423   290     36    2    541   551     19    5    351   267     16    8 •  376   356     22  -12   1490  1428
-12   20 •  424   173     38    2 •  444   210     21    5    380   326     18    8 •  391   284     20  -12 •  393    94
-10   20 •  423   255     39   -3 •  447    81     23    5    903   865     20    8 •  406   171     18  -12    492   549
 -8   20 •  422    73     37   -3 •  444   359     25    5 •  405   257     22    8 •  420    56     16  -12 •  378   290
 -6   20 •  420   233     35   -3 •  435   426     27    5 •  421   158     24    8    616   710     14  -12    475   513
 -4   20 •  416   221     33   -3 •  422   149     29    5   1192  1209     26    8    441   400     12  -12 •  368   206
 -2   20 •  412   394     31   -3    417   456     31    5 •  443   171     28    8 •  446   276    -10   12    645   615
  0   20 •  406   277     29   -3    809   744     33    5 •  447   139     30    8    540   594     -8   12 •  363   188
                          27   -3 •  369   135     38   -6 •  446   116     32    8 •  440   162     -6   12    608   588
                          25   -3    652   613     36   -6 •  441    92     39   -9 •  446   234     -4   12 •  365   258
  H    L        K = 2     23   -3   1738  1552     34   -6   1002   985     37   -9    540   481     -2   12    903   921
                          21   -3 •  254   130     32   -6 •  417   335     35   -9 •  442   169      0   12   1196  1229
  0    0    442   202     19   -3 •  238   124     30   -6 •  401   171     33   -9 •  435   223      2   12    378   343
  2    0 •   97   165     17   -3   1814  1754     28   -6    440   445     31   -9    459   324      4   12    418   415
  4    0    437   454     15   -3    207   266     26   -6    495   562     29   -9 •  410   102      6   12 •  393   254
  6    0   4608  4529     13   -3    652   614     24   -6 •  334   273     27   -9 •  397    55      8   12 •  402   125
  8    0    728   729     11   -3   3107  3175     22   -6    565   668     25   -9    891   789     10   12 •  411   439
 10    0    827   825      9   -3    188   211     20   -6 •  258   247     23   -9   1330  1326     12   12   1155  1120
 12    0   1957  2052      7   -3    537   576     18   -6   1896  1839     21   -9 •  355   110     14   12 •  430   200
 14    0    507   538      5   -3   1013  1049     16   -6    486   587     19   -9    677   668     16   12 •  438   267
 16    0    210   237      3   -3    133   123     14   -6    842   902     17   -9    813   790     18   12   1435  1352
 18    0    276   145      1   -3    635   537     12   -6   1826  1913     15   -9 •  263   148     20   12 •  447   166
 20    0    786   739      1    3    175   196     10   -6    860   952     13   -9    336   450     22   12 •  446   114
 22    0    445   476      3    3    260   231      8   -6   1518  1351     11   -9   2162  2287     37  -13 •  441   125
 24    0    226   232      5    3    513   535      6   -6   1191  1091      9   -9 •  247    85     35  -13 •  446   175
 26    0    331   261      7    3    200   246      4   -6 •  191   250      7   -9    409   442     33  -13 •  447   282
 28    0    523   600      9    3 •  189   182      2   -6   1320   820      5   -9   1935  2065     31  -13    538   515
 30    0   1114  1125     11    3    204   187      0    6   1700  1669     -3    9 •  245   117     29  -13 •  441   135
 32    0 •  423   200     13    3    828   799      2    6    717   651     -1    9 •  248   156     27  -13 •  435   122
 34    0    449   386     15    3    461   483      4    6    745   720      1    9   1190  1343     25  -13    490   520
 36    0 •  445   303     17    3   3161  2346      6    6   3608  3250      3    9 •  258    78     23  -13 •  419   103
 38    0 •  447   218     19    3    766   817      8    6    307   407      5    9    495   495     21  -13 •  412    86
 39   -1 •  446   175     21    3 •  344   162     10    6 •  240   125      7    9    790   838     19  -13    576   577
 37   -1 •  446   402     23    3    847   796     12    6    856   902      9    9 •  346   251     17  -13    567   698
 35   -1    592   607     25    3 •  383   346     14    6 •  324   133     11    9 •  359   255     15  -13 •  393   127
 33   -1 •  426    53     27    3 •  401   202     16    6 •  340   121     13    9 •  373   174     13  -13    554   622
 31   -1 •  410    41     29    3   1280  1289     18    6   3274  2634     15    9 •  386   266    -11   13   1002   883
 29   -1    965   976     31    3 •  433    75     20    6 •  376   214     17    9 •  400   210     -9   13 •  384   250
 27   -1 •  374   192     33    3 •  443    82     22    6    426   381     19    9 •  414   124     -7   13    394   411
-25    1 •  309   223     35    3    603   629     24    6 •  409   162     21    9 •  426   304     -5   13   1314  1153
-23    1   2286  2081     37    3 •  445    82     26    6 •  424    67     23    9    623   671     -3   13 •  387    51
-21    1 •  295   197     40   -4    835   803     28    6 •  436   141     25    9 •  444   388     -1   13 •  391   150
 19   -1 •  292   282     38   -4 •  446   317     30    6 •  444   117     27    9 •  447   259      1   13   1212  1069
-17    1   1707  1648     36   -4 •  440   165     32    6 •  447   349     38  -10 •  446   154      3   13 •  402   255
-15    1    264   270     34   -4 •  429   355     39   -7 •  447   263     36  -10 •  446   297      5   13 •  409   234
-13    1   1230  1206     32   -4 •  414   211     37   -7 •  445   442     34  -10    630   654      7   13    969   934
-11    1   3084  3345     30   -4    565   530     35   -7 •  438   196     32  -10 •  435   303      9   13 •  424    95
  9   -1    552   586     28   -4   1096  1043     33   -7 •  427   121     30  -10    572   608     11   13 •  432   348
  7   -1   1524  1438     26   -4 •  359   342     31   -7    527   608     28  -10    814   858     13   13 •  439   298
 -5    1   1563  1659     24   -4    683   604     29   -7    397   344     26  -10 •  400   256     15   13 •  444   240
 -3    1    295   230     22   -4    263   228     27   -7 •  381   168     24  -10    686   583     17   13 •  446   125
 -1    1    804   835     20   -4    891   944     25   -7    441   445     22  -10 •  375   161     38  -14 •  428   341
  1    1    966  1002     18   -4    571   582     23   -7    726   653     20  -10 •  363   297     36  -14    609   606
  3    1 •  155    83     16   -4 •  219   193     21   -7 •  333    80     18  -10    820   891     34  -14 •  445    96
  5    1   1382  1345     14   -4    403   419     19   -7    562   562     16  -10   1106  1095     32  -14 •  447    75
  7    1   1130  1097     12   -4   2050  2051     17   -7   2624  2266     14  -10    281   291     30  -14 •  446   147
  9    1    269   285     10   -4 •  180   166     15   -7 •  239   154     12  -10    623   645     28  -14   1062   949
 11    1    957   979      8   -4   1295  1086     13   -7 •  229   353     10  -10 •  265   165     26  -14 •  440   257
 13    1 •  200   145      6   -4   4572  4509     11   -7    935  1093      8  -10    800   974     24  -14 •  434   277
 15    1    270   254      4   -4    951   964      9   -7 •  215   161     -6   10    316   338     22  -14 •  428   212
 17    1   1742  1700      2   -4    757   648      7   -7    516   503     -4   10 •  262   228     20  -14 •  423   225
 19    1    373   361      0    4   2292  2317      5   -7   2783  2766     -2   10    493   506     18  -14 •  417   144
 21    1    301   268      2    4 •  163   159      3   -7    227   237      0   10 •  194   115     16  -14    691   721
 23    1   2107  1859      4    4 •  172    78      1   -7    942   987      2   10    334   310    -14   14 •  408   223
 25    1 •  306   158      6    4   3785  2797      1    7   1016  1038      4   10    885   886    -12   14    846   731
 27    1 •  385    57      8    4    365   337      3    7 •  222    54      6   10   2575  2256    -10   14    438   431
 29    1    755   783     10    4    436   413      5    7    327   347      8   10    501   544     -8   14    797   682
 31    1 •  420   290     12    4   2675  2482      7    7    267   286     10   10 •  373   138     -6   14    489   479
 33    1 •  434    62     14    4 •  238   200      9    7 •  305   164     12   10    385   375     -4   14 •  406   160
 35    1    615   729     16    4    275   307     11    7    336   308     14   10 •  397    87     -2   14 •  409   251
 37    1    459   431     18    4 •  328   207     13    7    334   258     16   10 •  410   164      0   14   1073  1039
 39    1 •  444    53     20    4    614   544     15    7 •  350   182     18   10   1067  1067      2   14 •  418   242
 38   -2 •  446   186     22    4    366   291     17    7 •  366   128     20   10 •  433    20      4   14    571   525
 36   -2    596   659     24    4   1465  1371     19    7    415   439     22   10 •  441   154      6   14    761   677
 34   -2   1003   978     26    4    403   371     21    7 •  399   249     24   10   1224  1135      8   14    435   415
 32   -2 •  416   184     28    4    419   376     23    7   1135  1074     26   10 •  447   204     10   14    440   454
 30   -2 •  399   116     30    4    524   543     25    7 •  428   335     28   10 •  443   122     12   14    928   886
 28   -2 •  380   213     32    4 •  443    62     27    7 •  439   136     21  -11 •  383   116     14   14 •  447   252
 26   -2    711   514     34    4 •  447   364     29    7    539   596     19  -11    503   542     35  -15 •  435   273
-24    2    654   456     36    4    457   458     31    7 •  447   346     17  -11    465   590     33  -15 •  442   312
-22    2    728   677     39   -5 •  447   234     33    7 •  443   109     15  -11 •  357   174     31  -15 •  446   402
 20   -2    259   262     37   -5 •  444   223     40   -8    880   893     13  -11    350   341     29  -15 •  447    57
-18    2    413   416     35   -5 •  435   189     38   -8 •  447   362     11  -11   1825  1698     27  -15 •  446   206
-16    2    508   535     33   -5 •  422   169     36   -8 •  444   162     -9   11 •  342   121     25  -15 •  444   218
-14    2   1353  1337     31   -5    803   734     34   -8 •  436   354     -7   11 •  341   244     23  -15 •  441   213
```

		IF0I	IFCI
21	-15	• 437	279
19	-15	584	717
-17	15	491	522
-15	15	• 426	162
-13	15	512	523
-11	15	• 422	396
-9	15	• 421	190
-7	15	422	347
-5	15	933	926
-3	15	• 425	240
-1	15	• 428	150
1	15	952	935
3	15	• 436	135
5	15	• 440	194
7	15	685	708
9	15	• 446	120
11	15	• 447	102
30	-16	• 443	235
28	-16	• 446	143
26	-16	• 447	95
24	-16	• 446	324
-22	16	601	680
-20	16	• 443	286
-18	16	• 441	169
-16	16	661	643
-14	16	• 438	393
-12	16	• 436	288
-10	16	• 436	221
-8	16	• 436	197
-6	16	1167	998
-4	16	777	678
-2	16	• 440	426
0	16	• 442	227
2	16	• 444	273
4	16	539	581
6	16	447	469
8	16	• 447	127
-25	17	• 445	373
-23	17	• 446	142
-21	17	• 447	114
-19	17	459	516
-17	17	• 446	92
-15	17	• 446	42
-13	17	510	480
-11	17	• 445	225
-9	17	• 445	30
-7	17	• 445	396
-5	17	834	817
-3	17	• 446	173
-1	17	• 447	288
1	17	571	499
3	17	• 446	47
5	17	• 445	51
7	17	704	654
-20	18	• 445	121
-18	18	• 446	265
-16	18	• 446	282
-14	18	• 447	260
-12	18	603	660
-10	18	792	779
-8	18	• 447	51
-6	18	• 446	140
-4	18	• 446	66
-2	18	• 445	368
0	18	• 444	120
2	18	• 441	230
4	18	• 438	102
H	L		K = 3
1	0	• 115	140
3	0	3566	4495
5	0	725	818
7	0	624	607
9	0	3856	3716
11	0	1071	1097
13	0	535	514
15	0	3271	3223
17	0	771	750
19	0	• 169	183
21	0	897	966
23	0	415	399
25	0	642	608
27	0	• 384	319
29	0	543	523
31	0	• 420	183
33	0	• 435	227
35	0	• 445	335
37	0	1106	1189
39	0	447	405
41	0	• 437	51
43	0	• 418	349
42	-1	• 434	112
40	-1	• 446	145
38	-1	• 450	72
36	-1	• 446	89
34	-1	• 438	133
32	-1	485	445
30	-1	• 407	32
28	-1	• 369	125
26	-1	882	880
-24	1	308	134
-22	1	• 303	48
-20	1	902	823
18	-1	• 235	149
-16	1	699	674
-14	1	1443	1410
12	-1	270	349

		IF0I	IFCI
-10	1	1105	1059
-8	1	1209	1147
-6	1	215	267
-4	1	634	694
-2	1	1059	1069
0	1	225	217
-2	-1	735	762
4	1	• 196	136
6	1	267	174
8	1	705	645
10	1	542	488
12	1	• 194	97
14	1	229	269
16	1	• 228	93
18	1	• 245	227
20	1	1133	1073
22	1	• 307	175
24	1	• 307	101
26	1	604	613
28	1	• 400	183
30	1	• 417	68
32	1	• 432	253
34	1	• 444	226
36	1	• 449	24
38	1	• 448	361
40	1	• 440	215
43	-2	945	911
41	-2	• 443	520
39	-2	• 449	90
37	-2	542	598
35	-2	441	302
33	-2	428	428
31	-2	861	814
29	-2	• 395	136
-27	2	1650	1537
-25	2	727	698
23	-2	626	647
-21	2	1543	1395
19	-2	241	253
17	-2	724	691
15	-2	• 315	341
13	-2	• 193	160
11	-2	1510	1345
-9	2	3147	3490
7	-2	928	948
-5	2	698	747
-3	2	1724	2067
-1	2	376	403
-1	-2	• 126	126
3	2	7120	6226
5	2	466	440
7	2	612	558
9	2	5720	5109
11	2	• 195	220
13	2	574	506
15	2	425	352
17	2	704	687
19	2	• 260	185
21	2	934	903
23	2	708	731
25	2	403	333
27	2	398	414
29	2	• 415	201
31	2	581	652
33	2	597	681
35	2	• 449	177
37	2	• 449	344
39	2	• 441	174
42	-3	• 439	108
40	-3	• 448	282
38	-3	• 449	130
36	-3	• 444	102
34	-3	• 434	198
32	-3	• 419	255
30	-3	• 402	98
28	-3	384	379
26	-3	395	429
24	-3	• 344	170
22	-3	• 266	141
20	-3	804	868
18	-3	• 234	131
16	-3	• 219	223
14	-3	811	772
12	-3	• 188	76
10	-3	• 174	220
8	-3	1366	1210
6	-3	• 148	93
4	-3	947	862
2	-3	309	227
0	3	• 142	120
2	3	175	208
4	3	817	714
6	3	• 170	69
8	3	292	290
10	3	352	352
12	3	233	285
14	3	872	833
16	3	791	813
18	3	• 262	142
20	3	930	824
22	3	369	344
24	3	• 379	90
26	3	• 398	340
28	3	• 415	198
30	3	• 430	73
32	3	784	679
34	3	• 449	62
36	3	• 449	94
38	3	• 442	165

		IF0I	IFCI
43	-4	584	621
41	-4	• 445	170
39	-4	• 450	308
37	-4	884	849
35	-4	• 439	240
33	-4	890	863
31	-4	1009	1063
29	-4	• 393	452
27	-4	453	486
25	-4	479	457
23	-4	453	490
21	-4	1012	1024
19	-4	953	940
17	-4	825	809
15	-4	527	525
13	-4	722	691
11	-4	1908	1746
9	-4	1691	1467
7	-4	• 167	192
5	-4	880	821
3	-4	3773	3207
1	-4	733	700
1	4	1173	1122
3	4	6397	7126
5	4	441	461
7	4	• 193	175
9	4	780	699
11	4	233	248
13	4	• 235	175
15	4	2989	3085
17	4	764	756
19	4	461	418
21	4	1377	1253
23	4	• 381	143
25	4	• 399	115
27	4	• 416	145
29	4	• 431	443
31	4	• 442	214
33	4	• 449	105
35	4	• 449	190
37	4	• 442	304
42	-5	• 441	60
40	-5	• 448	142
38	-5	• 449	156
36	-5	• 444	166
34	-5	• 434	230
32	-5	• 420	225
30	-5	• 403	84
28	-5	• 386	270
26	-5	903	779
24	-5	• 333	128
22	-5	• 330	69
20	-5	628	639
18	-5	• 242	36
16	-5	• 229	129
14	-5	2076	2022
12	-5	• 205	212
10	-5	695	687
8	-5	1146	1153
6	-5	• 179	132
4	-5	417	384
2	-5	1144	999
0	5	• 161	115
2	5	868	863
4	5	1071	975
6	5	• 204	111
8	5	• 215	190
10	5	241	271
12	5	241	201
14	5	561	555
16	5	• 329	88
18	5	• 347	157
20	5	• 366	137
22	5	• 385	192
24	5	• 402	257
26	5	922	816
28	5	• 433	80
30	5	• 443	114
32	5	• 449	344
34	5	• 449	78
36	5	• 442	67
43	-6	768	832
41	-6	• 445	257
39	-6	• 449	409
37	-6	638	698
35	-6	• 441	485
33	-6	429	364
31	-6	964	955
29	-6	• 398	163
27	-6	936	882
25	-6	1309	1300
23	-6	• 346	177
21	-6	625	692
19	-6	256	364
17	-6	1086	1180
15	-6	• 232	49
13	-6	390	499
11	-6	300	324
9	-6	246	197
7	-6	281	321
5	-6	1765	1733
3	-6	5268	5078
-1	6	782	840
1	6	577	565
3	6	237	210
5	6	• 216	159
7	6	445	463
9	6	3737	4009
11	6	270	238

		IF0I	IFCI
13	6	277	373
15	6	2475	2371
17	6	• 355	55
19	6	• 372	224
21	6	770	785
23	6	491	504
25	6	433	312
27	6	587	640
29	6	• 445	218
31	6	• 449	54
33	6	• 448	455
35	6	• 440	249
42	-7	• 439	215
40	-7	• 448	134
38	-7	• 449	311
36	-7	• 446	66
34	-7	• 437	312
32	-7	• 425	159
30	-7	• 410	125
28	-7	• 395	253
26	-7	• 379	170
24	-7	• 362	69
22	-7	345	365
20	-7	780	926
18	-7	• 258	97
16	-7	• 247	132
14	-7	550	613
12	-7	• 229	149
10	-7	• 222	92
8	-7	559	575
6	-7	• 213	119
4	-7	803	697
2	-7	1032	1160
0	7	• 181	123
2	7	529	569
4	7	• 230	185
6	7	• 238	57
8	7	• 248	134
10	7	• 259	41
12	7	• 271	41
14	7	347	330
16	7	416	430
18	7	• 380	157
20	7	430	455
22	7	• 411	333
24	7	• 426	108
26	7	• 438	312
28	7	• 446	207
30	7	• 449	67
32	7	• 447	362
34	7	• 438	194
43	-8	442	347
41	-8	• 443	363
39	-8	605	635
37	-8	639	690
35	-8	• 444	40
33	-8	• 435	381
31	-8	1293	1309
29	-8	• 408	165
27	-8	• 394	252
25	-8	510	564
23	-8	490	489
21	-8	688	671
19	-8	1272	1233
17	-8	340	241
15	-8	720	691
13	-8	267	386
11	-8	1261	1318
9	-8	1377	1517
7	-8	456	501
5	-8	1085	1176
-3	8	472	497
-1	8	• 237	125
1	8	951	1028
3	8	2345	2435
5	8	583	575
7	8	604	595
9	8	2904	3050
11	8	344	290
13	8	• 358	112
15	8	1082	1081
17	8	• 389	123
19	8	• 404	176
21	8	1682	1686
23	8	• 431	145
25	8	• 441	202
27	8	• 448	125
29	8	• 449	244
31	8	• 446	179
33	8	814	726
42	-9	• 434	26
40	-9	• 445	166
38	-9	• 449	114
36	-9	• 448	151
34	-9	• 443	227
32	-9	• 434	116
30	-9	• 422	41
28	-9	• 409	328
26	-9	478	506
24	-9	• 381	82
22	-9	378	348
20	-9	627	603
18	-9	• 329	30
16	-9	340	357
14	-9	492	545
12	-9	• 257	157
10	-9	• 253	131
8	-9	1547	1645
6	-9	• 248	34

		IF0I	IFCI
-4	9	269	303
-2	9	560	630
0	9	• 193	98
2	9	273	255
4	9	766	811
6	9	• 273	70
8	9	441	475
10	9	• 358	235
12	9	• 371	194
14	9	• 385	90
16	9	• 399	17
18	9	• 412	105
20	9	• 425	119
22	9	• 436	187
24	9	• 445	197
26	9	• 447	326
28	9	• 449	210
30	9	• 443	182
41	-10	• 437	156
39	-10	• 446	190
37	-10	1200	1221
35	-10	• 448	202
33	-10	• 443	125
31	-10	• 434	367
29	-10	• 423	30
27	-10	• 411	191
25	-10	1694	1608
23	-10	• 386	247
21	-10	595	508
19	-10	757	768
17	-10	502	564
15	-10	• 344	329
13	-10	564	526
11	-10	652	646
9	-10	1385	1305
-7	10	640	552
-5	10	938	849
-3	10	996	943
-1	10	523	485
1	10	1143	1023
3	10	2019	1862
5	10	• 351	211
7	10	361	362
9	10	1139	1064
11	10	• 384	259
13	10	396	436
15	10	2049	1967
17	10	• 421	168
19	10	• 432	271
21	10	612	627
23	10	• 448	333
25	10	• 449	97
27	10	1369	1391
29	10	• 439	126
40	-11	• 438	80
38	-11	• 447	269
36	-11	• 450	142
34	-11	• 448	138
32	-11	• 443	95
30	-11	• 436	84
28	-11	• 426	247
26	-11	• 415	54
24	-11	• 404	200
22	-11	394	351
20	-11	• 384	145
18	-11	• 374	167
16	-11	• 366	213
14	-11	834	777
12	-11	• 353	145
10	-11	• 349	149
-8	11	397	414
-6	11	• 346	123
-4	11	• 348	137
-2	11	772	741
0	11	• 174	176
2	11	437	482
4	11	369	354
6	11	• 378	76
8	11	• 388	169
10	11	• 398	188
12	11	• 409	77
14	11	• 420	317
16	11	• 430	143
18	11	• 439	28
20	11	• 446	104
22	11	• 449	286
24	11	• 449	84
39	-12	• 435	301
37	-12	• 446	132
35	-12	• 449	47
33	-12	• 449	341
31	-12	1094	1055
29	-12	• 437	442
27	-12	• 430	205
25	-12	879	813
23	-12	• 412	368
21	-12	• 403	391
19	-12	738	700
17	-12	• 387	155
15	-12	1448	1561
13	-12	1028	1116
11	-12	694	676
-9	12	400	393
-7	12	• 368	187
-5	12	769	743
-3	12	• 371	77
-1	12	• 375	171
1	12	794	671
3	12	522	597

```
          IF0I  IFCI              IF0I  IFCI              IF0I  IFCI              IF0I  IFCI              IF0I  IFCI

  5  12    395   365      7  16    714   750     26  -2 •  369   203     34   4 •  447   261     17   7 •  375   386
  7  12    888   812      9  16   1300  1212    -24   2 •  447   123     36   4 •  443   156     19   7 •  391   171
  9  12   1013  1086     11  16 •  445   368    -22   2    466   397     41  -5 •  442   294     21   7    406   440
 11  12 •  421   384     28 -17 •  442    88     20  -2 •  252   267     39  -5 •  447   214     23   7   1285  1164
 13  12 •  430   297     26 -17 •  446   268     18  -2    236   206     37  -5    446   520     25   7 •  433   440
 15  12    767   870    -24  17 •  448    18     16  -2 •  220   190     35  -5 •  440   397     27   7 •  442   290
 17  12 •  445   219    -22  17 •  449   290    -14   2    483   404     33  -5 •  428   111     29   7   1227  1165
 19  12 •  449   224    -20  17 •  449   162    -12   2    839   772     31  -5    863   747     31   7 •  447   201
 21  12   1622  1626    -18  17 •  449    52    -10   2    430   453     29  -5    743   727     33   7 •  445   174
 23  12 •  446   116    -16  17 •  449   255      8  -2    175   277     27  -5 •  380   188     35   7    841   838
 36 -13 •  445    15    -14  17 •  448   143      6  -2   1903  2059     25  -5    754   669     40  -8 •  443   430
 34 -13 •  449   130    -12  17 •  448    46     -4   2 •  286   263     23  -5   1107  1198     38  -8 •  447   174
 32 -13 •  449   152    -10  17 •  448   307     -2   2    274   318     21  -5 •  325   109     36  -8 •  446    74
 30 -13 •  447   170     -8  17 •  448   290      0   2   1957  2113     19  -5    252   251     34  -8 •  446   393
 28 -13 •  442   329     -6  17 •  448   175      2   2 •  274    57     17  -5   2697  3173     32  -8 •  430   270
 26 -13 •  436    99     -4  17 •  449   101      6   2    723   697     15  -5    225   262     30  -8 •  417   190
 24 -13 •  428   167     -2  17    487   471      8   2 •  173   118     13  -5    230   354     28  -8    403   342
 22 -13 •  421   319      0  17 •  459   148     10   2    189   191     11  -5   2039  2163     26  -8 •  389   262
 20 -13 •  413   332      2  17 •  449   120     12   2    292   293      9  -5 •  208   100     24  -8    594   653
 18 -13 •  406    95      4  17 •  448   155     14   2    283   415      7  -5   1019   978     22  -8    359   271
 16 -13 •  401   350      6  17 •  446    75     16   2 •  239    83      5  -5   2804  3078     20  -8 •  345   250
 14 -13 •  396   298    -27  18    767   673     18   2    408   360      3  -5    330   305     18  -8   1128  1206
 12 -13 •  392   174    -25  18 •  439   180     20   2    340   302      1  -5   1710  1561     16  -8    430   486
-10  13 •  390   292    -23  18 •  443    30     22   2    539   446      1   5    693   601     14  -8    308   300
 -8  13    618   647    -21  18 •  445   241     24   2    732   692      3   5 •  191   192     12  -8 •  245   144
 -6  13 •  390    55    -19  18    986   902     26   2 •  391   195      5   5 •  201   134     10  -8    555   559
 -4  13 •  391   171    -17  18 •  448   251     28   2 •  409   198      7   5    230   245      8  -8    438   444
 -2  13    564   530    -15  18 •  449   246     30   2    796   738      9   5 •  224   199      6  -8    636   693
  0  13 •  399   122    -13  18    449   440     32   2 •  438   232     11   5 •  237   157      4  -8 •  281    25
  2  13 •  404    31    -11  18 •  449   354     34   2 •  446   250     13   5    763   771     -2   8    234   274
  4  13    554   525     -9  18 •  449    92     36   2 •  447   182     15   5    522   529      0   8   1121  1108
  6  13 •  418    92     -7  18 •  449   469     38   2 •  443   156     17   5   1299  1358      2   8 •  243   140
  8  13 •  425   343     -5  18 •  448   206     41  -3 •  441   256     19   5   1042   970      4   8    250   279
 10  13    523   498     -3  18    604   595     39  -3 •  447   313     21   5 •  378   235      6   8    878   999
 12  13 •  439   177     -1  18    446   516     37  -3    447   441     23   5   1211  1148      8   8 •  327   135
 14  13 •  445   143      1  18    599   604     35  -3 •  440   377     25   5    412   452     10   8    340   302
 16  13 •  446   114      3  18    441   414     33  -3 •  428    85     27   5 •  427   229     12   8   1423  1283
 18  13 •  449   119                             31  -3    499   551     29   5   1420  1336     14   8 •  369    29
 35 -14 •  443   393                             29  -3   1592  1543     31   5 •  446   270     16   8 •  384   180
 33 -14    448   499      H   L        K = 4     27  -3 •  377   112     33   5 •  447   104     18   8    788   728
 31 -14    640   722                             25  -3 •  358   273     35   5    924   988     20   8    413   229
 29 -14 •  448   168      0   0   1170  1172     23  -3   1990  1909     40  -6 •  445   176     22   8 •  426   146
 27 -14    458   472      2   0 •  131   148     21  -3 •  346   223     38  -6 •  447   131     24   8 •  437    84
 25 -14    534   548      4   0 •  134    26     19  -3 •  245    47     36  -6 •  444   178     26   8 •  444   159
 23 -14    436   386      6   0    686   643     17  -3   2590  2803     34  -6 •  436   317     28   8 •  447   157
 21 -14    467   703      8   0    162   152     15  -3    287   359     32  -6 •  423   289     30   8 •  445   315
 19 -14   1373  1335     10   0    188   192     13  -3   1223  1256     30  -6 •  408   151     32   8 •  437   230
 17 -14 •  420   213     12   0    451   436     11  -3   3982  4263     28  -6 •  392   181     34   8 •  421   183
 15 -14 •  415   281     14   0    182   143      9  -3    511   527     26  -6    430   481     36   8 •  399   180
 13 -14 •  412   212     16   0 •  225   212      7  -3   1008   940     24  -6    388   401     41  -9 •  436   408
 11 -14 •  410   367     18   0    258   254      5  -3   2244  2007     22  -6    350   284     39  -9 •  445   456
  9 -14    551   487     20   0    217   199      3  -3    268   288     20  -6 •  323   330     37  -9    472   519
  7 -14    952   869     22   0    409   328      1  -3   1900  1509     18  -6   1009  1206     35  -9 •  445   172
  5 -14    410   398     24   0    507   538      1   3   1980  1844     16  -6    323   401     33  -9 •  439   161
  3 -14 •  412   313     26   0 •  377   243      3   3 •  152    29     14  -6 •  229   177     31  -9    579   553
  1 -14 •  416    46     28   0    453   546      5   3    170   151     12  -6   1593  1773     29  -9 •  417   233
  1  14    877   875     30   0    622   608      7   3    544   536     10  -6    350   443     27  -9 •  404   312
  3  14    449   475     32   0 •  429    43      9   3    324   325      8  -6    321   381     25  -9    960   894
  5  14 •  431   210     34   0 •  441   131     11   3   1446  1304      6  -6    441   393     23  -9    706   644
  7  14    437   497     36   0    603   618     13   3    521   493      4  -6    596   599     21  -9 •  364    41
  9  14 •  442   301     38   0 •  447   184     15   3    261   333      2  -6    202   244     19  -9    733   702
 11  14 •  446    80     40   0 •  439   149     17   3   1680  1710      0   6    702   681     17  -9   1609  1635
 13  14    461   528     41  -1 •  436   312     19   3    621   518      2   6 •  206   175     15  -9 •  332   198
 15  14   1713  1702     39  -1 •  445    76     21   3    362   405      4   6 •  214   257     13  -9    348   323
 17  14 •  448   331     37  -1    485   566     23   3   1813  1669      6   6   1052  1037     11  -9   2065  1938
 34 -15 •  440    92     35  -1    924   881     25   3    402   369      8   6 •  234   171      9  -9 •  309   194
 32 -15 •  446   173     33  -1 •  432   154     27   3 •  409   107     10   6 •  246   102      7  -9 •  306   144
 30 -15 •  449   129     31  -1    465   396     29   3   1532  1487     12   6   1155  1257     -5   9   2640  2379
 28 -15 •  449   170     29  -1    835   831     31   3 •  438   252     14   6 •  332   127     -3   9 •  307   274
 26 -15 •  448    47     27  -1 •  381    73     33   3 •  445    90     16   6 •  349   227     -1   9   1057   943
 24 -15 •  446   194     25  -1    371   381     35   3    885   870     18   6   1395  1295      1   9   1860  1811
 22 -15 •  443   208    -23   1   2778  2742     37   3 •  443   286     20   6 •  384    95      3   9 •  323   116
 20 -15 •  439   122    -21   1 •  307   188     40  -4 •  445   195     22   6 •  400    47      5   9    731   648
-18  15 •  435   132    -19   1    497   490     38  -4 •  447   309     24   6    626   656      7   9    392   387
-16  15    432   349    -15   1    293   222     36  -4 •  444   182     26   6 •  430   196      9   9 •  354   144
-14  15    429   329    -13   1    631   608     34  -4 •  434   199     28   6 •  440   164     11   9    469   477
-12  15 •  427   157     11  -1   2780  2888     32  -4 •  420   203     30   6 •  446   108     13   9 •  380   344
-10  15 •  426   205     -9   1    389   348     30  -4 •  404   194     32   6 •  447   247     15   9 •  394   190
 -8  15 •  426   215      7  -1   1486  1515     28  -4 •  386   257     34   6 •  441   251     17   9 •  408    32
 -6  15 •  427   119     -5   1   1485  1554     26  -4    368   454     36   6 •  428   195     19   9    444   516
 -4  15 •  429   206     -3   1 •  219   223     24  -4 •  320    95     41  -7 •  441   274     21   9 •  432   289
 -2  15    522   542     -1   1 •  217   180     22  -4 •  330   190     39  -7 •  447   276     23   9    825   880
  0  15 •  434   185      1   1    431   483     20  -4    450   491     37  -7 •  447   473     25   9 •  446   429
  2  15 •  438   155     -3  -1    411   386     18  -4    908   905     35  -7 •  442   188     27   9 •  447   180
  4  15    480   548      5   1   1116  1152     16  -4    225   235     33  -7 •  432   287     29   9    443   450
  6  15 •  445   151      7   1   1207  1213     14  -4    607   636     31  -7    977   798     31   9 •  433   366
  8  15 •  448   128      9   1    545   573     12  -4   1890  2014     29  -7    643   651     33   9 •  415   135
 10  15 •  449   156     11   1   1591  1586     10  -4    185   310     27  -7 •  389    90     35   9   1017  1017
 12  15 •  449   117     13   1   1466  1432      8  -4    196   155     25  -7    778   709     40 -10 •  436   256
 33 -16    459   474     15   1    519   529      6  -4   2747  2873     23  -7   1515  1580     38 -10 •  446   215
 31 -16 •  442   354     17   1   2857  2945      4  -4    312   346     21  -7 •  341   186     36 -10 •  447   108
 29 -16 •  446   333     19   1    783   738      2  -4 •  158    82     19  -7    757   747     34 -10 •  445   194
 27 -16 •  449    97     21   1    333   235      0   4   1325  1185     17  -7   1971  2237     32 -10 •  439   163
 25 -16    841   860     23   1   2046  1783      2   4 •  168   134     15  -7 •  245   178     30 -10    430   504
-23  16 •  449   258     25   1 •  294   267      4   4 •  177   114     13  -7 •  235   152     28 -10 •  419   306
-21  16 •  448   356     27   1    393   305      6   4    414   377     11  -7   2720  3128     26 -10 •  407   189
-19  16 •  446   345     29   1   1652  1533      8   4    337   330      9  -7    221   273     24 -10    870   876
-17  16 •  444   217     31   1 •  427    61     10   4 •  216   148      7  -7    867   896     22 -10    483   541
-15  16 •  442   247     33   1 •  439    97     12   4    453   450      5  -7   2710  2808     20 -10 •  372   176
-13  16   1146  1014     35   1    791   833     14   4    280   375      3  -7 •  215    91     18 -10 •  280   317
-11  16 •  440   139     37   1 •  447   328     16   4    317   264     -1   7    503   473     16 -10    694   676
 -9  16    824   748     39   1 •  441   186     18   4    871   785      1   7   2128  2036     14 -10 •  343   111
 -7  16 •  440   342     40  -2 •  444   162     20   4 •  355   188      3   7 •  228   160     12 -10 •  336   347
 -5  16    783   733     38  -2 •  447    65     22   4 •  375   127      5   7   1054  1138     10 -10 •  331   126
 -3  16 •  443   113     36  -2    445   444     24   4    965   973      7   7    881   985      8 -10 •  328   224
 -1  16 •  445   109     34  -2    473   542     26   4 •  410   124      9   7    364   376     -6  10    418   399
  1  16 •  446   245     32  -2 •  422   270     28   4 •  425   186     11   7    306   410     -4  10 •  328   220
  3  16    637   720     30  -2 •  406   289     30   4 •  438   299     13   7    461   455     -2  10 •  331   204
  5  16 •  449   210     28  -2 •  388   334     32   4 •  445   211     15   7    358   307      0  10    349   336
```

```
              IFØI   IFCI
  2   10 •  342    195
  4   10    350    347
  6   10    883    754
  8   10 •  370     98
 10   10 •  381     89
 12   10    560    629
 14   10 •  405    248
 16   10 •  417    146
 18   10 •  428    103
 20   10 •  438     94
 22   10 •  444     99
 24   10 •  447    407
 26   10 •  446    130
 28   10 •  440    163
 30   10 •  427    348
 39  -11 •  439    217
 37  -11    484    450
 35  -11 •  447    227
 33  -11 •  445    358
 31  -11    594    550
 29  -11 •  432    278
 27  -11 •  422     32
 25  -11    959    983
 23  -11    934    953
 21  -11 •  391     48
 19  -11    796    786
 17  -11    736    686
 15  -11 •  365     26
 13  -11    834    858
 11  -11   2746   2236
  9  -11 •  351    295
 -7   11 •  349    141
 -5   11   2063   1915
 -3   11 •  352     40
 -1   11 •  356    268
  1   11   1712   1492
  3   11 •  368    204
  5   11    536    536
  7   11   1468   1290
  9   11 •  395    176
 11   11    547    571
 13   11 •  416    347
 15   11 •  426    356
 17   11 •  436    313
 19   11 •  443    111
 21   11 •  447    300
 23   11 •  447     51
 25   11 •  444    354
 27   11 •  435    389
 29   11    875    815
 38  -12 •  439    205
 36  -12 •  445    355
 34  -12 •  447    336
 32  -12 •  446    185
 30  -12    442    585
 28  -12    620    602
 26  -12 •  427     54
 24  -12 •  418    244
 22  -12    650    655
 20  -12 •  401     81
 18  -12 •  393    244
 16  -12 •  386    296
 14  -12 •  380    143
-12   12 •  376    302
-10   12 •  373    214
 -8   12 •  371    311
 -6   12 •  371     45
 -4   12 •  373    157
 -2   12 •  376    265
  0   12    838    748
  2   12 •  386    125
  4   12 •  393    153
  6   12    836    740
  8   12 •  409    265
 10   12 •  418     65
 12   12 •  427    320
 14   12 •  435    173
 16   12 •  442    139
 18   12 •  446    335
 24   12 •  439    319
 20   12 •  447    156
 22   12 •  445     56
 37  -13 •  438    161
 35  -13    445    471
 33  -13    447    311
 31  -13    447    535
 29  -13 •  444    142
 27  -13 •  439    342
 25  -13    496    586
 23  -13 •  426    219
 21  -13 •  419    231
 19  -13    933    905
 17  -13    919    873
 15  -13 •  400    201
 13  -13    535    542
-11   13   1272   1200
 -9   13 •  392    155
 -7   13    425    447
 -5   13   1202   1182
 -3   13 •  395    267
 -1   13 •  399    246
  1   13   1812   1739
  3   13 •  409    162
  5   13 •  416    464
  7   13    933    861
  9   13 •  430     97
 11   13 •  437    421
 13   13    480    557
 15   13 •  446    180

              IFØI   IFCI
 17   13 •  447    355
 19   13 •  446    175
 21   13 •  441    164
 34  -14 •  443    318
 32  -14 •  447    167
 30  -14 •  447    216
 28  -14 •  446    446
 26  -14 •  443    145
 24  -14 •  439    339
 22  -14 •  434    182
 20  -14 •  429    277
 18  -14 •  424    285
 16  -14 •  419    191
-14   14 •  415    359
-12   14 •  413    175
-10   14 •  411    177
 -8   14    470    422
 -6   14    858    775
 -4   14 •  413    166
 -2   14 •  416    221
  0   14   1152   1003
  2   14    436    430
  4   14 •  430     76
  6   14    526    570
  8   14 •  440    192
 10   14 •  444    128
 12   14 •  447    140
 14   14 •  447    120
 16   14 •  446     66
 18   14 •  442    284
 33  -15 •  440    338
 31  -15    445    444
 29  -15 •  447    237
 27  -15 •  447    216
 25  -15    540    571
 23  -15 •  444    134
 21  -15 •  441     61
 19  -15    776    817
-17   15    526    567
-15   15 •  432     98
-13   15    897    734
-11   15    428    383
 -9   15 •  428    227
 -7   15    593    572
 -5   15   1825   1523
 -3   15 •  431     86
 -1   15 •  434    256
  1   15    912    907
  3   15 •  440    146
  5   15 •  443     91
  7   15   1097   1106
  9   15 •  447    145
 11   15    447    477
 13   15 •  446    519
 15   15 •  441    180
 30  -16 •  441    282
 28  -16 •  445    159
 26  -16 •  447    179
 24  -16 •  447    208
-22   16 •  447    212
-20   16 •  446    305
-18   16 •  445     43
-16   16 •  443     83
-14   16 •  442    326
-12   16    595    536
 -8   16 •  440    244
 -6   16    825    705
 -4   16    442    430
 -2   16 •  443     55
  0   16 •  445    479
  2   16 •  446    320
  4   16 •  447    128
  6   16 •  447    345
  8   16 •  447     57
 10   16 •  444    130
 12   16    451    410
 29  -17 •  434    145
-27   17 •  440    256
-25   17    481    447
-23   17 •  446     30
-21   17 •  447    376
-19   17    604    615
-17   17 •  447    144
-15   17 •  447    312
-13   17    837    763
-11   17    792    687
 -9   17 •  447    178
 -7   17    447    501
 -5   17    603    700
 -3   17 •  447    299
 -1   17 •  447    426
  1   17   1042   1016
  3   17 •  446    206
  5   17 •  444    198
  7   17    920    912
  9   17 •  435    130
 11   17 •  427     53
 13   17    778    618
-20   18 •  443    243
-18   18 •  445    214
-16   18 •  446     99
-14   18 •  446    188
-12   18    446    444
-10   18 •  446    377
 -8   18 •  446     97
 -6   18 •  446    284
 -4   18 •  445    309
 -2   18 •  444    277
  0   18    442    446

              IFØI   IFCI
  2   18 •  439    131

  H    L           K = 5

  1    0    371    332
  3    0   3724   4585
  5    0    464    487
  7    0    843    827
  9    0   3318   3537
 11    0    614    625
 13    0    373    356
 15    0    194    123
 17    0    719    717
 19    0    406    375
 21    0   1442   1334
 23    0    659    574
 25    0 •  371    125
 27    0    412    405
 29    0 •  408    128
 31    0    572    658
 33    0    589    638
 35    0 •  444    287
 36   -1 •  445    197
 34   -1 •  439    236
 32   -1    609    611
 30   -1 •  412     50
 28   -1 •  395     57
-26    1    782    732
-24    1    322    298
-22    1 •  295     93
-20    1    685    681
 18   -1 •  241    219
-16    1    570    550
-14    1   2187   2212
-12    1    465    443
 10   -1 •  171    115
  8   -1    254    245
 -6    1 •  132    234
 -4    1 •  247     70
 -2    1   1577   1617
  0    1    257    300
 -2   -1    529    572
 -4   -1    360    387
  6    1 •  254     92
  8    1    855    819
 10    1    350    348
 12    1 •  200    156
 14    1   1203   1240
 16    1 •  234    104
 18    1 •  250    162
 20    1    465    420
 22    1 •  305    156
 24    1 •  293     18
 26    1   1121   1119
 28    1 •  405    371
 30    1 •  421    123
 32    1 •  435     77
 34    1 •  443    217
 37   -2    930    938
 35   -2 •  441    281
 33   -2    522    481
 31   -2    563    554
 29   -2    401    363
 27   -2 •  382    333
 25   -2    383    418
 23   -2    462    469
-21    2   1396   1406
 19   -2    299    351
-17    2    825    739
-15    2   1257   1148
 13   -2    635    656
 11   -2   1247   1245
  9   -2   2298   2233
 -7    2    560    551
 -5    2    615    634
 -3    2   3383   3620
 -1    2    356    311
  1    2    448    461
  3    2   4230   4392
  5    2 •  327    192
  7    2    294    255
  9    2   1130   1118
 11    2    638    669
 13    2    493    503
 15    2   3120   3168
 17    2    781    771
 19    2    439    472
 21    2 •  346    103
 23    2 •  366    202
 25    2    385    268
 27    2    426    439
 29    2    481    561
 31    2 •  434    149
 33    2 •  442    302
 36   -3 •  443     67
 34   -3    448    406
 32   -3    435    536
 30   -3 •  408    117
 28   -3 •  390    169
 26   -3 •  372    112
 24   -3 •  300    130
 22   -3 •  332    223
 20   -3   1781   1905
 18   -3 •  240    219
 16   -3 •  224    190
 14   -3    209    300
 12   -3    199    200
 10   -3    332    294

              IFØI   IFCI
  8   -3   1651   1719
  6   -3 •  152     93
  4   -3   1086   1004
  2   -3    548    506
  0    3    237    239
  2    3    502    442
  4    3    161    222
  6    3 •  175    216
  8    3    608    619
 10    3    205    219
 12    3    220    346
 14    3    578    592
 16    3    470    509
 18    3 •  327    200
 20    3    900    759
 22    3 •  367    193
 24    3 •  385    241
 26    3    574    519
 28    3 •  420    412
 30    3 •  433    236
 32    3    596    591
 34    3 •  445    202
 37   -4    538    559
 35   -4 •  440    170
 33   -4    430    301
 31   -4    821    802
 29   -4 •  399    211
 27   -4   1302   1371
 25   -4    891    849
 23   -4    344    339
 21   -4 •  325    203
 19   -4 •  250    159
 17   -4    800    863
 15   -4 •  221    209
 13   -4 •  207    137
 11   -4    657    752
  9   -4   1739   1740
  7   -4    762    778
  5   -4   1327   1307
  3   -4   2950   3261
  1   -4    841    794
  1    4    384    378
  3    4   1819   1836
  5    4 •  186    159
  7    4 •  199     54
  9    4   4626   4854
 11    4 •  226    123
 13    4    528    542
 15    4   1421   1452
 17    4 •  331    153
 19    4 •  350    259
 21    4    690    565
 23    4    583    605
 25    4    405    359
 27    4    482    461
 29    4 •  434    106
 31    4 •  442    262
 36   -5 •  443    233
 34   -5 •  436    236
 32   -5 •  424    107
 30   -5 •  409    111
 28   -5 •  392    257
 26   -5    973    985
 24   -5 •  357    287
 22   -5    357    340
 20   -5    643    696
 18   -5 •  248     34
 16   -5    316    362
 14   -5   1166   1230
 12   -5    210    231
 10   -5    754    711
  8   -5   2036   2028
  6   -5 •  184    165
  4   -5    196    291
  2   -5    491    478
  0    5 •  178    108
  2    5    416    410
  4    5   1163   1099
  6    5 •  209    172
  8    5    526    566
 10    5    267    268
 12    5 •  247     74
 14    5 •  319    238
 16    5    407    380
 18    5 •  355    152
 20    5    779    711
 22    5 •  391    298
 24    5 •  407    223
 26    5    791    684
 28    5 •  435    140
 30    5 •  443     29
 37   -6    880    779
 35   -6 •  441    212
 33   -6    901    854
 31   -6   1088   1168
 29   -6 •  404    198
 27   -6 •  388    135
 25   -6    500    474
 23   -6    405    408
 21   -6    713    816
 19   -6    891   1017
 17   -6    395    410
 15   -6    244    302
 13   -6 •  227    106
 11   -6   1344   1420
  9   -6    883    797
  7   -6    221    294
  5   -6    891    854
  3   -6    471    455

              IFØI   IFCI
  1   -6    257    289
  1    6    970    925
  3    6   3945   4304
  5    6    461    452
  7    6 •  232    237
  9    6   1777   1879
 11    6 •  255    103
 13    6 •  328    148
 15    6   1464   1425
 17    6    415    495
 19    6 •  379    297
 21    6   1507   1416
 23    6 •  411    229
 25    6 •  426    204
 27    6 •  437     96
 29    6 •  444    321
 36   -7 •  444     71
 34   -7 •  439     30
 32   -7 •  429    192
 30   -7 •  415    246
 28   -7    400    428
 26   -7 •  385    234
 24   -7 •  369    122
 22   -7    363    365
 20   -7    508    505
 18   -7 •  323    139
 16   -7 •  309    141
 14   -7    974   1172
 12   -7 •  235    252
 10   -7 •  227     73
  8   -7    543    593
  6   -7 •  219    133
  4   -7 •  218    215
  2   -7   1151   1163
  0    7 •  187     65
  2    7 •  228    253
  4    7 •  235    308
  6    7 •  244    125
  8    7 •  254    282
 10    7    523    510
 12    7 •  339     48
 14    7 •  355    189
 16    7    381    385
 18    7 •  386    252
 20    7    838    886
 22    7 •  416    299
 24    7 •  430     72
 26    7 •  439     83
 28    7 •  444    124
 37   -8    930    876
 35   -8 •  443    272
 33   -8 •  436    224
 31   -8 •  426    392
 29   -8 •  413     74
 27   -8 •  400    375
 25   -8   1467   1322
 23   -8 •  371    176
 21   -8    631    625
 19   -8    371    353
 17   -8    854    870
 15   -8 •  318    341
 13   -8    273    326
 11   -8    411    446
  7   -8 •  237     86
  5   -8   1112   1183
 -3    8   2536   2702
 -1    8    769    848
  1    8    742    779
  3    8   1056   1070
  5    8    272    344
  7    8    281    326
  9    8   1690   1789
 11    8 •  351    125
 13    8 •  366    170
 15    8   2245   2114
 17    8 •  395    177
 19    8 •  409    286
 21    8    983    841
 23    8 •  434    231
 25    8 •  442    329
 27    8   1363   1013
 36   -9 •  445    225
 34   -9 •  443    212
 32   -9 •  436    173
 30   -9 •  426     81
 28   -9    501    570
 26   -9    792    678
 24   -9 •  388    200
 22   -9 •  375     91
 20   -9 •  362    311
 18   -9    350    255
 16   -9    483    501
 14   -9   1186   1140
 12   -9 •  327    248
 10   -9 •  259    224
  8   -9    917   1027
  6   -9 •  254     69
 -4    9 •  254    294
 -2    9    738    717
  0    9 •  189    217
  2    9 •  265    283
  4    9    875    959
  6    9 •  342    107
  8    9    427    479
 10    9 •  365    233
 12    9 •  378    281
 14    9    910    856
 16    9 •  404    229
 18    9 •  417     76
```

```
               IFØI   IFCI
  20    9 •  429    243
  22    9 •  438    163
  24    9 •  444    268
  26    9    601    565
  35  -10 •  445     63
  33  -10 •  443    122
  31  -10   1133   1202
  29  -10 •  427    270
  27  -10 •  416    293
  25  -10    756    717
  23  -10 •  393    379
  21  -10    487    480
  19  -10    910    921
  17  -10 •  360     93
  15  -10   1199   1313
  13  -10    800    807
  11  -10    877    902
   9  -10    967    931
   7  -10    332    348
  -5   10    960    861
  -3   10    382    389
  -1   10 •  338    191
   1   10    843    716
   3   10   1014    972
   5   10    359    334
   7   10    858    761
   9   10   1900   1812
  11   10 •  391    289
  13   10 •  402    176
  15   10   1267   1140
  17   10 •  425    147
  19   10 •  435    144
  21   10   1428   1576
  23   10 •  445     92
  34  -11 •  445    353
  32  -11 •  443    268
  30  -11 •  437     58
  28  -11 •  430     53
  26  -11 •  420    246
  24  -11 •  410    304
  22  -11    434    359
  20  -11    390    392
  18  -11 •  381     61
  16  -11 •  373    260
  14  -11    763    736
  12  -11 •  361    130
  10  -11 •  356    328
   8  -11 •  355    373
  -6   11 •  354    130
  -4   11 •  355    307
  -2   11   1290   1168
   0   11 •  364    226
   2   11    369    408
   4   11    376    309
   6   11 •  385     32
   8   11 •  394    266
  10   11 •  404    395
  12   11 •  414    235
  14   11 •  424    270
  16   11 •  433    273
  18   11 •  440     93
  33  -12 •  445    237
  31  -12    444    409
  29  -12 •  439     67
  25  -12    841    840
  23  -12 •  417    323
  21  -12    685    624
  19  -12    984    967
  17  -12    393    364
  15  -12 •  387    330
  13  -12 •  382    163
  11  -12    410    437
  -9   12    976   1006
  -7   12    664    609
  -5   12    507    480
  -3   12 •  378    309
  -1   12    392    346
   1   12    951    937
   3   12    966    953
   5   12 •  400    368
   7   12 •  408    356
   9   12    780    704
  11   12 •  425    187
  13   12 •  433    407
  15   12   1675   1682
  17   12 •  444    256
  32  -13 •  445     59
  30  -13 •  445    219
  28  -13 •  442    122
  26  -13 •  437    152
  24  -13 •  431     71
  22  -13    514    578
  20  -13    826    794
  18  -13 •  412    101
  16  -13 •  406    368
  14  -13 •  402    453
  12  -13 •  398     77
 -10   13    454    413
  -8   13   1349   1235
  -6   13 •  396    154
  -4   13 •  397    191
  -2   13 •  400    261
   0   13 •  407     97

               IFØI   IFCI
   2   13 •  410    328
   4   13    503    540
   6   13 •  422    271
   8   13 •  429    151
  10   13    435    438
  12   13 •  440    116
  14   13 •  444    220
  31  -14    747    659
  29  -14 •  445    348
  27  -14 •  444    214
  25  -14    873    824
  23  -14 •  438    180
  21  -14    445    426
  19  -14    465    506
  17  -14 •  424    158
  15  -14    926    916
 -13   14   1208   1082
 -11   14 •  415    216
  -9   14    474    501
  -7   14 •  414    186
  -5   14    820    784
  -3   14 •  417     63
  -1   14 •  420    160
   1   14    425    411
   3   14 •  429    173
   5   14 •  434    237
   7   14    820    766
   9   14   1087   1080
  11   14 •  444    324
  24  -15 •  444    328
  22  -15 •  442    191
  20  -15 •  440    380
  18  -15 •  437    221
 -16   15    435    349
 -14   15    583    575
 -12   15 •  430    159
 -10   15 •  430     83
  -8   15 •  430    360
  -6   15 •  430     89
  -4   15 •  432    407
  -2   15 •  434    390
   0   15 •  429    242
   2   15 •  439    146
   4   15    741    710
   6   15 •  444    129
  21  -16 •  445    410
 -19   16   1220   1037
 -17   16 •  443    170
 -15   16 •  442    219
 -13   16 •  441    295
 -11   16 •  441    328
  -9   16 •  441    247
  -7   16    533    482
  -5   16 •  442    122
  -3   16    443    487
  -1   16 •  444    295
   1   16    634    646
   3   16 •  445    295

   H    K            L = 0

   0    6   4777   6089
   2    6    314    297
   4    6 •  155     29
   6    6    489    478
   8    6 •  158    147
  10    6    207    229
  12    6   1646   1613
  14    6   1075   1066
  16    6    290    290
  18    6    584    524
  20    6    182    186
  22    6    280    306
   1    7 •  161     46
   3    7   1336   1273
   5    7    217    206
   7    7    202    189
   9    7    410    354
  11    7    504    486
  13    7    575    594
  15    7   1523   1526
  17    7    392    404
  19    7    218    287
  21    7    939   1013
   0    8   1557   1581
   2    8    305    280
   4    8    400    351
   6    8   3503   3836
   8    8    775    765
  10    8    445    413
  12    8   1882   1948
  14    8    335    360
  16    8    251    251
  18    8    361    377
   1    9    237    203
   3    9   1047    961
   5    9 •  165    174
   7    9 •  164    146
   9    9    593    539
  11    9    357    299
  13    9 •  151     95
  15    9   1145   1190

               IFØI   IFCI
   0   10   2025   1941
   2   10 •  159    140
   4   10    244    292
   6   10   1336   1284
   8   10    200    192
  10   10    665    659
  12   10    529    499
   1   11 •  135    164
   3   11   2078   2177
   5   11    447    486
   7   11 •  112    116

   H    K            L = 1

 -25    6 •  276    106
 -23    6    541    559
 -21    6 •  305    128
 -19    6 •  303    180
 -17    6   2133   2351
 -15    6    338    402
 -13    6   1104   1119
 -11    6   1398   1475
  -9    6    389    450
  -7    6    442    472
  -5    6    310    286
  -3    6    219    289
  -1    6   1073   1106
   1    6    721    715
   3    6 •  268    196
   5    6 •  271     67
   7    6   1146   1095
   9    6    279    209
  11    6   1819   1792
  13    6    471    423
  15    6 •  297     87
  17    6    691    625
  19    6    552    568
  21    6 •  302    292
  23    6   1474   1567
 -24    7 •  263     83
 -22    7 •  292    243
 -20    7   2150   2217
 -18    7    391    347
 -16    7    490    320
 -14    7   1443   1500
 -12    7 •  295     62
 -10    7    647    657
  -8    7   2259   2381
  -4    7   1340   1397
  -2    7 •  284    153
   0    7    284    316
   2    7   1138   1117
   4    7    330    285
   6    7 •  288    183
   8    7    335    349
  10    7    378    359
  12    7    614    636
  14    7   2103   2194
  16    7    949    932
  18    7 •  303    261
  20    7   1319   1347
  22    7 •  279    129
 -23    8 •  239    110
 -21    8 •  281    205
 -19    8    434    482
 -17    8 •  302    107
 -15    8 •  303    105
 -13    8 •  303    204
 -11    8    623    604
  -9    8    346    243
  -7    8    726    720
  -5    8    453    452
  -3    8 •  297    167
  -1    8    244    148
   1    8    931    904
   3    8 •  298    143
   5    8    684    657
   7    8    544    533
   9    8 •  301    132
  11    8    389    371
  13    8    814    727
  15    8    248    261
  17    8    486    387
  19    8 •  289    105
  21    8 •  262    292
  23    8    497    690
 -20    9   1029   1079
 -18    9 •  284    198
 -16    9    655    667
 -14    9   1684   1760
 -12    9    350    432
 -10    9    905    876
  -8    9    720    685
  -6    9 •  305    128
  -4    9 •  305    213
  -2    9    781    773
   0    9 •  188    169
   2    9    699    632
   4    9    631    655
   6    9    305    270
   8    9   1407   1350
  10    9   1139   1166

               IFØI   IFCI
  12    9 •  302     75
  14    9    541    586
  16    9    237    249
  18    9 •  272    329
  20    9   1832   1918
 -17   10    845    895
 -15   10    280    204
 -13   10 •  291     54
 -11   10   1088   1108
  -9   10    301    256
  -7   10    738    756
  -5   10   1089   1063
  -3   10 •  306    157
  -1   10    394    325
   1   10 •  306    207
   3   10 •  306    125
   5   10 •  304    310
   7   10 •  302    302
   9   10 •  299    181
  11   10    694    622
  13   10    611    610
  15   10 •  269    215
  17   10   1572   1569
 -12   11 •  266    103
 -10   11    598    612
  -8   11   1122   1042
  -6   11    336    258
  -4   11    735    790
  -2   11    588    614
   0   11 •  151     14
   2   11 •  295    212
   4   11 •  293    244
   6   11 •  289    130
   8   11    326    336
  10   11    350    151

   H    K            L = 2

 -24    6 •  447    140
 -22    6 •  451    158
 -20    6    815    774
 -18    6 •  443    377
 -16    6 •  435     86
 -14    6 •  425    281
 -12    6 •  414    359
 -10    6 •  403    151
  -8    6    778    677
  -6    6   4118   4640
  -4    6    736    630
  -2    6    624    568
   0    6   1710   1857
   2    6 •  356    216
   4    6 •  358     78
   6    6   2152   2416
   8    6    427    417
  10    6 •  381    317
  12    6   2363   2499
  14    6 •  409    185
  16    6 •  423    107
  18    6    505    580
  20    6 •  450    360
  22    6 •  455    274
  24    6    891    870
 -21    7    821    776
 -19    7 •  453    366
 -17    7    634    604
 -15    7 •  445    207
 -13    7 •  438    157
 -11    7 •  430    135
  -9    7    485    452
  -7    7    475    433
  -5    7    569    653
  -3    7   2055   2197
  -1    7    451    519
   1    7 •  388     56
   3    7 •  387    147
   5    7 •  389     62
   7    7 •  393    188
   9    7   2377   2731
  11    7 •  409    272
  13    7 •  420    331
  15    7    526    550
  17    7 •  443     78
  19    7 •  452    214
  21    7 •  454    470
  23    7 •  443    401
 -20    8 •  450    224
 -18    8 •  454    263
 -16    8 •  455    287
 -14    8    900    947
 -12    8   1816   1783
 -10    8    510    556
  -8    8    664    649
  -6    8    655    622
  -4    8 •  424    291
  -2    8 •  419    279
   0    8   3635   3803
   2    8 •  413     95
   4    8 •  413    128
   6    8   2664   2935
   8    8 •  419    114
  10    8    599    573

               IFØI   IFCI
  12    8   1403   1428
  14    8    801    703
  16    8    517    404
  18    8   1041    998
  20    8 •  450    449
 -19    9 •  442     92
 -17    9 •  452    287
 -15    9 •  456    132
 -13    9 •  457    337
 -11    9 •  455    272
  -9    9   1101   1141
  -7    9 •  448    146
  -5    9    626    505
  -3    9    670    732
  -1    9 •  436    130
   1    9 •  434    149
   3    9   1359   1370
   5    9    500    348
   7    9 •  435    167
   9    9   1589   1649
  11    9 •  443    167
  13    9 •  448    222
 -16   10 •  442    275
 -14   10 •  451    340
 -12   10 •  455    442
 -10   10 •  457    300
  -8   10    643    683
  -6   10   1805   1930
  -4   10 •  453    409
  -2   10 •  450    371
   0   10    892    920
   2   10 •  447     99
   4   10 •  446    227
   6   10   1772   1797
   8   10 •  447    352
  10   10 •  449    194
  12   10   1094   1031
 -15   11    484    594
 -13   11 •  435    299
 -11   11    513    526
  -9   11   1154   1110
  -7   11    736    488
  -5   11 •  453     63
  -3   11   2043   2149
  -1   11 •  452    227
   1   11 •  451    246
   3   11   1748   1743
   5   11 •  449    104
 -12   12 •  400    160
 -10   12    481    445
  -8   12 •  427     90
  -6   12    501    619
  -4   12 •  438    103
  -2   12 •  439    256
   0   12 •  439    300

   K    L            H = 0

   7    3 •  185    235
   9    3 •  187     84
  11    3 •  131    110
   6    4   1554   1538
   8    4   2777   2813
  10    4   1977   1876
   7    5 •  189    104
   9    5 •  179    175
   6    6   1927   1861
   8    6   1742   1740
  10    6   1283   1305
   7    7 •  330    141
   9    7 •  148    108
   6    8   1410   1339
   8    8   1229   1189
   7    9 •  160    121
   6   10   1277   1385

   H    K      L = K-H/3

  12   -6 •  258    228
   6   -7 •  290    152
   9   -6 •  316    215
   6   -6    371    275
   9   -5   1073   1029
   3   -7   1201   1124
   3   -6 •  339    149
   9    6 •  336    250
  12    7 •  338    235
  15    8 •  246    333
   6    6   2827   3096
   9    7 •  336     40
  12    8   1979   2190
   3    6 •  338    153
   6    7 •  335    252
   9    8 •  299    135
   3    7 •  331    183
   6    8   2007   2137
   3    8    291    171
```

TABLE 15

Atomic coordinates of α-$Zn_2P_2O_7$ (e.s.d's in parentheses)

(a) Layer A

Configurated coordinates

	x/a	y/b	z/c	B
Zn(I)	-0.0130(1)	-0.3122(5)	0.0232(2)	-
Zn(II)	0.0130	0.3117(6)	-0.0232	-
P(I)	-0.0661(2)	0.0153(12)	0.2940(6)	-
P(II)	0.0660(4)	0.0256(14)	0.2026(9)	-
O1	0.0010(12)	0.0874(15)	0.2437(27)	0.81(14)
O2(I)	-0.1242(10)	-0.0003(36)	0.1405(26)	1.08(29)
O2(II)	0.1233(7)	0.0103(30)	0.3537(18)	0.26(17)
O3(CI)	-0.0827(10)	0.1655(31)	0.3869(22)	1.13(27)
O3(CII)	0.0836(6)	0.1512(24)	0.1024(13)	-0.01(11)*
O3(TI)	-0.0461(6)	-0.1375(22)	0.3760(13)	0.35(13)
O3(TII)	0.0577(7)	-0.1416(24)	0.1152(15)	0.71(17)

Anisotropic thermal coordinates (A^2 x 10^4)

	U_{11}	U_{22}	U_{33}	U_{12}	U_{13}	U_{23}	
Zn(I)	124(10)	1(20)	24(8)	-28(13)	6(7)	-34(14)	*
Zn(II)	22(7)	130(28)	98(12)	26(12)	-10(7)	46(16)	
P(I)	-17(10)	8(34)	-11(13)	-2(21)	-10(10)	-18(25)	*
P(II)	154(23)	36(44)	78(24)	-34(31)	-8(20)	-23(36)	

TABLE 15 (continued)

(b) Layer B

Configurational coordinates

	x/a	y/b	z/c	B	
Zn(I)	0.1641(2)	0.1838(5)	0.0008(4)	-	
Zn(II)	0.1829(2)	0.8112(5)	-0.0251(5)	-	
P(I)	0.1016(3)	0.5075(12)	0.2824(7)	-	
P(II)	0.2400(3)	0.5203(12)	0.2000(7)	-	
O1	0.1648(6)	0.5607(24)	0.2134(13)	0.05(12)	
O2(I)	0.0399(8)	0.4969(33)	0.1414(19)	0.21(18)	
O2(II)	0.2935(5)	0.5094(23)	0.3570(10)	-0.04(10)	*
O3(CI)	0.0969(7)	0.6509(29)	0.3852(17)	0.31(17)	
O3(CII)	0.2530(11)	0.6575(42)	0.1055(26)	1.35(32)	
O3(TI)	0.1197(8)	0.3535(29)	0.3696(17)	0.50(19)	
O3(TII)	0.2372(11)	0.3627(35)	0.1153(26)	1.01(29)	

Anisotropic thermal coordinates ($A^2 \times 10^4$)

	U_{11}	U_{22}	U_{33}	U_{12}	U_{13}	U_{23}	
Zn(I)	101(10)	25(21)	41(11)	6(14)	-20(8)	-31(15)	
Zn(II)	47(9)	70(21)	75(12)	-34(12)	5(9)	-13(15)	
P(I)	96(17)	-32(35)	29(19)	-31(26)	34(15)	-126(25)	*
P(II)	-13(10)	65(38)	18(17)	-4(24)	14(12)	62(26)	*

TABLE 15 (continued)

(c) Layer C

Configurational coordinates

	x/a	y/b	z/c	B
Zn(I)	0.3181(2)	0.3106(5)	0.0228(5)	-
Zn(II)	0.3371(2)	0.3511(5)	-0.0011(5)	-
P(I)	0.2629(3)	-0.0156(14)	0.2964(8)	
P(II)	0.3980(3)	-0.0064(14)	0.2138(7)	-
O1	0.3352(11)	-0.0542(36)	0.2755(26)	1.56(32)
O2(I)	0.2156(6)	-0.0103(27)	0.1334(14)	0.50(15)
O2(II)	0.4596(9)	0.0075(34)	0.3568(22)	0.51(22)
O3(CI)	0.2457(7)	-0.1615(32)	0.3884(16)	0.22(15)
O3(CII)	0.4094(7)	-0.1531(20)	0.1221(18)	0.48(19)
O3(TI)	0.2668(10)	0.1465(35)	0.3817(25)	0.94(29)
O3(TII)	0.3848(10)	0.1429(37)	0.1179(23)	1.31(31)

Anisotropic thermal coordinates (A^2 x 10^4)

	U_{11}	U_{22}	U_{33}	U_{12}	U_{13}	U_{23}
Zn(I)	109(11)	23(21)	54(12)	-40(12)	-34(9)	-8(15)
Zn(II)	34(8)	104(23)	78(11)	-9(13)	26(7)	-40(16)
P(I)	113(20)	71(41)	38(22)	15(33)	-10(18)	97(32) *
P(II)	24(14)	175(55)	35(19)	31(27)	-27(13)	151(27) *

* Non positive definite

TABLE 16

Molecular geometry of α-$Zn_2P_2O_7$

Bond lengths (A)

	Layer A	Layer B	Layer C
P(I)-O1	1.65	1.63	1.55
P(II)-O1	1.54	1.58	1.57
P(I)-O2(I)	1.55	1.51	1.52
P(II)-O2(II)	1.53	1.53	1.53
P(I)-O3(CI)	1.59	1.53	1.56
P(II)-O3(CII)	1.49	1.51	1.53
P(I)-O3(TI)	1.46	1.49	1.54
P(II)-O3(TII)	1.58	1.49	1.49

(average error 0.04 A)

O1-O2(I)	2.53	2.46	2.41
O1-O2(II)	2.46	2.58	2.45
O1 - O3(CI)	2.48	2.46	2.47
O1-O3(CII)	2.43	2.39	2.46
O1-O3(TI)	2.54	2.55	2.51
O1-O3(TII)	2.64	2.51	2.55
O2(I)-O3(CI)	2.54	2.53	2.55
O3(II)-O3(CII)	2.49	2.53	2.48
O2(I)-O3(TI)	2.54	2.52	2.47
O2(II)-O3(TII)	2.53	2.49	2.53
O3(CI)-O3(TI)	2.62	2.51	2.57
O3(CII)-O3(TII)	2.48	2.46	2.49

(average error 0.07A)

TABLE 16 (continued)

Note: Primed O3 atoms are in adjacent layers to cations

Zn(I)-O2(I)	2.03	2.09	2.06
Zn(I)-O2(II)	2.08	2.10	2.08
Zn(I)-O3(1)	2.00	2.00	1.95
Zn(I)-O3(2)	2.01	2.14	2.03
Zn(I)-O3'(1)	2.02	2.09	2.07
Zn(I)-O3'(2)	3.35	2.17	3.32
Zn(I)-O1	3.22	3.36	3.18
Zn(II)-O2(I)	2.10	2.04	1.99
Zn(II)-O2(II)	2.07	2.02	2.07
Zn(II)-O3(1)	1.93	1.92	2.07
Zn(II)-O3(2)	2.04	2.02	2.07
Zn(II)-O3'(1)	2.10	2.12	2.14
Zn(II)-O3'(2)	3.21	3.15	2.18
Zn(II)-O1	3.12	3.09	3.34

(average error 0.06 A)

Angles

	Layer A	Layer B	Layer C
P(I)-O1-P(II)	139°	147°	150°
O1-P(I)-O2(I)	104°	103°	104°
O1-P(II)-O2(II)	106°	112°	105°
O1-P(I)-O3(CI)	100°	102°	105°
O1-P(II)-O3(CII)	106°	102°	105°

TABLE 16 (continued)

O1-P(I)-O3(TI)	109°	110°	109°
O1-P(II)-O3(TII)	116°	109°	113°
O2(I)-P(I)-O3(CI)	109°	113°	112°
O2(II)-P(II)-O3(CII)	111°	113°	109°
O2(I)-P(I)-O3(TI)	115°	115°	113°
O2(II)-P(II)-O3(TII)	109°	110°	114°
O3(CI)-P(I)-O3(TI)	118°	113°	113°
O3(CII)-P(II)-O3(TII)	108°	110°	111°

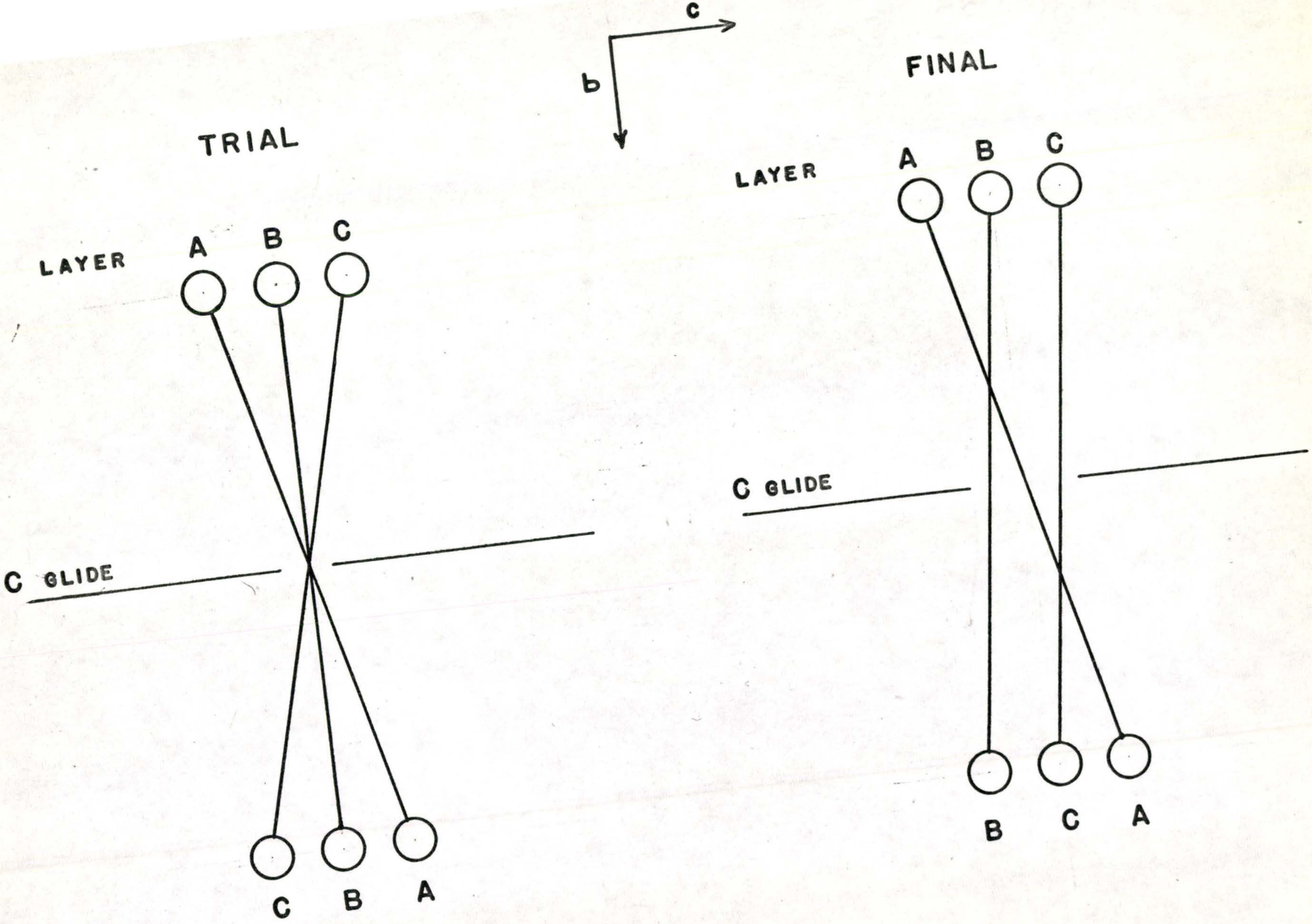

Figure 3

Schematic representation of the appearance of the cations of in projection down the a axis in the "trial" and "final" structures

CHAPTER 5: CRYSTAL CHEMISTRY OF "SMALL CATION" PYROPHOSPHATES

(A) Description of Structures

The general description of the structure of thortveitite was given in Chapter 1(A). This description applies to β-$Cu_2P_2O_7$ as it does to the other high temperature members of this series, and the structures of the low temperature forms are similar. Here we shall compare the small differences between the high temperature structures and in turn compare them with the structures of the low temperature forms of $Cu_2P_2O_7$, $Zn_2P_2O_7$, and $Mg_2P_2O_7$. Of particular interest are the nature of the differences in the distortion of the environment of the cation, the thermal motion of the central oxygen atom in the β phase and the P-O-P angle of the α phase. The pertinent bond lengths and interatomic angles of the structures of β-$Mg_2P_2O_7$, β-$Zn_2P_2O_7$ and $Mn_2P_2O_7$ are compared with those of β-$Cu_2P_2O_7$ in Table 17.

In the β phase, the distortion of the octahedral environment of the cations consists of (a) an elongation of the bonds to two oxygen ligands "O3'" on opposite sides of the cation and (b) a rotation of the pair of O3 ligands about the twofold axis by angles of the order of 25° from the positions they would occupy if the octahedron were regular. The significance of the long bonds, to be referred to as the M-O3' bonds, in all the β phases may be further understood by comparing their structure with that of $PbSb_2O_6$ (Magneli, 1941). If we replace the X-O-X group, in compounds with the formula $M_2X_2O_7$, by the single Pb^{+2} ion, the structures are now similar and the octahedra of oxygen atoms surrounding the Sb^{+5} ions are nearly regular. It is then easily seen from Figure 4 that the structure of $M_2X_2O_7$ must accommodate the strain caused by the anisotropic shape of the X-O-X group, rather than the spherical Pb^{+2} ion, by elongating the M-O3$'$ bonds. All the β phase structures show longer axial cation oxygen bond lengths, that is the M-O3$'$ bonds, than equatorial bonds. The case of β-$Cu_2P_2O_7$ is, however, extreme. Here the axial bond lengths are 2.58 A and the equatorial average 1.9 A. This extra distortion is manifested in an anomalous ratio of the a to b axial lengths as compared to other structures having the thortveitite structure (Au and Calvo, 1967). These long bonds are nearly parallel to the P-O1 bonds. Other effects of the long M-O3$'$ bonds are to decrease the length of these P-O1 bonds in β-$Cu_2P_2O_7$ and to increase the length of the vector <u>a</u>-<u>c</u> as may be seen by inspection of Tables 17 and 2. Cruickshank's curve predicts P-O(-P) and P-O bond length of 1.58 A and 1.53 A respectively for a linear P-O-P group. All of the P-O(-P) bond lengths in Table 17 are shorter than their predicted value by 0.01 to 0.04 A. However, these are not necessarily the true time averaged bond lengths because the O1 atoms of each structure shows a large component of motion perpendicular to the P-P vector. In order to make the proper correction, it is necessary to know the manner in which the motion of the O1 atoms is correlated with the motion of the P atoms. However, we can make a minimum correction without such knowledge (Busing and Levy, 1964). This correction increases the P-O(-P) distance in β-$Cu_2P_2O_7$ to 1.564 A. Minimum corrections for thermal motion calculated for the terminal P-O bond lengths are not significant. In $Mn_2P_2O_7$, β-$Mg_2P_2O_7$ and β-$Zn_2P_2O_7$, the average length of the P-O bonds in the anion is significantly greater than the predicted average of 1.53 A for the isolated $P_2O_7^{-4}$ group. This suggests some delocalization of electrons toward the cation. One would not expect the behaviour of β-$Cu_2P_2O_7$ to be different from the other members of the group. However, the proper corrections for thermal motion would possibly bring β-$Cu_2P_2O_7$ more in line with the others. For instance, corrections based on an "uncorrelated model" increase the P-O2 and P-O3 bond lengths to 1.528 and 1.526 A respectively.

A further indication of the dependence of the chemistry of the anion on its crystalline environment is provided by an examination of the manner in which two cations and one phosphorus atom are bonded to each terminal oxygen atom. In Table 18 are tabulated the three angles subtended by its three ligands at each independent terminal oxygen atom of some of the pertinent structures. In each case the sum of the angles total nearly 360°, indicating a nearly planar distribution of the four atoms. The terminal oxygen atom would then be expected to have some sp^2 hybridization although the individual angles deviate considerably from the ideal 120°. If the terminal oxygen atoms are partially sp^2 hybridized, the total number of electrons in the anion would be affected. It appears then that the deviations from the predicted bond lengths arise from the effects of the environment, which were not considered by Cruickshank, and the fact that the P-O-P angle is not necessarily 180°.

(B) Comparison of Low Temperature Structures

The c glide plane and the doubled c axis is common to all the low temperature structures of the "small ion" pyrophosphates. Further, in each case they only contain bent P-O-P groups in the anions. Thus the c glide plane might be closely related to the bending of the pyrophosphate ion. For the purpose of discussion the structures may be considered to consist of layers perpendicular to the a^* vector and cutting the unit cell at x = 0 and $\frac{1}{2}$. The cations and O1 atoms lie nearly at the middle of these layers.

The c glide plane in the α-$Cu_2P_2O_7$ structure may now be constructed from the mirror plane in the β-$Cu_2P_2O_7$ structure in the following way. One central oxygen atom is first displaced along the positive b direction by 0.39 Å (#1 in Figure 4). In order to retain pseudo-tetrahedral symmetry about the phosphorus atoms, the terminal oxygen atoms must be rotated about an axis perpendicular to the P-P vector and the b axis, and which also passes through the P atom. The largest effect of this operation is to move the O3 atoms about 0.16 A in the a - c direction (#2 in Figure 4). At one end of the anion each member of the pair of O3 atoms moves in opposite directions by an equal amount. These oxygen atoms are each bonded to one Cu^{+2} cation in the same layer. The cations are then moved by almost equal amounts in the same direction as their respective O3 atoms (#3 in Figure 4). The O3 atoms bonded to the other side of the cations must also be moved in the same direction and by an equal amount (#4 in Figure 4). This rotates one end of the $P_2O_7^{-4}$ groups removed from the first by c/2 but in the opposite sense. This displaces the O1 atoms of these anions in the opposite direction to the displacement of the first (#5 in Figure 4). This mechanism generates the c glide plane and the double periodicity in the c direction. The octahedra of ligands surrounding the two cation bonded through the O3 atoms of one anion, share edges with two other octahedra. The cations of these octahedra are each displaced in the opposite direction from the direction of displacement of those cations in the first two octahedra (Figure 13). The displacements of all atoms in one layer are then interdependent.

The displacements of the cations and the O3 atoms are both in the same direction as those of the long Cu^{+2}-O3' bonds, which is nearly the a - c direction, and have a very marked effect on these bonds. The two atoms which make up each of these bonds are moved in opposite directions such that half of the bonds are shortened from 2.58 A to 2.32 A and the other half are lengthened to 2.94 A. This is an abnormally long distance for a Cu^{+2}-O bond. Since there is only one independent Cu^{+2} site in α-$Cu_2P_2O_7$, each cation has five ligands within 2.32 A and one at 2.94 A.

The P-O(-P) distance of 1.577 A in α-$Cu_2P_2O_7$ is slightly longer than in the high temperature form. The P-O2 bond length has increased significantly from 1.516 A in β-$Cu_2P_2O_7$ to 1.552 in α-$Cu_2P_2O_7$. This change is not generated by the bending of the anion from its configuration in β-$Cu_2P_2O_7$. It involves a shift of the O2 atom in the c direction a distance of 0.05 A towards the Cu^{+2} cation. This is the largest atomic shift not associated with the bent anion and its explanation may be in the different temperature at which the structures were observed. Since the P-O-P angle in α-$Cu_2P_2O_7$ is 156° the P-O(-P) separations, according to Cruickshanks curve, should lie between 1.58 and 1.64 A which correspond to P-O-P angles of 180° and 120° respectively. Similarly the P-O separations should be between 1.51 and 1.53 A respectively. If corrections for thermal motion could be made to the data, all of these bond lengths except that of the P-O2 bond would probably lie within their predicted limits.

The structure of α-$Mg_2P_2O_7$ as reported by Calvo (1967d) is similar to that of α-$Cu_2P_2O_7$. The pertinent bond angles and interatomic angles of α-$Mg_2P_2O_7$ are presented in Table 19. The space group $B2_1/c$ is centrosymmetric. The anions are bent but the displacement of the central oxygen atom from its centric position in β-$Mg_2P_2O_7$ is not restricted to lie along a twofold rotation axis in the b direction as in α-$Cu_2P_2O_7$. Nevertheless, the component of this displacement in the a,c plane is small. The doubling of the a axis and the change in symmetry gives rise to two independent cation sites. One cation maintains octahedral coordination with nearest neighbour distances ranging from 2.062 to 2.150 A. The other Mg^{+2} ion is five coordinated. One of the ligands bonded to this cation by one of the long Mg^{+2}-$O3'$ bonds of length 2.15 A in β-$Mg_2P_2O_7$ is 3.35 A away in α-$Mg_2P_2O_7$. The sixth nearest neighbour to this cation is, in fact, an O1 atom at a distance of 3.057 A. The α phase may obtain some degree of stabilization from the interaction of the O1 atom and the cation. The other five bonds to the five coordinated cations range from 1.985 to 2.120 A. The bonding between the cation and the $O3'$ atom at a distance of 3.354 A is either non-existent or severely weakened. This should allow the other bonds to the $O3'$ atom to be strengthened. Its P-$O3'$ bond length and the nearest cation distance are 1.469 A and 1.985 A respectively. These are the shortest phosphorous oxygen and cation oxygen distances in α-$Mg_2P_2O_7$. In contrast, there is no short terminal P-O bond length in α-$Cu_2P_2O_7$.

The P-O-P angle in α-$Mg_2P_2O_7$ is 144°. One would expect the P-O(-P) distances to be slightly greater than in α-$Cu_2P_2O_7$. They are 1.610 A and 1.571 A as opposed to 1.577 A in β-$Cu_2P_2O_7$. Except for the short P-$O3'$ bond length of 1.469 A, the P-O bonds do not deviate significantly from the predicted range of 1.51 A to 1.53 A. The structures of α-$Ni_2P_2O_7$ (Łukaszewicz, 1967a) and α-$Co_2P_2O_7$ (Calvo, 1967c) are very similar to that of α-$Mg_2P_2O_7$. Both structures are only partially refined and will not be discussed here.

As is the case in the low temperature structures described above, the c glide plane in α-$Zn_2P_2O_7$ is generated by bent $P_2O_7^{-4}$ anions and is transmitted throughout the crystal by the displaced cation octahedra. Two of the six independent cations have octahedral coordination with Zn^{+2}-O bond lengths ranging from 1.99 A to 2.18 A. The four other cations are five coordinated with bond lengths ranging from 1.92 A to 2.12 A and each has a long Zn^{+2}-$O3'$ bond which would be 2.28 A long in β-$Zn_2P_2O_7$ and which has been lengthened to about 3.25 ± 0.10 A in α-$Zn_2P_2O_7$. Also an O1 atom is within 3.16 ± 0.06 A of these cations. α-$Zn_2P_2O_7$ has the smallest fraction of octahedrally coordinated cations. Because of correlation problems discussed in Chapter 4, the resolution of the oxygen atoms in α-$Zn_2P_2O_7$ is not sufficient to make a meaningful comparison of the individual P-O bond lengths and the predicted values. However, the average P-O(-P) and P-O bond lengths which are 1.58 A and 1.53 A, agree well. The three independent P-O-P angles are 139°, 147° and 150°.

If the effects of thermal vibrations are ignored, the low temperature structures would appear to be in better agreement with Cruickshank's predictions than the high temperature structures. The main differences between the structures of the α forms of $Zn_2P_2O_7$, $Mg_2P_2O_7$ and $Cu_2P_2O_7$ are associated with the way they transform to the β phase and will be discussed further in Chapter 8. The geometries of the anions as found in each of these structures are compared in Figure 5.

TABLE 17

Molecular geometry of the high temperature forms of the "small cation" pyrophosphates, $M_2P_2O_7$ (e.s.d's in parantheses)

(a) Bond lengths (A)

M	Mn^{+2}	Mg^{+2}	Zn^{+2}	Cu^{+2}
M-O2	2.14	2.05	2.061	2.003(15)
M-O3	2.11	2.02	2.001	1.936(15)
M-O3'	2.27	2.15	2.275	2.577(15)
P-O1	1.57	1.557(2)	1.569(5)	1.542(4)
P-O2	1.57	1.534(10)	1.556(19)	1.516(15)
P-O3	1.54	1.542(9)	1.554(13)	1.503(15)

(b) Angles

O1-P-O2	104.8°	103.3°	102.1°	105.5°
O1-P-O3	108.2°	106.8°	110.0°	108.7°
O2-P-O3	113.0°	113.3°	110.9°	111.0°
O3-P-O3	109.1°	112.6°	112.6°	111.8°

Source

$Mn_2P_2O_7$ - Further refinement of the results of Łukaszewicz and Smajkiewicz (1961) with some additional data added.

β-$Mg_2P_2O_7$ - Calvo 1965c

β-$Zn_2P_2O_7$ - Calvo 1965b

TABLE 18

Sums of angles subtended at terminal oxygen atoms of the pyrophosphate ion in some "small cation" pyrophosphates.

(a) β-$Cu_2P_2O_7$

P-O2-Cu	129.6°	P-O3-Cu	118.1°
P-O2-Cu'	129.6°	P-O3-Cu'	135.6°
Cu-O2-Cu'	99.8°	Cu-O3-Cu'	103.2°
	359.0°		356.9°

(b) α-$Cu_2P_2O_7$

P-O2-Cu	126.2°	P-O31-Cu	124.4°
P-O2-Cu'	131.6°	P-O31-Cu'	130.3°
Cu-O2-Cu'	100.9°	Cu-O31-Cu'	101.8°
	358.7°		356.5°
P-O32-Cu	110.2°		
P-O32-Cu'	142.6°		
Cu-O32-Cu'	103.7°		
	356.5°		

(c) α-$Mg_2P_2O_7$

P(I)-O2(I)-Mg(II)	128.6°	P(II)-O2(II)-Mg(II)	128.1°
P(I)-O2(I)-Mg(I)	132.1°	P(II)-O2(II)-Mg(I)	132.6°
Mg(I)-O2(I)-Mg(II)	98.8°	Mg(I)-O2(II)-Mg(II)	97.8°
	359.5°		358.5°
P(I)-O3(CI)-Mg'(I)	128.7°	P(II)-O3(CII)-Mg(II)	124.2°
P(I)-O3(CI)-Mg(I)	127.9°	P(II)-O3(CII)-Mg(I)	129.6°
Mg(I)-O3(CI)-Mg'(I)	102.4°	Mg(I)-O3(CII)-Mg(II)	102.1°
	359.0°		355.9°

TABLE 18 (continued)

P(II)-O3(TI)-Mg'(II)	164.4°	P(II)-O3(TII)-Mg(II)	113.9°
P(II)-O3(TI)-Mg(II)	94.2°	P(II)-O3(TII)-Mg(I)	144.8°
Mg(II)-O3(TI)-Mg'(II)	100.0°	Mg(I)-O3(TII)-Mg(II)	98.5°
	358.6°		357.2°

(d) α-$Zn_2P_2O_7$

	Layer A	Layer B	Layer C
P(I)-O2(I)-Zn(I)	134.7°	125.8°	131.1°
P(I)-O2(I)-Zn(II)	125.1°	129.1°	131.0°
Zn(I)-O2(I)-Zn(II)	100.2°	101.3°	97.9°
	360.0°	356.2°	360.0°
P(II)-O2(II)-Zn(I)	134.1°	126.7°	131.1°
P(II)-O2(II)-Zn(II)	127.6°	133.6°	124.4°
Zn(I)-O2(II)-Zn(II)	98.3°	97.0°	100.5°
	360.0°	357.3°	356.0°
P(I)-O3(CI)-Zn(I)	126.1°	134.7°	129.0°
P(I)-O3(CI)-Zn(II)	127.1°	123.4°	124.3°
Zn(I)-O3(CI)-Zn(II)	98.9°	100.8°	99.9°
	352.1°	358.9°	353.2°
P(II)-O3(CII)-Zn(I)	135.0°	127.7°	128.7°
P(II)-O3(CII)-Zn(II)	123.3°	127.8°	127.6°
Zn(I)-O3(CII)-Zn(II)	99.8°	100.3°	100.4°
	358.1°	355.8	356.7°
P(I)-O3(TI)-Zn(I)	159.0°	101.9°	141.7°
P(I)-O3(TI)-Zn(II)	100.1°	154.0°	114.4°
Zn(I)-O3(TI)-Zn(II)	100.0°	102.1°	100.6°
	359.1°	358.0°	356.7°

TABLE 18 (continued)

P(II)-O3(TII)-Zn(I)	135.0°	140.3°	127.6°
P(II)-O3(TII)-Zn(II)	123.3°	117.9°	128.7°
Zn(I)-O3(TII)-Zn(II)	99.8°	99.6°	100.4°
	358.1°	357.8°	356.7°

TABLE 19

Molecular geometry of α-$Mg_2P_2O_7$ (from Calvo, 1967d)

(a) Bond lengths (A)

P(I)-O1	1.610	O1-O2(I)	2.46
P(II)-O1	1.571	O1-O2(II)	2.51
P(I)-O2(I)	1.533	O1-O3(CI)	2.47
P(II)-O2(II)	1.532	O1-O3(CII)	2.41
P(I)-O3(CI)	1.502	O1-O3(TI)	2.51
P(II)-O3(CII)	1.525	O1-O3(TII)	2.53
P(I)-O3(TI)	1.469	O2(I)-O3(CI)	2.52
P(II)-O3(TII)	1.517	O2(II)-O3(CII)	2.55
		O2(I)-O3(TI)	2.53
		O2(I)-O3(TII)	2.52
		O3(CI)-O3(TI)	2.46
		O3(CII)-O3(TII)	2.51
Mg(I)-O2(I)	2.066	Mg(II)-O2(I)	2.047
Mg(I)-O2(II)	2.086	Mg(II)-O2(II)	2.057
Mg(I)-O3(CI)	2.062	Mg(II)-O3(CII)	2.026
Mg(I)-O3'(CI)	2.140	Mg(II)-O3(TI)	3.354
Mg(I)-O3(CII)	2.129	Mg(II)-O3'(TI)	1.985
Mg(I)-O3(TII)	2.150	Mg(II)-O3(TII)	2.120
		Mg(II)-O1	3.057

TABLE 19 (continued)

b Angles

P(I)-O1-P(II)	144.1°		
O1-P(I)-O2(I)	102.8°	O2(I)-P(I)-O3(CI)	114.8°
O1-P(II)-O2(II)	107.8°	O2(II)-P(II)-O3(CII)	111.2°
O1-P(I)-O3(CI)	105.8°	O2(I)-P(I)-O3(TI)	112.0°
O1-P(II)-O3(CII)	102.4°	O2(II)-P(II)-O3(TII)	113.3°
O1-P(I)-O3(II)	109.3°	O3(CI)-P(I)-O3(TI)	111.9°
O1-P(II)-O3(TII)	110.2°	O3(CII)-P(II)-O3(TII)	111.5°

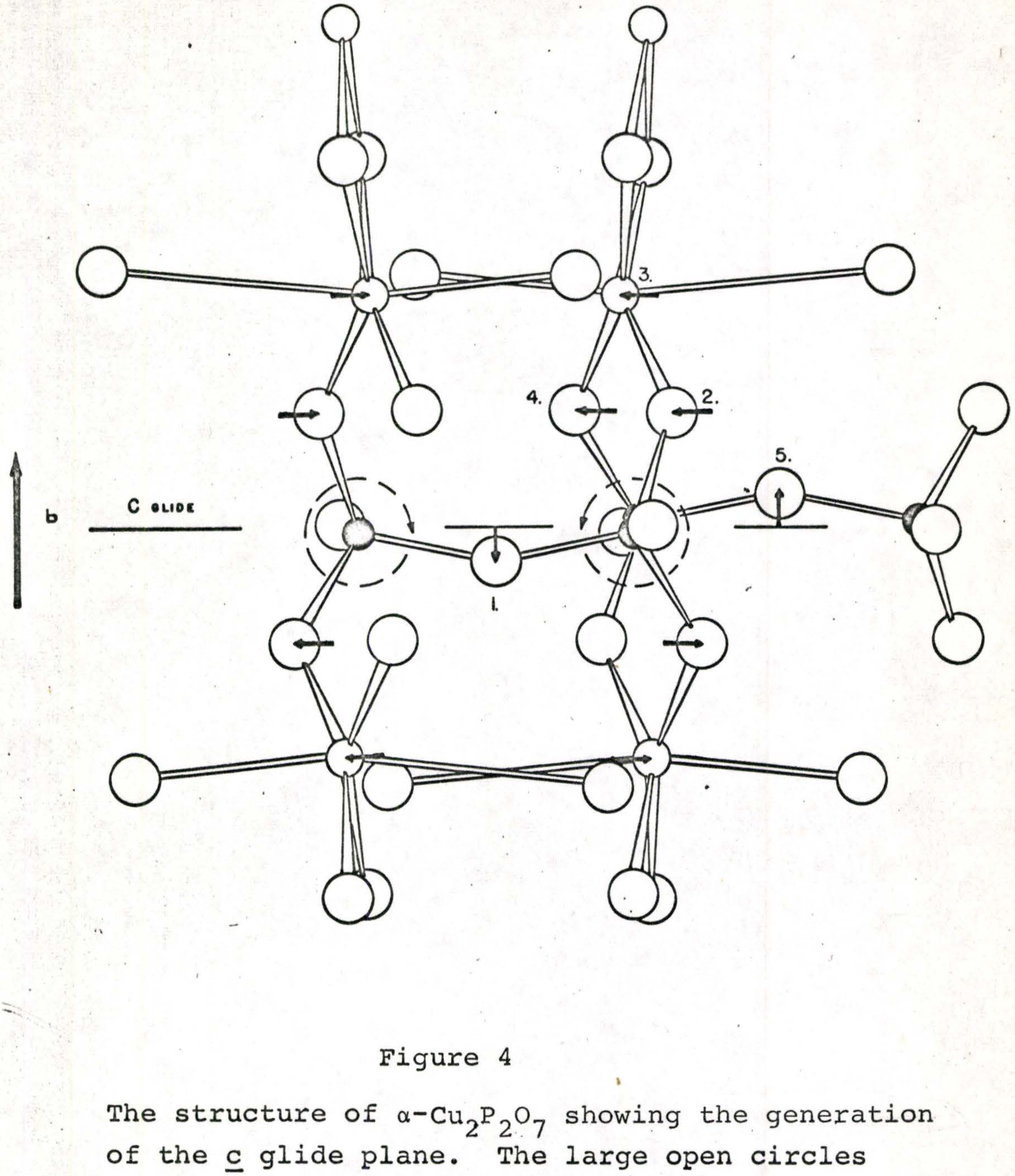

Figure 4

The structure of α-$Cu_2P_2O_7$ showing the generation of the c glide plane. The large open circles represent oxygen atoms, the small open circles represent the cations and the small solid spheres are the phosphorus atoms.

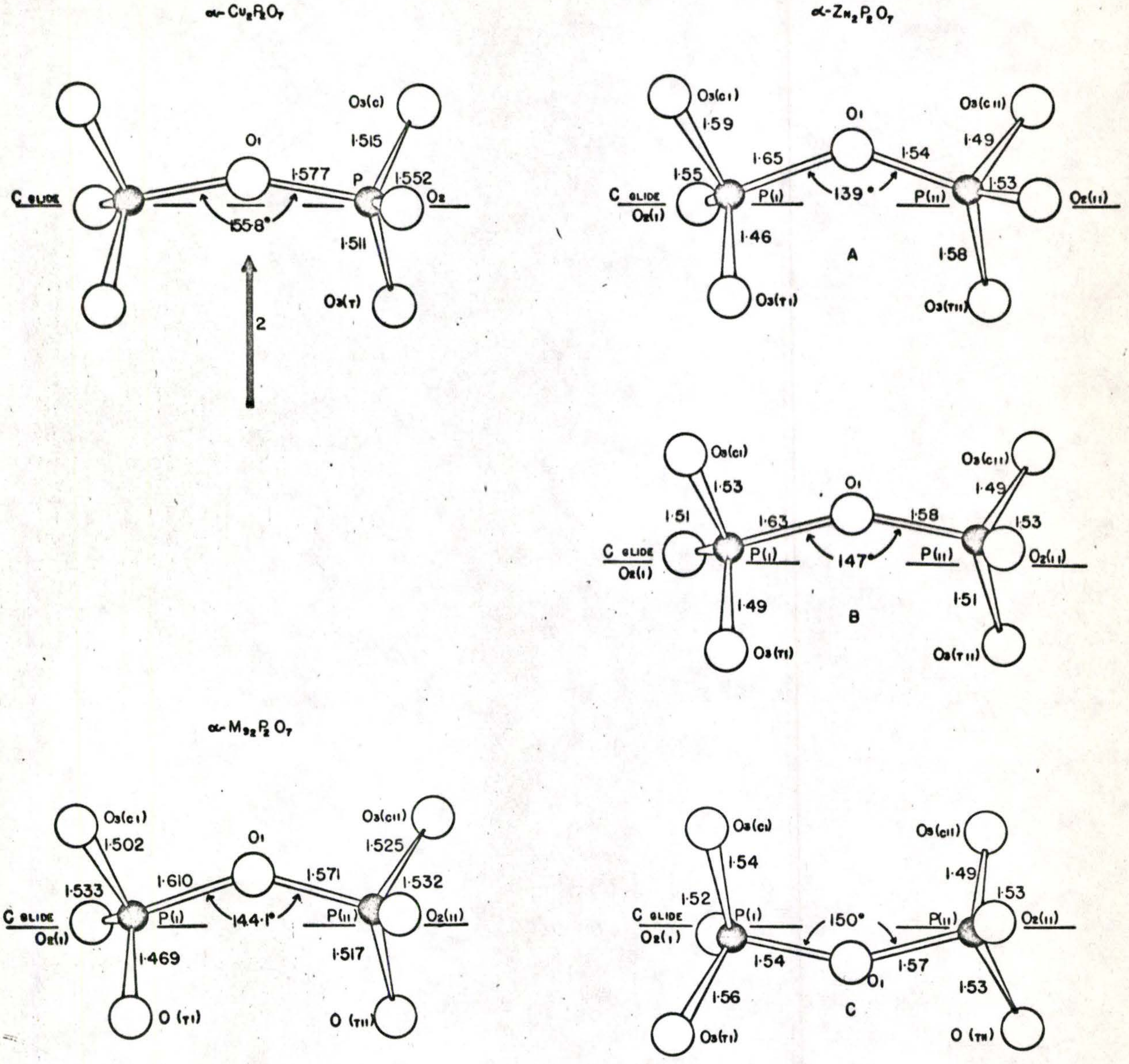

Figure 5

The geometry of the pyrophosphate anion in the low temperature forms of the "small cation" pyrophosphates. The atoms are represented as in Figure 4. The two-fold axis through O1 in α-$Cu_2P_2O_7$ is indicated.

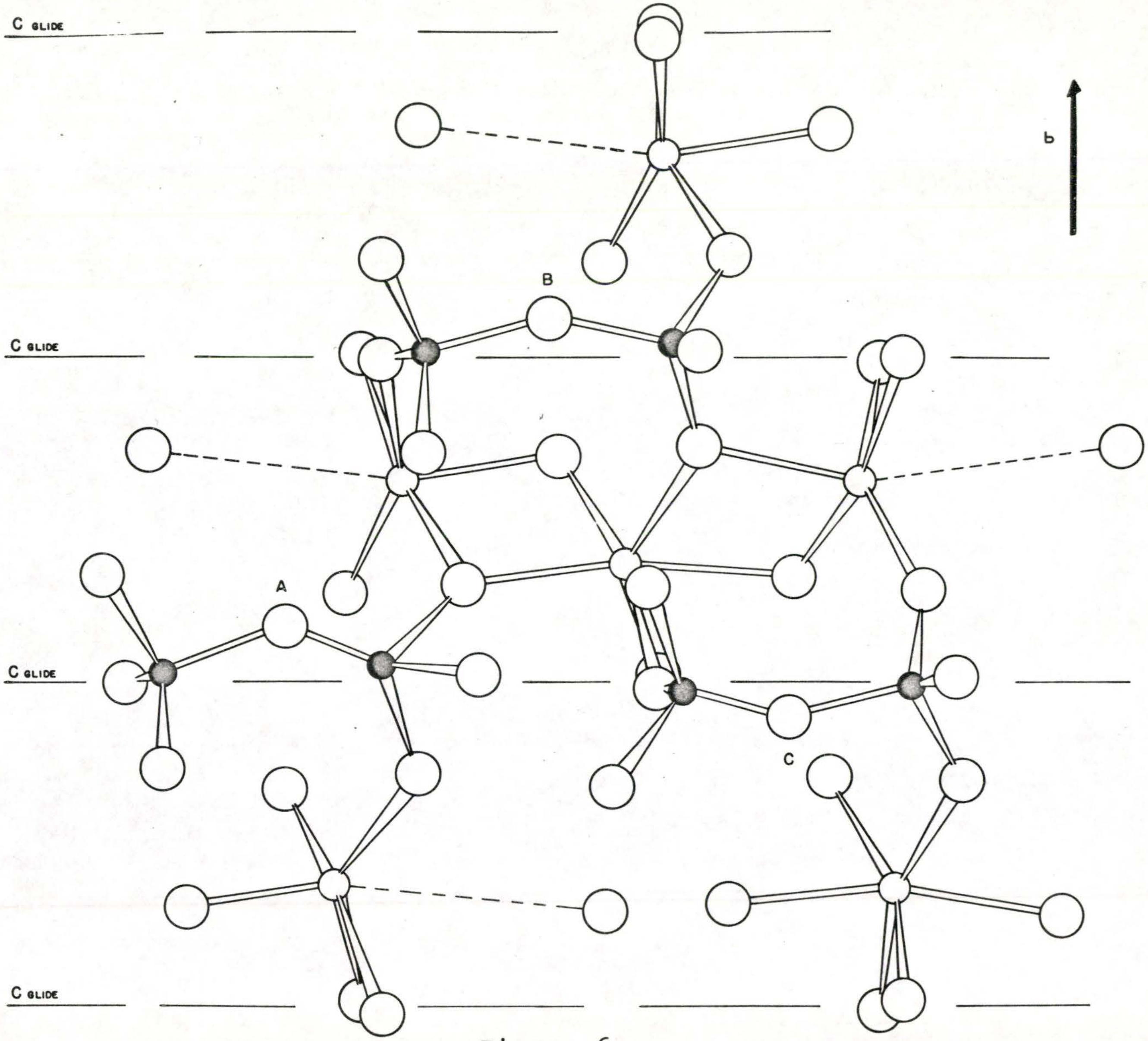

Figure 6
The structure of α-$Zn_2P_2O_7$ in projection down the _b_ axis .The atoms are represented as in Figure 4

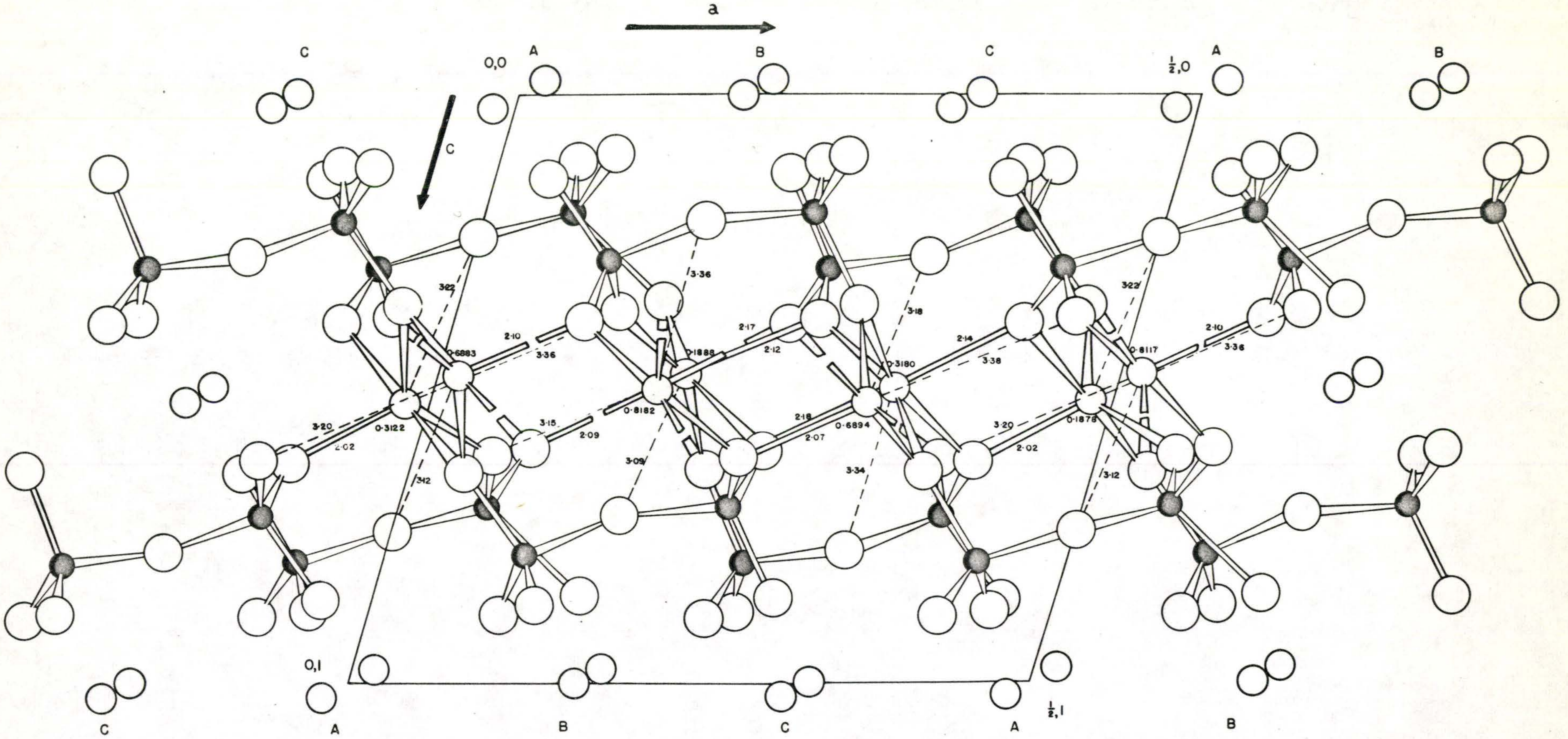

Figure 7

The structure of α-$Zn_2P_2O_7$ in projection down the b axis. The atoms are represented as in Figure 4.

CHAPTER 6: DIFFUSE STREAKS IN $Cu_2P_2O_7$

(A) Investigation of the Phase Transformation

The occurrence of a phase transformation in $Cu_2P_2O_7$ was originally mentioned by Roy et. al. (1948). The details of the transformation as reported here were found by observing its single crystal diffraction pattern as a function of temperature which indicated that the unit cell halved along the c axis at about 70°C (Robertson, 1965). This phase change is manifested by a disappearance of those reflections having indices with ℓ odd when referred to the α unit cell. It should be noted that because of the doubled c axis, these reflections would have half integral values of ℓ when referred to the β unit cell.

The heating apparatus in these experiments consisted of a coil of nichrome wire mounted in the end of a layer line screen and the current was supplied by a "powerstat" transformer. With this apparatus, it was difficult to maintain a constant temperature and to accurately monitor the absolute temperature. Further experiments, overcoming these difficulties, have been carried out using a Nonius "Hi-Lo" Weissenberg camera. This camera is fitted with an attachment consisting of a double-walled silvered glass cylinder which is inserted inside the layer line screen and adjusted to be within a few millimeters of the crystal. An inert gas is flushed down the axis of the cylinder and heated by a resistance coil coaxial with and within the dewar. A A copper constantan thermocouple extends slightly beyond the axis of the cylinder. It was found that this thermocouple gave temperature readings which were approximately 10% too high. In order to calibrate the system another thermocouple was substituted at the position of the crystal and the temperature difference recorded as the overall temperature was changed. It was found that the thermocouples differed by about 12°C in the temperature region of interest with the thermocouple in the dewar reading higher. Later experiments with a crystal in thermal contact with a thermocouple showed that the readings taken with the thermocouple located in the dewar were, in fact, about 8° higher than the actual temperature of the crystal. The errors in temperature were assumed to be caused by thermal conduction in the large thermocouple leads which caused the thermocouples to act as heat sinks. The thermocouple in the dewar was heated by radiation from the resistance coil in the dewar. Temperatures quoted below have been measured at the crystal or were corrected by the subtraction of roughly 8°C from the temperature as measured with the thermocouple in the dewar.

A crystal was mounted on a glass fiber with Stycast 2651 high temperature cement and aligned about the [$\bar{1}$11] axis. In this orientation only the odd layer lines contain reflections with ℓ odd. In order to ensure that the proper conditions for diffraction existed and to observe reflections which were sensitive to the phase transformation, both the o'th and first layer lines were allowed to pass through the layer line screen to the recording film.

It was observed on a twenty hour exposure taken at 77 ± 3°C that the first layer line had disappeared and all of the reflections of that layer line had been replaced by very faint streaks. Further study of these streaks was warranted but their low intensity made it necessary to optimize the experimental situation. Since their relative intensity appeared to be proportional to the intensity of the Bragg peak which they replaced, it was desirable to choose an area of reciprocal space containing a number of relatively strong reflections with odd ℓ. Further, in order to decrease the necessary exposure time and to minimize temperature drift the oscillation range of the camera spindle angle was limited to about 60°. Photographs were taken at several temperatures ranging from room temperature to 120°C.

The general nature of the streaks could be determined from these photographs. By 50°C the intensity of those reflections with odd values of ℓ had begun to decrease in relation to those with even ℓ. The streaks first appeared at about 70°C. The Bragg peak remained, however, until the temperature was raised a few degrees further. Beyond 73°C the intensity of the streaks decreased monotonically as the temperature was raised further and could still be seen as a faint smudge on a 24 hour exposure at 120°C. The intensity distribution was remarkably flat along their length and did not blend into the Bragg peak. There was a marked discontinuity in intensity between the peak and the streaks.

Photographs of the streaks taken with the crystal aligned in several orientations showed that the length of the streaks paralleled the $\underline{a}^*$ direction.

X-rays which are not scattered into a region within a few minutes of arc of the direction defined by the Laue equations, arise because of some imperfections in the three-dimensional translational symmetry of the crystal. One source of such imperfections is the thermal vibration of atoms. This type of diffuse scattering has been well documented (Guinier, 1963; Wooster, 1961; and Ramachandran, 1963) but can not explain these diffuse streaks in $Cu_2P_2O_7$. Another class of imperfection in the translational symmetry is caused by a positional disordering of the atoms. Since the streaks extend only in the $\underline{a}^*$ direction the disordering must produce a loss of translational symmetry only in that direction.

The resolved structures of the α and β phases afford an opportunity to speculate on the details of how planes perpendicular to the $\underline{a}^*$ vector become disordered. The layers perpendicular to $\underline{a}^*$, as mentioned in Chapter I, should be able to maintain a high degree of order because of the manner in which the non-linear anions are joined by the cation octahedra but the layers themselves might be susceptible to a particular type of disordering. If the direction of bending of all the anions in one layer is reversed, that is, if their sense of the displacement of the central oxygen atoms from the y = constant plane of P atoms is reversed, then the bonding between layers will not be disrupted since only small changes in the primary bonding sphere are necessary. The structural implications of this operation will be discussed in detail in Chapter 7. The generation of the "disordered" layer is equivalent to the translation of the origin of that layer by c/2. If half of these layers are reversed with no long range correlations between them, then the atoms in the two halves of the unit cell related by the c glide plane will appear to be superimposed into an "average" unit cell with the length of the c axis halved. Also, in place of the c glide operation, there will now be a mirror plane. For convenience, we shall define a normal layer on α-$Cu_2P_2O_7$ as a type I layer and the reversed or disordered layer will be defined as type II.

(B) Measurement of Intensity Profiles

An apparatus was set up to provide better control of the temperature of the crystal. The experimental arrangement is shown in Figure 8. When the e.m.f. generated by the copper-constantan thermocouple falls below a predetermined value on the temperature control device, the relay is closed and the 8Ω impedance is by-passed. The voltage across the heater coils is then increased by 20% and the temperature increases. A standard Croyden P4 thermocouple potentiometer was used to measure the e.m.f. from the chromel-alumel thermocouple mounted on the side of the collimator. The galvanometer leads were connected to a Leeds and Northrup 2430D galvanometer which greatly enhanced the sensitivity of the instrument. The 0.8°C variations in temperature could easily be measured as the relay switched on and off and an additional 0.1°C variation in temperature could be observed as the Weissenberg film holder moved back and forth on its track. It was found that variations in the temperature of the crystal due to changes in room temperature and the gradual heating of the entire camera could be decreased by increasing the rate of flow of the inert gas bathing the crystal.

A crystal was carefully selected and affixed to a glass fiber with modelling clay. Several photographs were taken to find the direction of the $\underline{c}$ axis. A copper-constantan thermocouple consisting of 0.0036 gauge wire was inserted into a ceramic rod which was mounted on a goniometer head.

The crystal was remounted on the thermocouple junction with Stycast cement so that the c axis was nearly coincident with the goniometer's rotation axis. The crystal was now aligned about the c axis and photographs were taken in the temperature range of the phase transition which contained both the hk0 and hkl layer lines. In all these experiments, a region near the a^* axis was photographed since here the first layer line contained a number of strong reflections.

This mounting of the crystal proved inadequate for the collection of intensity distribution data because the scattering from the thermocouple raised the background level on the film to such an extent that the streaks were not well defined. However, this arrangement was useful in establishing the absolute temperature at which the various phenomena occurred. The variation in temperature during each exposure of this series was kept to within 2°C. Thus from the large number of exposures recorded with overlapping temperature ranges it was possible to assign the temperature at which the streaks first appeared as 71.0 ± 1.0°C and the temperature at which the Bragg peak disappeared as 74.0 ± 1.0°C.

The original crystal used to study the nature of the streaks was now used to collect data for the intensity distribution. This crystal had been mounted on a thin fiber with a minimum amount of glue and the background on the photographs obtained was very low. It could also be realigned about the c axis. The temperature was monitored by the chromel-alumel thermocouple as shown in Figure 8. Photographs were taken over the entire range of temperatures associated with the phase transition but only five photographs were used for detailed analysis. Two strong peaks were chosen which had a relatively smooth background. A tracing of the intensity of each streak was obtained with a Joyce-Loebl MKIIIC densitometer. The background level and coarse grain of the film was still such that the high sensitivity of the densitometer produced very erratic fluctuations in the intensity tracings. The rough outline of the streaks was drawn by hand through the fluctuations. A photograph taken at 69^{o} and showing only the Bragg peaks and background was used to subtract the background from each of the other tracings in the transition region. The normal white radiation streaks associated with the Bragg peaks appeared in the photographs and passed through the diffuse streaks. However, they decreased in intensity as the Bragg peaks decreased in intensity and therefore the background above 71.0 ± 1.0^{o}C was markedly different than on the photograph at 69^{o}C. In order to complete the background curve above this temperature, a smooth line was drawn which joined the background curves in the regions not affected by the white radiation streaks. The height of the intensity profile and the associated background was noted at intervals of 0.05 $\underline{a}^{*}$. Each diffuse streak extends on either side of a Bragg peak and the intensity profile of each half must be nearly identical although they will register slightly different on a photographic film because of the effects of absorption and the Lp factor. It was assumed, however, that these effects were linear with $\sin\Theta/\lambda$ over the small range of Θ through which each streak appears. Then they may be cancelled by averaging the two halves of each streak. The curves obtained from the two streaks in this way were then themselves averaged. A further correction is required to account for the fact that the streaks have been convoluted by the mosaic spread and size of the crystal, the divergence and dispersion of the x-ray beam and the width of the light beam used to measure the intensity of the streaks. The width of the tracing of the Bragg peak provides a rough estimate of the magnitude of the effect of convolutions. This width was observed to be $0.05 \pm 0.01\underline{a}^*$ The intensity profiles were observed to have two portions that were linear within experimental error. These were at the points when the streaks faded into the background and near the Bragg peak. These two linear parts were extended $0.05\ \underline{a}^*$ towards each other and then joined by a continuous curve with the same general character as the uncorrected curve. These corrections are illustrated in Figure 10. The dashed lines are the corrected intensity profiles used to analyse the disorder. The intensity is plotted against the dimensionless quantity ξ describing the fractional distance in reciprocal space between the reflections $hk\ell$ and $(h+1)k\ell$.

The first curve shows the streaks as they first appear at $71.0 \pm 1.0^{\circ}$C. On the scale shown, the Bragg peak extends to 280 units along the ordinate. The curve representing the profile of the streak at 74.0 ± 1.0°C has a central peak extending to 55 units and at 75.0 ± 1.0°C there are no central peaks. The photographs from which these curves were obtained were taken over a finite range of temperature and therefore they probably contain some additional error, particularly at 71.0 ± 1.0°C where the experimental conditions under which the profile was measured extend into a temperature region where the streaks may not exist. The other three curves are flat within experimental error from the origin out to 0.125 $\underline{a}^*$. They then fall off to zero intensity with approximate Gaussian character. Beyond 74°C the only apparent change is an overall decrease in intensity.

(C) Derivation of the Intensity Profiles

A derivation of the relation between the distribution of intensity in the streak and the nature of the disorder may be found in Wilson (1949). An alternate discussion of the relationship will be presented here which will be better suited to the case of $Cu_2P_2O_7$.

Let $F'(hk\ell)$ represent the structure factor of one layer of type I (see Chapter 6A) made up of the contents of a half unit cell extending from x = 0 to x = a/2 and from $-\infty$ to $+\infty$ in both the y and z directions. The structure factor of the entire crystal is obtained by summing the $F'(hk\ell)$ of all the layers with the appropriate phase factor depending on the displacement of the layer from an arbitrary origin. Adjacent layers in the α phase, or the pure β phase, since it is described by an averaged unit cell, are C centered. However, in the transformation region, adjacent layers of opposite type are I centered. We can then define the structure factor of the n'th layer $A^n(hk\ell)$, with its appropriate phase factors as

$$A^n(hk\ell) = F'(hk\ell)\exp(2\pi i\ \nu_n\ k/2)\exp(2\pi i\ \gamma_n\ \ell/2)$$

where ν_n is a selector factor which is 0 if the layer is type I and 1 if the layer is of type II, and γ_n is 0 if n is odd and 1 if n is even. We may now write the structure of the entire crystal in terms of the $A^n(hk\ell)$. However, we shall be interested in the scattering of x-rays in the vicinity of the Bragg peaks where h is not integral. We therefore define a new quantity h' such that $h'\underline{a}^* = h\underline{a}^* + \xi\underline{a}^*$. Then the structure factor of a crystal consisting of N layers is

$$F(h'k\ell) = \sum_{n=1}^{N} A^{n}(h'k\ell)\ \exp(2\pi inh'/2)$$

The measured intensity $I(h'k\ell)$ as recorded on a photographic film, will be proportional to $F(h'k\ell)F^*(h'k\ell)$. The product may be written

$$I(h'k\ell)\ \alpha\ N\{|F(h'k\ell)|^2 + \frac{1}{N}\sum_{n=1}^{N}\sum_{j=1}^{N-n} A^{j}(h'k\ell)A^{j+n*}(h'k\ell)\exp(-\pi inh') + (C.C$$

where C.C. is the complex conjugate of the second term in the brackets. If we now substitute for $A^j(h'k\ell)$ and $A^{j+n*}(h'k\ell)$ and consider the behaviour of the exponentials, we find that their value depends only on the evenness of k or ℓ. We also substitute for h' and obtain

$$I(h'k\ell)\ \alpha\ N\ |F(h'k\ell)|^2\{\ 1+\frac{2}{N}\sum_{n=1}^{N}\sum_{j=1}^{N-n}\ (-)^{n(h+k)}\,[(-)^{\nu_j}(-)^{\nu_{j+n}}]^{\ell}\ \cos n\pi\xi\}$$

The quantity $[(-)^{\nu_j}(-)^{\nu_{j+n}}]$ is 1 if the layers j and j+n are the same type (ie, both type I or both type II) and -1 if they are different. It is reasonable to assume that the probability that the two layers are different depends on their separation n and not on the running index j. The second summation may then be averaged and the average value of $[(-)^{\nu_j}(-)^{\nu_{j+n}}]$ will be denoted by β_n. Consider the case when $\xi = 0$, ℓ is even and h + k is odd. Then

$$I(hk\ell)\ \alpha\ N\ |F'(hk\ell)|^2\ \{1 + \frac{2}{N}\sum_{n=1}^{N-1}\ (N-n)(-)^{n}\}$$

If we assume the crystal contains only complete unit cells, N is even and the summation gives directly -N/2 and I(hkℓ) is zero. The values of β_n depend on the degree of disorder and thus I(hkℓ) is not necessarily zero if both ℓ and h + k are odd. The area of reciprocal space corresponding to these reflections were studied in the temperature region where the crystal is partially disordered but no scattered x-rays were observed.

In order to obtain an expression which is independent of the integrated intensity of each diffuse streak, we shall define the quantity I(ξ) as

$$I(\xi) = \frac{I(h'k\ell)}{N|F(h'k\ell)|^2}$$

We shall further assume that $F'(h'k\ell) = F'(hk\ell)$ throughout the region of a diffuse streak. The appearance of the streaks suggests that this is a good approximation and the averaging of four "half" streaks should minimize any errors arising from this approximation. Then

$$I(\xi) = 1 + 2 \sum_{n=1}^{N-1} \frac{N-n}{N} \beta_n \cos n\pi\xi$$

(D) Fourier Transforms of the Intensity Profiles

We have measured $I(\xi)$ and now wish to find β_n. From the form of the expression for $I(\xi)$ we may express β_n as the Fourier transform of $I(\xi)$. It is then desirable to describe $I(\xi)$ analytically. The central peak in the ideal case is a delta function and the streak contains a flat part and appears to decay to zero approximately as a Gaussian of half width σ Thus

$$I(\xi) = \begin{cases} C_1 \ \delta(\xi-0) + C_2 & (-x < \xi < x) \\ C_2 \ \exp\left\{-(\xi - |x|)/2\sigma^2\right\} & (\xi \geqslant |x|) \end{cases}$$

where C_1 and C_2 are constants and x is the value of ξ where the intensity of the streaks begins to decrease. $I(\xi)$ is an even function and the period of integration will be 2. Therefore, if the expression for $I(\xi)$ may be written

$$\frac{a_o}{2} + a_1 \cos\pi\xi + a_2 \cos 2\pi\xi + \ldots..$$

then a_n is given by

$$a_n = \int_{-1}^{1} I(\xi) \cos n\pi\xi d\xi$$

$I(\xi)$ has been measured in arbitrary units, but

$$a_n \ \alpha \ \frac{2(N-n)}{N} \beta_n \text{ and since } \beta_o = \left[(-)^{\nu_j}\right]^2, \ \beta_o = 1$$

Furthermore, if n is much less than the total number of layers in the crystal (N-n) is nearly equal to N.

Then

$$\beta_n = a_n/a_o$$

Also, if α_n is the probability that the j'th and (j+n)'th layers are the same type, $\beta_n = (+1)\alpha_n + (-1)(1-\alpha_n)$

Therefore

$$\alpha_n = \frac{\beta_n + 1}{2} .$$

We must now evaluate a_n for any n, where

$$a_n = \int_{-1}^{+1} I(\xi)\cos(n\pi\xi)d\xi = C_1 + 2C_2\,\frac{\sin(n\pi x)}{n\pi}$$

$$+C_2\int_{x}^{+1} \exp\left\{-\frac{(\xi-x)^2}{2\sigma^2}\right\}\cos(n\pi\xi)d\xi + C_2\int_{-1}^{-x} \exp\left\{-\frac{(\xi+x)^2}{2\sigma^2}\cos(n\pi\xi)d\xi\right.$$

For convenience the limits of integration will be changed to $\pm\infty$. The contribution to the integrals when $|\xi|>|1|$ will be negligible. Also the cosines will be changed to exponentials. In the first integral, we shall substitute $t = (\xi-x)/(\sqrt{2}\sigma)$ and in the second $t = -(\xi+x)/(\sqrt{2}\sigma)$. Then the integrals become

$$\sqrt{2}\sigma C_2\left[\int_0^\infty \exp-\{t^2-\pi in(\sqrt{2}\sigma t+x)\}\,dt + \int_0^\infty \exp-\{t^2+\pi in(\sqrt{2}\sigma t+x)\}dt\right]$$

These integrals may be evaluated by completing the square of the arguments of the integrands. The substitutions

$$U = t-\pi in\sigma/\sqrt{2} \text{ and } U = t+\pi in\sigma/\sqrt{2}$$

will now be made in the first and second integrals respectively. Then we have

$$\sqrt{2}\sigma C_2\exp\left(-\frac{\pi^2n^2\sigma^2}{2}\right)\left[\exp(\pi inx)\left\{\int\limits_{\substack{0\\ \frac{\pi in\sigma}{\sqrt{2}}}}^{\infty} e^{-U^2}dU+\int_{\frac{-\pi in\sigma}{\sqrt{2}}}^{0} e^{-U^2}dU\right\}+\exp(-\pi inx)\right.$$

$$\left.\left\{\int_0^\infty e^{-U^2}dU - \int_0 e^{-U^2}dU\right\}\right]$$

The integrals from o to ∞ both give $\sqrt{\pi}/2$. In the other integrals we replace U by -iy and +iy. Then the expression becomes

$$\sqrt{2}\sigma C_2 \exp\left(\frac{-\pi^2 n^2 \sigma^2}{2}\right)\cos(n\pi x)\ \left[\sqrt{\pi} + \frac{\sqrt{2}i}{\pi}\operatorname{erf}\left(\frac{\pi n\sigma}{\sqrt{2}}\right)\right]$$

where erf(Z) is the error function of Z. We only require the real part of a_n. Therefore

$$a_n = C_1 + 2C\ \frac{\sin(n\pi x)}{n\pi} + \sqrt{2\pi}\ \sigma\ C_2\ \exp\ \left(\frac{-\pi^2 n^2 \sigma^2}{2}\right)\cos(n\pi x)$$

The quantities a_n, β_n and α_n were calculated for $n = 1, 2....100$ and at temperature of $71 \pm 1^{\circ}C$, $73 \pm 1^{\circ}C$ and $75 \pm 1^{\circ}C$. The results depend only on the shape of the curve defining the streaks and not the height. Only the height of the curve changes above $75^{\circ}C$ so there was no additional information to be gained from the α_n above this temperature. Strictly speaking, the model for the transition as has been presented cannot account for a change in the total number of photons diffracted into one Bragg peak and its associated diffuse streak. This point will be discussed in Chapter 7.

The width "σ" of the Gaussian part of the intensity distribution was estimated from the curves in Figure 10. The values of σ, x (the length of the flat portion of the streak), C_1 (the height of the Bragg peak), C_2 (the height of the flat portion of the peak), and α_n, $n = 0,1,2...50$ are listed in Table 20, as determined at the three temperatures mentioned previously. Also α_n is plotted as a function of n for $n = 0,1 ....20$ in Figure 11.

TABLE 20

Probability $\alpha_n(T)$ that the layers j and $j+n$ are identical as a function of n and the temperature T.

	$T = 71\pm1^{\circ}C$	$T=74\pm1^{\circ}C$	$T=75\pm1^{\circ}C$
Height of central peak	200.0	20.0	0.0
Length of flat portion	0.025 a*	0.125 a*	0.125 a*
Height of flat portion	80.0	36.0	32.0
Half width of Gaussian	0.110 a*	0.100 a*	0.100 a*
n	α_n	α_n	α_n
0	1.0000	1.0000	1.0000
1	0.9970	0.9827	0.9634
2	0.9891	0.9384	0.8701
3	0.9789	0.8849	0.7572
4	0.9690	0.8383	0.6589
5	0.9611	0.8055	0.5896
6	0.9560	0.7843	0.5450
7	0.9530	0.7697	0.5142
8	0.9515	0.7580	0.4894
9	0.9507	0.7482	0.4687
10	0.9504	0.7411	0.4538
11	0.9501	0.7376	0.4464
12	0.9500	0.7379	0.4470
13	0.9498	0.7416	0.4548
14	0.9495	0.7478	0.4679
15	0.9493	0.7553	0.4838
16	0.9490	0.7630	0.5000
17	0.9488	0.7698	0.5143
18	0.9485	0.7748	0.5250
19	0.9483	0.7776	0.5309
20	0.9480	0.7781	0.5318
21	0.9477	0.7763	0.5280
22	0.9474	0.7727	0.5204
23	0.9471	0.7680	0.5106

TABLE 20 (continued)

24	0.9468	0.7630	0.5000
25	0.9465	0.7584	0.4903
26	0.9462	0.7548	0.4827
27	0.9459	0.7527	0.4782
28	0.9456	0.7522	0.4773
29	0.9453	0.7534	0.4797
30	0.9450	0.7559	0.4850
31	0.9447	0.7593	0.4922
32	0.9444	0.7630	0.5000
33	0.9441	0.7665	0.5074
34	0.9439	0.7693	0.5132
35	0.9436	0.7709	0.5168
36	0.9433	0.7714	0.5177
37	0.9431	0.7705	0.5159
38	0.9428	0.7686	0.5118
39	0.9426	0.7660	0.5062
40	0.9424	0.7630	0.5000
41	0.9421	0.7602	0.4941
42	0.9419	0.7579	0.4893
43	0.9418	0.7565	0.4863
44	0.9416	0.7561	0.4856
45	0.9414	0.7568	0.4869
46	0.9413	0.7584	0.4902
47	0.9411	0.7605	0.4948
48	0.9410	0.7630	0.5000
49	0.9409	0.7653	0.5050
50	0.9408	0.7673	0.5090

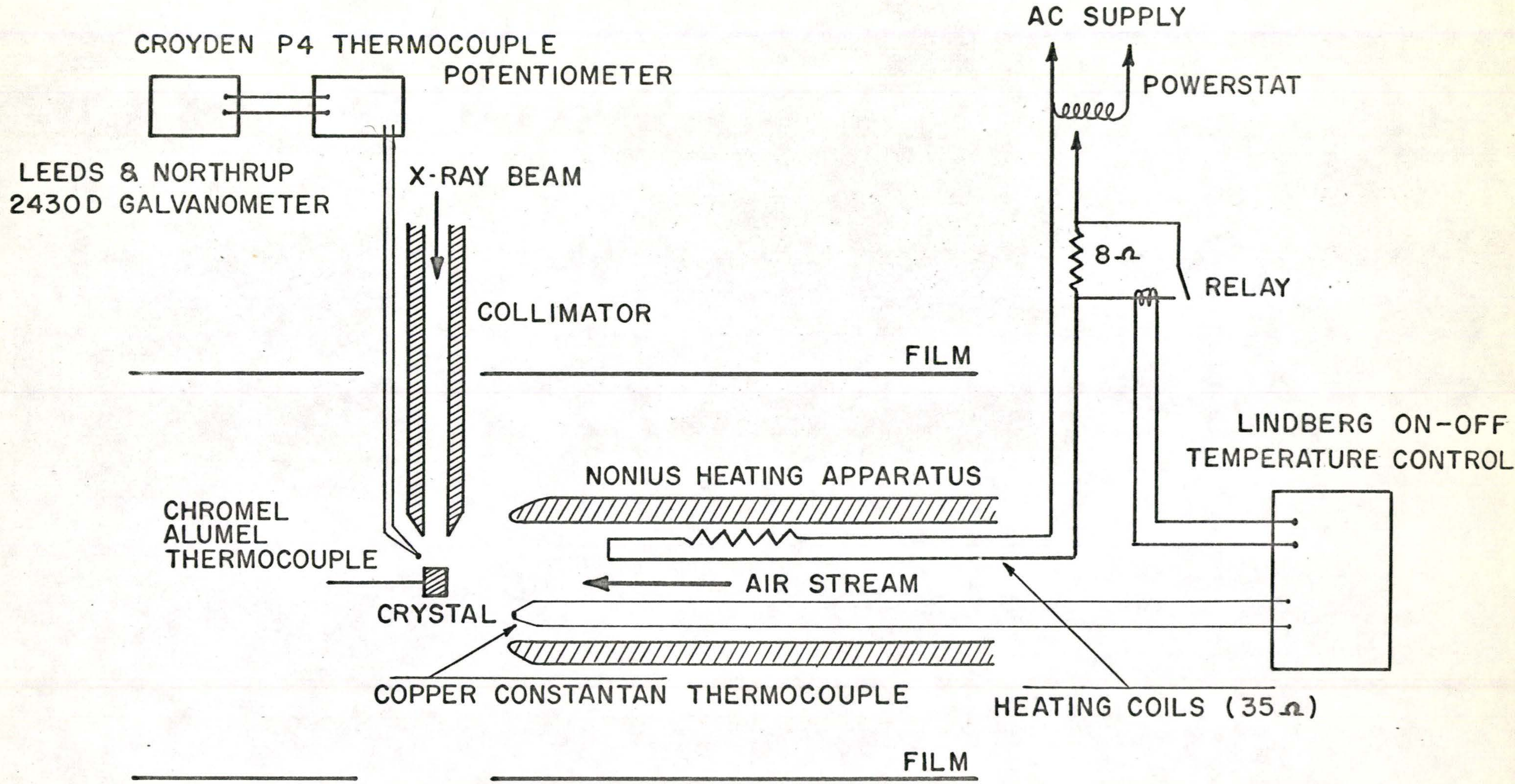

Figure 8

Experimental arrangement used to record diffuse streaks

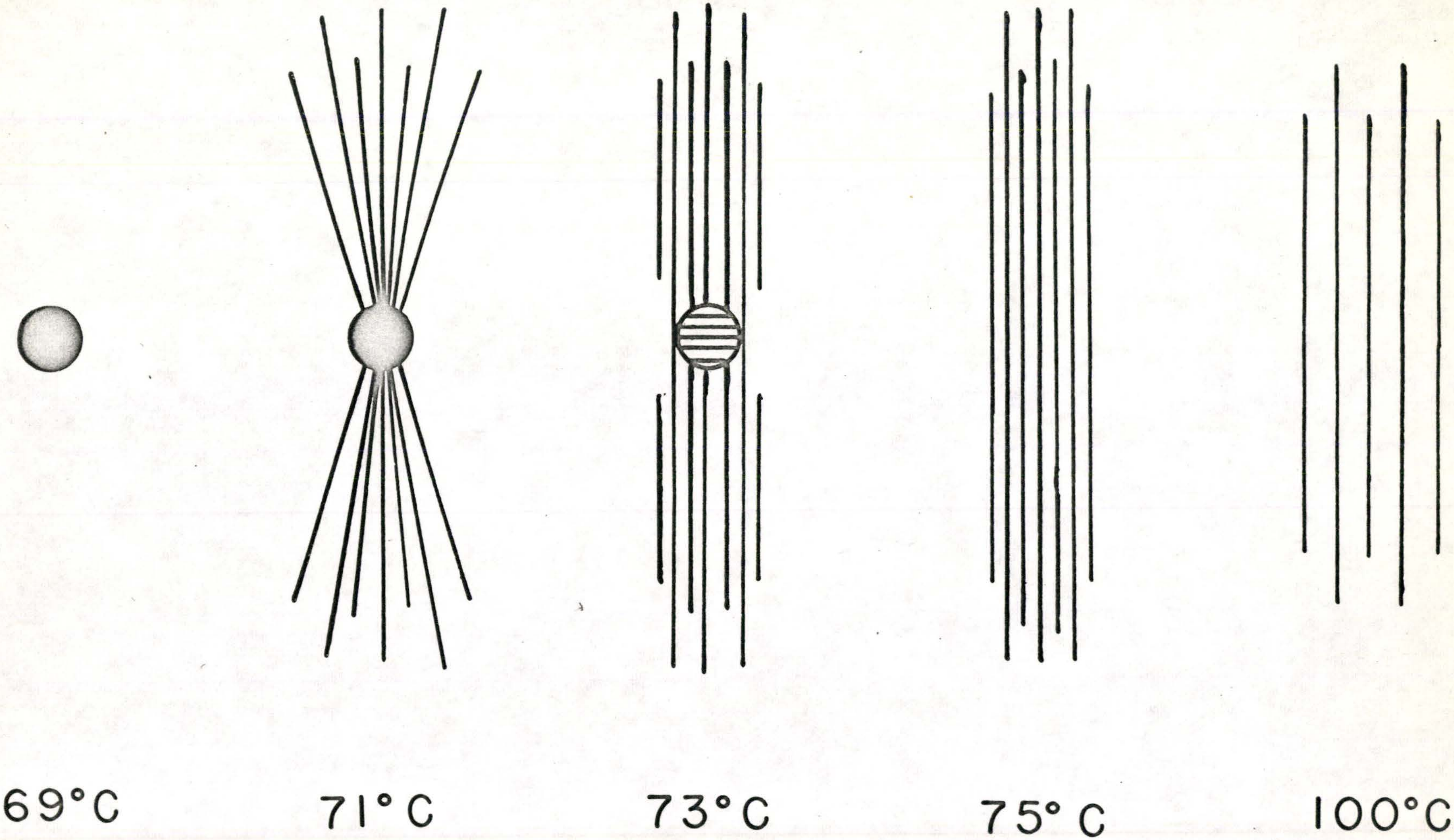

Figure 9

Schematic representation of the appearance of the diffuse streaks as a function of temperature. (Attempts to reproduce the x-ray films showing the streaks have not been successful because of their low intensity.)

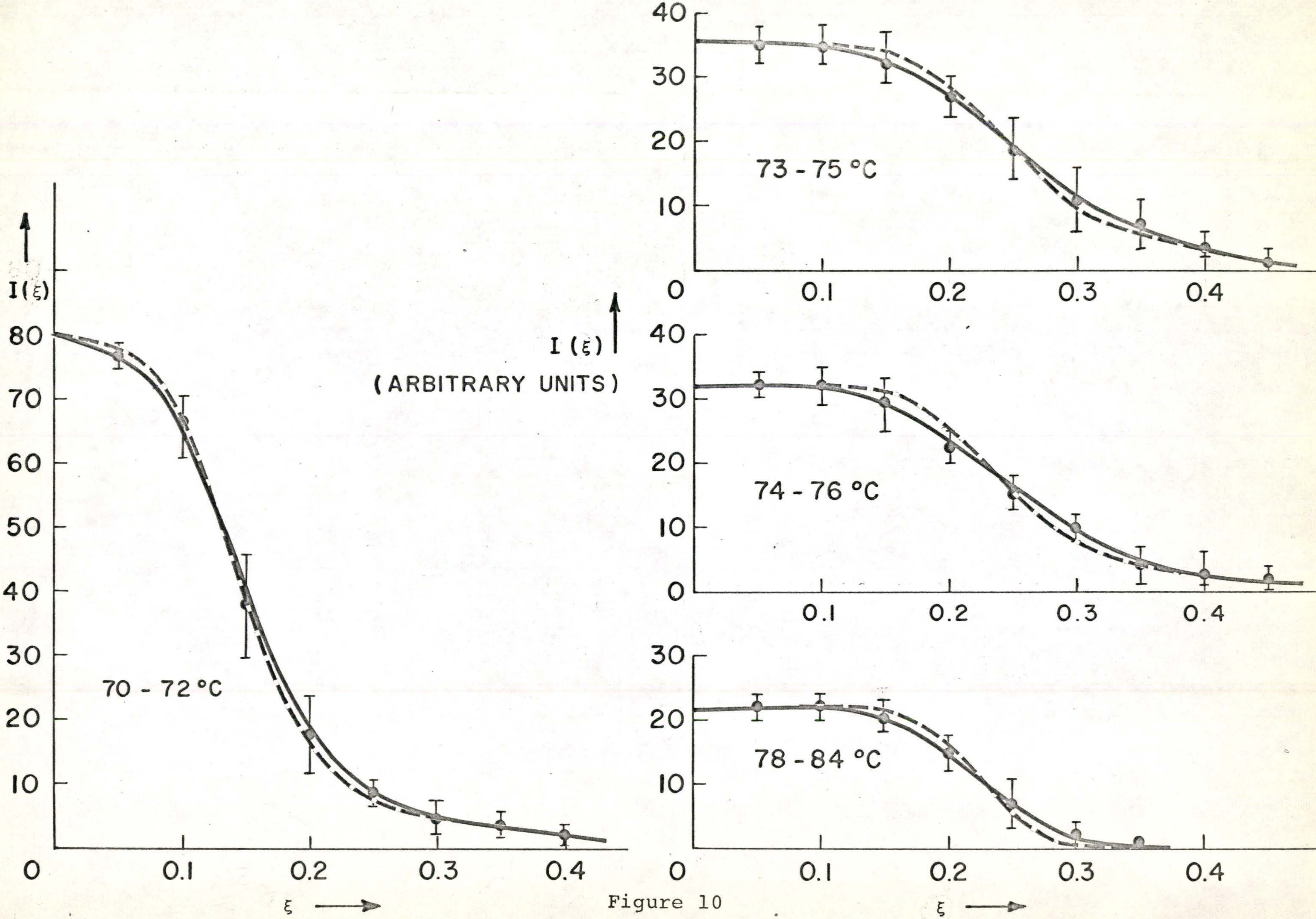

Figure 10
Intensity profiles of diffuse streaks

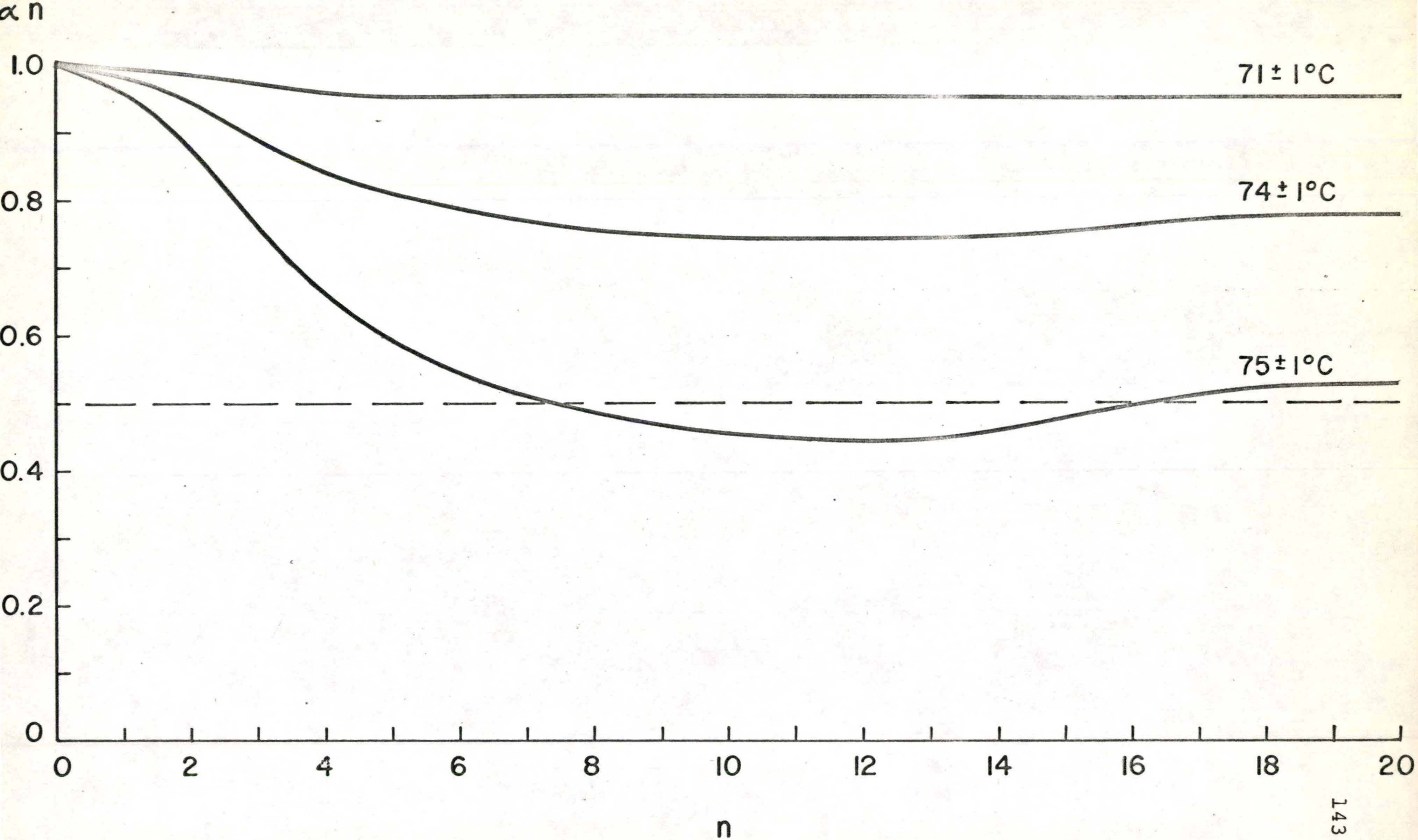

Figure 11

Probability $\alpha_n(T)$ calculated from the intensity profiles of the diffuse streaks.

CHAPTER 7: PHASE TRANSFORMATION STUDIES

(A) Theoretical Aspects

"Phases" are usually defined only in terms of two states of a system which are related by a "phase" transformation. A more general definition is provided by Guggenheim (1950). "If a system is not homogeneous, in order to describe its thermodynamic state we have to consider it as composed of a number, small or large, of homogeneous parts called phases, each of which is described by specifying its contents and a sufficient number of other properties." In addition to the more common phase changes which involve a change of state, a phase change may involve two liquid phases such as normal Helium I and the superfluid Helium II or two solid phases. Haas (1965) has classified the changes which may occur in a solid as follows.

(I) A continuous change without a change of symmetry. In this case there is no phase transition. (It should be noted that the change from the normal to superconducting state of a crystal is one case of a second order phase transition in a solid where there is no symmetry change.)

(ii) An abrupt change by a first order transition. At the transition temperature there are two phases in equilibrium with each other. There are no symmetry requirements for a first order phase transition to be possible.

(III) In a second order phase transition the properties of the crystal change gradually until at a certain transition temperature the change is complete. This type of transition is only possible if certain stringent conditions for the symmetry above and below the transition point are fulfilled.

Unless an energy barrier inhibits the transformation from one phase to another, a system will be found in the phase having the lowest Gibbs free energy at a given temperature and pressure. A transformation corresponds then to the intersection of the Gibbs free energy curves of two different phases of a system since at the transformation temperature the two phases coexist in equilibrium and therefore have the same Gibbs free energy density. The Gibbs free energy of one phase G_i is given by

$$G_i = U_i - TS_i + PV_i$$

where U_i is the internal energy of the system in the phase i, T is the temperature, S_i the entropy, P the pressure and V_i the volume of the system.

Ehrenfest (1933) has classified phase transitions according to the behaviour of the derivations of the Gibbs free energy. If at least one of the first derivatives of G, for example, $-\left(\frac{\partial G}{\partial T}\right)_P$ and $\left(\frac{\partial G}{\partial P}\right)_T$ are discontinuous the transition is denoted as "first order". These derivatives are respectively equal to the entropy and volume. If at least one of the second derivatives of G, notably the specific heat at constant pressure ($C_p = T(\frac{\partial S}{\partial T})_p$) and/or the coefficient of thermal expansion ($\alpha = \frac{1}{V}(\frac{\partial V}{\partial T})_p$) are discontinuous, while the first derivatives are not, the phase transition is denoted as "second order". Higher order transitions would be similarly defined but none have been observed in nature.

Most of the second order phase transitions which have been studied exhibit infinite changes in the second derivatives which are not analogous to the finite changes accompanying a first order transition. Callen (1960) has remarked that the phase transition of metals to the superconducting state in zero magnetic field appears to be the only second order phase transition exhibiting a single finite change in the second derivatives of G.

A more complete phenomenological description of second order phase transitions has been presented by Tisza (Smoluchowski, Mayer and Weyl, 1951). This description applies to second order phase transitions involving infinite changes in the second derivatives including some order-disorder phenomena. According to Tisza's theory, if U is the internal energy of the system and x_i are the set of t variables defining the system, then a second order phase transition occurs if the quadratic form

$$d^2U = \frac{1}{2}\sum_{j,k}^{t-1} \frac{\partial^2 U}{\partial x_j \partial x_k} dx_j dx_k$$

is positive semidefinite; ie. d^2U may be only zero or positive and the second order transition occurs when d^2U becomes zero. If d^2U is allowed to become negative a first order transition will occur. If the inflection point is such that $\frac{d^2U}{dSdx_i} = 0$ where S is the entropy and x_i is any other variable or linear combination of them, then the transformation is an order-disorder phenomenon. Tisza has called this a transformation of the second kind to distinguish his theory from that of Ehrenfest. Because of the fact that the curvature of the energy surface is changing sign or going to zero, that is, going from absolute stability to absolute instability, the transformation has also been called a critical phenomenon.

Both of the aforementioned treatments of second order phase transformations are essentially macroscopic in nature. Landau (Landau and Lifshitz, 1962) has formulated a set of necessary conditions for the existence of a second order phase transformation which relates to the microscopic processes involved. Haas (1965) has recently presented a discussion of Landau's theory and applied it to the phase changes in ferromagnetic and ferroelectric materials. Following Haas, Landau's theory may be summarized as follows:

(I) In order for a second order transformation to occur, the change of symmetry between two phases is such that the space group of one phase of the crystal is a subgroup of that of the other phase.

(II) Further, the symmetry operators corresponding to only one irreducible representation of the more symmetric phase may be lost in the change of phase.

(III) The change in electron density caused by the transformation may be described by a set of n functions belonging to the representation of order n associated with the transformation. If each of these n functions ϕ_i contribute a fractional amount γ_i to the change in electron density then the free energy G may be expanded about G_o at the transformation temperature in terms of homogeneous functions $f^{(j)}$ of order j in the γ_i. That is,

$$G = G_o + Af^{(1)} + Bf^{(2)} + Cf^{(3)} + Df^{(4)} + \ldots.$$

The free energy must be invariant to the operations of the group of the high symmetry phase which transforms the coefficients γ_i into each other. In order for the free energy to be invariant, the first and third order terms must vanish.

Landau and Lifshitz have derived a fourth condition for a second order phase transformation arising from the requirement that the crystal be stable against spatial inhomogeneity. The necessity of the fourth condition is a matter of current debate and in particular a number of second order phase transformations have been studied which are not homogeneous. Landau's theory is similar to that of Ehrenfest in that it cannot account for infinities in the specific heat curves.

First order phase transformations in covalent crystals are usually characterized by the breaking of bonds and volume discontinuities. In elemental crystals or ordered alloys the first order transition involves a rearrangement of packing, for instance, from face centered cubic to hexagonal close packed. Second order transformations are best exemplified by the ordering of alloys or cooperative phenomena such as the transformation to ferromagnetic or ferroelectric states in some solid state systems. A number of second order phase transformations involve entropy as one of the critical variables in the internal energy U.

In the expression for G, the PV term is relatively unimportant in second order transformations of condensed phases since the volume is continuous across the phase change. At high temperatures the term TS is dominant and the additional entropy of disorder makes the disordered phase energetically more favorable even though the internal energy U of the disordered phase may be greater. At lower temperatures the internal energy term becomes dominant and the ordered phase is stable. The specific heat of most second order transformations seems to diverge logarithmically in contrast to the simple discontinuity suggested by Ehrenfest. This specific heat curve is often broadened or "diffuse" with a tail above the critical or transformation temperature and hence is called a "λ" curve. The present understanding of phase transformations is best illustrated by a statement of Smoluchowski (Condon and Odishaw, 1958) which still remains true. "The field of phase transformations in solids is characterized by a huge amount of experimental (often only quantitatively significant) material and by a relative scarcity of satisfactory theories. This is particularly true of theories of the atomic mechanism and of kinetics of transformations."

(B) The Phase Transformations in $Cu_2P_2O_7$, $Mg_2P_2O_7$ and $Zn_2P_2O_7$

The transformation in $Cu_2P_2O_7$ is the easiest to understand and will be considered first since it may shed some light on the transformations in $Mg_2P_2O_7$ and $Zn_2P_2O_7$.

The specific heat Cp of $Cu_2P_2O_7$ has been investigated by Melkvi, Stager and Calvo (1967a). They used a continuous heating method to measure the heat capacity. The sample was suspended inside an adiabatic heat shield and the energy supplied to the sample and its temperature were monitored . The results of these experiments are shown in Figure 12. Because of the limited sensitivity of the equipment, the results for $Cu_2P_2O_7$ were difficult to obtain and should not be considered conclusive. The Cp curve for $Cu_2P_2O_7$ has a broad peak centered about 75°C with two additional discontinuities at 54°C and 85°C, although the discontinuity at 54°C may not be significant.

The height of the peak above the base line, which may be obtained by joining the curve below 54°C to the curve above 85°C by a smooth line, is only about 2.0 cal/mole-degree.

X-ray photographs show that the intensity of the reflections with odd values of ℓ in the α phase start to weaken with respect to the intensity of reflections with ℓ even as the temperature is raised above 50 or 60°C. It is difficult to fix the exact temperature at which this occurs because the magnitude of the change is very small in this region but the rate of intensity change increases with the temperature. Above 74.0 ± 1.0°C the Bragg peak is no longer observable. The streaks were first observed at 71.0 ± 1.0°C and their intensity decreased monotonically as the temperature was raised further. The diffuse streaks indicate that the crystal has become disordered. The specific heat anomally represents the energy required to produce the disordering and the shape of the Cp curve could suggest that the disordering takes place over the wider temperature region between 54°C and 85°C with the maximum rate of disordering appearing at 75°C. In their n.m.r. experiments, Stager and Atkinson (1967) have observed a change in the slope of the chemical shift of the ${}_{15}P^{31}$ nucleus plotted against temperature at 80 ± 5°C.

The lattice parameters of $Cu_2P_2O_7$ have been measured at room temperature and 100°C and show no large differences at the two temperatures. The photographs used to study the transformation were all taken over a small range of temperatures which overlap and cover the entire temperature range of the transformation. No broadening of the Bragg peaks was observed on these photographs. This evidence would seem to discount the possibility of a volume discontinuity associated with the phase transformation in $Cu_2P_2O_7$.

The direction of the streaks in reciprocal space is perpendicular to the layers of the structure as defined in Chapter 1(A). These layers must then be disordered; i.e. there is a loss of the translational symmetry between these layers. Such an inhomogeneity may occur either by a variation in the distance between the layers or a variation in the atomic arrangement in individual layers. Also, because the diffuse streaks appear only at reflections with ℓ odd, the variation in the atomic arrangements must correspond to a shift c/2 of some layers from their positions in α-$Cu_2P_2O_7$. The resolved structures of the high and low temperature structures of $Cu_2P_2O_7$ permit one to speculate as to what is the nature of the disordering mechanism.

In Chapter 5(A) the manner in which the c glide plane was generated throughout one layer was discussed. The layers are joined to one another by the bonding of terminal oxygen atoms of an anion in one layer to the cations in an adjacent layer. The terminal oxygen atoms are the O3 and O2 atoms. The major component of the displacement of the O2 atoms from their positions in α-$Cu_2P_2O_7$ to their positions in β-$Cu_2P_2O_7$ is in the c direction and is independent of the sign of the displacement of the central oxygen atoms; ie the sense of bending of the anion. As a result of the bending of the anion, the O3 atoms are displaced in the same direction as that of their bonds to the cations in neighbouring layers. If a layer of one type is situated between two layers of opposite type, then the most significant change from the bonding which would occur if all the layers were of the same type is that the long

Cu-O3' bonds that were of length 2.322 A and 2.946 A in α-$Cu_2P_2O_7$ now have lengths of 2.629 A and 2.632 A respectively. The two crystallographically independent Cu-O2 bond lengths are changed only from 1.962 A and 1.988 A to 1.954 A and 1.996 A respectively by the operation.

In a disordered or type II layer, we have assumed that all the anions have reversed their direction of bending and the cations have been moved such that their coordinates are consistent with those of the anions. The model for the phase transformation is illustrated in Figure 13. The cross hatched atoms belong to a type II layer. The type II layer appears the same as if it had been translated by *c*/2. When half of the layers have become type II, an arbitrarily chosen atom has equal probability of being in either type of layer, which is defined with respect to some fixed layer of type I, and therefore the effective length of the *c* axis appears to be halved. However the layers as seen by x-rays do not have full translational symmetry in the *a* direction.

The refinement of the structure of β-$Cu_2P_2O_7$ with the disordered model was an attempt to verify this picture for β-$Cu_2P_2O_7$. The R factors obtained in this way were slightly higher than those obtained with the fully anisotropic model although the latter contains more least squares variables. The weighted R factors were analysed using Hamilton's (1965) significance tables which showed a preference for the anisotropic model. These results are not conclusive, however, because of the problems encountered in the refinement of the disordered model. Also the unweighted R factors are nearly equal. The atomic positions given by this analysis are similar to those obtained by adding the root mean square of the principal axis of the thermal ellipsoid to the configurational coordinates of the completely anisotropic model of the structure. It is also noteworthy that the $Cu\text{-}O_3'$ distance in $\alpha\text{-}Cu_2P_2O_7$ is 2.58 ± 0.02 A and the average $Cu\text{-}O_3'$ distance between two layers of different types is 2.63 ± 0.02 A.

The functional dependence of bond energy on bond lengths is not known and therefore the difference between the energy of all inter-layer bonds between two given layers before and after one of them has been "disordered" can not be explicitly evaluated. However, the average bond length is not changed drastically and therefore the magnitude of the energy difference particularly for the cation should be small since it arises mainly from non-linearities in the energy versus bond length function since the average $Cu\text{-}O_3'$ bond length in the β phase is the mean of those in the α phase.

The decrease in intensity of the reflections with odd ℓ implies that there is a decrease in the deviations from the symmetry of the β phase at a lower temperature than that at which the streaks appear. Some disordering may take place at these temperatures such that the resultant streaks would be too weak to be observed. In addition there can be changes in the geometry of the anion. In particular the P-O-P angle may decrease as a function of temperature. In α-$Cu_2P_2O_7$ the displacement of the central O_1 atom out of the c glide plane, is 0.39 A. The structure of β-$Cu_2P_2O_7$ as resolved at 100°C gives a value of 0.21 ± 0.02 A for this displacement for both the disordered model and the root mean square displacement as determined from the thermal parameter of the anisotropic model. This displacement is a measure of the P-O-P angle. Although it has only been measured at two points it would appear that the P-O-P angle decreases with temperature. Further, the thermal expansion parameters of the crystal as measured at room temperature and 100°C show that the crystal expands as the temperature increases primarily by increasing the length of the a-c vector which is, in fact, nearly parallel to the P-P vector of the anion. The expansion in the crystal might be accommodated by an increase in the P-P distance or an increase in the long Cu-$O3'$ bonds but if the former is the case, the P-O-P angle will tend to approach nearer to 180°. The possible change in the anion geometry is illustrated in Figure 14 where the atomic coordinates obtained from the disordered model of β-$Cu_2P_2O_7$ are compared with those of α-$Cu_2P_2O_7$.

The apparent magnitude of the change in the P-O-P angle as indicated by the crystal structure of α- and β-$Cu_2P_2O_7$ seems rather large. This effect may be magnified by the thermal behaviour of the anion. The total area under the diffuse streaks and the Bragg peaks varies monotonically with temperature as may be seen by inspection of Figure 10. This is not consistent with the model of the phase transformation as has been presented at this point. When the layers are completely disordered the probability that a given layer is type I or type II will be completely independent of its environment and the quantities β_n discussed in Chapter 7(D) would only be non-zero when $n = 0$. The intensity profile $I(\xi)$ will then be a constant independent of ξ and at high temperatures we should find streaks of nearly constant intensity running along rows or reciprocal space for which k and ℓ are constant and extending in the $\underline{a}^*$ direction. Attempts were made to observe streaks of this nature but they did not appear to exist. Also from Figure 10 it may be seen that the total integrated intensity of the streaks decreases as the temperature is raised.

As the temperature is raised above the region of the transformation, the anions should find less hindrances to changing their sense of bending and individual layers would be able to change more rapidly from type I to type II configurations. It might then be expected that there would be some loss of homogeneity within the individual layers. This disorder would consist of a partial loss of the $\underline{c}$ glide operation and the $\underline{b}$ translation. There is some evidence for disorder within layers in that the diffuse streaks become broader as the temperature is raised. It would then appear most likely that the diffuse scattering from the disordered lattice is spread over all of reciprocal space and is therefore not observable. As the temperature is raised still further, the anion might assume a state of enhanced thermal motion with the central O1 oscillating anharmonically across a multi-well potential. This effect would cause the O1 atom to appear nearer the c glide plane than in a model based on a disordering of the α-$Cu_2P_2O_7$ structure at room temperature.

The Fourier transform of the diffuse streaks permits one to speculate as to the distribution of the two types of layers. Table II lists the probabilities $\alpha_n(T)$, that at the temperature T, the layers m and m + n are of the same type. Since the shape of the intensity profiles of the streaks does not change above 75°C the transforms are only listed at 71 ± 1°C, 74 ± 1°C and 75 ± 1°C. This analysis has not taken into account the effects of the aforementioned disordering within the layers and therefore cannot account for the changes in the total integrated intensity of the streaks. The simplest approximation to the profile of the streaks is a step function and therefore α_n might be expected to be oscillatory. This then suggests that the layers form small groups of the same type.

The α_n curves fall off smoothly and then perform small oscillations about an average value determined by the height of the Bragg peak. If the height of the Bragg peak is zero, the oscillations are about the value 0.50. If we postulate a model for the layer distribution consisting of groups of layers of the same type imbedded in a sea of completely disordered layers, we can estimate the average number of layers in each group by noting the number "n" where the α_n curve first reaches the value about which it oscillates. These numbers are then 40 at $71 \pm 1^{\circ}C$ and 7 at both $74 \pm 1^{\circ}C$ and $75 \pm 1^{\circ}C$. There must still be some long range order in the crystal above that implied by the width of the aforementioned groups of layers since they are not large enough to prevent broadening of the central peak.

The phase transformation in $Mg_2P_2O_7$ has been studied by a number of workers. Roy, Middleswarth and Hummel (1948) found evidence of a volume discontinuity near $70^{\circ}C$. Their study of the Debye-Scherrer pattern of $Mg_2P_2O_7$ also indicated that in contrast to $Cu_2P_2O_7$ the high and low temperature phases were distinct and coexisted over a small temperature range. Calvo, Leung and Datars (1967) have also observed the coexistance phenomenon in the e.p.r spectrum and the single crystal diffraction pattern of $Mg_2P_2O_7$. It appears that there is a continuous change in the relative amounts of each phase and the size of the α and β phase regions in the crystal are macroscopic since there appears to be no line broadening of the e.p.r. spectra. Calvo (1967d) has observed index of refraction discontinuities in crystals of $Mg_2P_2O_7$ near the transformation region with a hot stage microscope. These discontinuities moved laterally in a direction perpendicular to the layers which are involved in the disordering mechanism in the case of $Cu_2P_2O_7$. These striations are a manifestation of the volume discontinuity in $Mg_2P_2O_7$, and this behaviour would suggest some similarity between the transformations in $Mg_2P_2O_7$ and $Cu_2P_2O_7$. However, the volume discontinuity would suggest that there is a more significant change in the interatomic bonding than in $Cu_2P_2O_7$. This in fact is the case since not only does the P-O-P angle in α-$Mg_2P_2O_7$ deviate further from linearity than in α-$Cu_2P_2O_7$ but the change in the length of the long cation-oxygen bonds is more pronounced. One interatomic distance to one of the two crystallographically independent cations is decreased in length from 3.35 A to 2.15 A in going from the α to the β form of $Mg_2P_2O_7$.

The specific heat at constant pressure Cp of $Mg_2P_2O_7$ has been recently measured by Melkvi, Stager and Calvo (1967b). They found a large peak at 66.5°C of height greater than 500 cal/mole-degree which is roughly 250 times the height of the peak in $Cu_2P_2O_7$. The enthalpy of the transformation ΔH is obtained by integrating the area under the peaks of the Cp curves. The accuracy of the curve associated with the transformation in $Cu_2P_2O_7$ does not permit a realistic assessment of ΔH but it would appear to be considerably less than the ΔH of 729 ± 4 cal/mole determined by Oetting and McDonald (1963).

From the evidence presented above this phase transformation must be first order although high and low temperature phases coexist over a finite range of temperature. Mayer and Streeter (1939) have introduced the term "diffuse first order" to describe a transformation such as this.

The e.p.r. parameters of Cu^{+2} and Mn^{+2} ions in solid solution in $Zn_2P_2O_7$ have been studied in detail by Chambers, Datars and Calvo (1964). Above 155°C only one e.p.r. site appears but below this temperature there are two sites. At 132°C there is an abrupt change in the spectra with the appearance of at least one more nonequivalent site. Furthermore the axial splitting parameter D, which describes the interaction of the effective spin component S_z with external fields, was found to assume two values at 155° which diverged continuously as the temperature was lowered to 132° where the discontinuity occurred.

The discontinuous e.p.r. parameters at 132° must result from a discontinuous change in electron density which is characteristic of a first order phase transformation. The possibility of a volume discontinuity in $Zn_2P_2O_7$ at 132° has not been investigated although the lattice parameters at room temperature referred to the β unit cell are considerably different from those of the β phase above 155°C. The crystal structure of α-$Zn_2P_2O_7$ shows larger deviations from that of β-$Zn_2P_2O_7$. In particular four Zn-O3$'$ interatomic distances have been increased by approximately one angstrom. A volume discontinuity would then not be unexpected. The appearance of two crystallographically independent cation sites between 132° and 155° is not consistent with the space group C2/m although the single crystal x-ray pattern does not show any definitive change from that of β-$Zn_2P_2O_7$ in this temperature region. The principal axis of the magnetic moment tensor which is constrained to lie along the b axis in β-$Zn_2P_2O_7$ was observed to be slightly removed from colinearity with this axis in the intermediate phase region. These results are not consistent with the space group C2. Also the observed e.p.r. spectrum is not consistent with the symmetry imposed on the cations by the mirror plane if the space group were Cm . These, however, are the only space groups allowed by the Laue symmetry and extinctions.

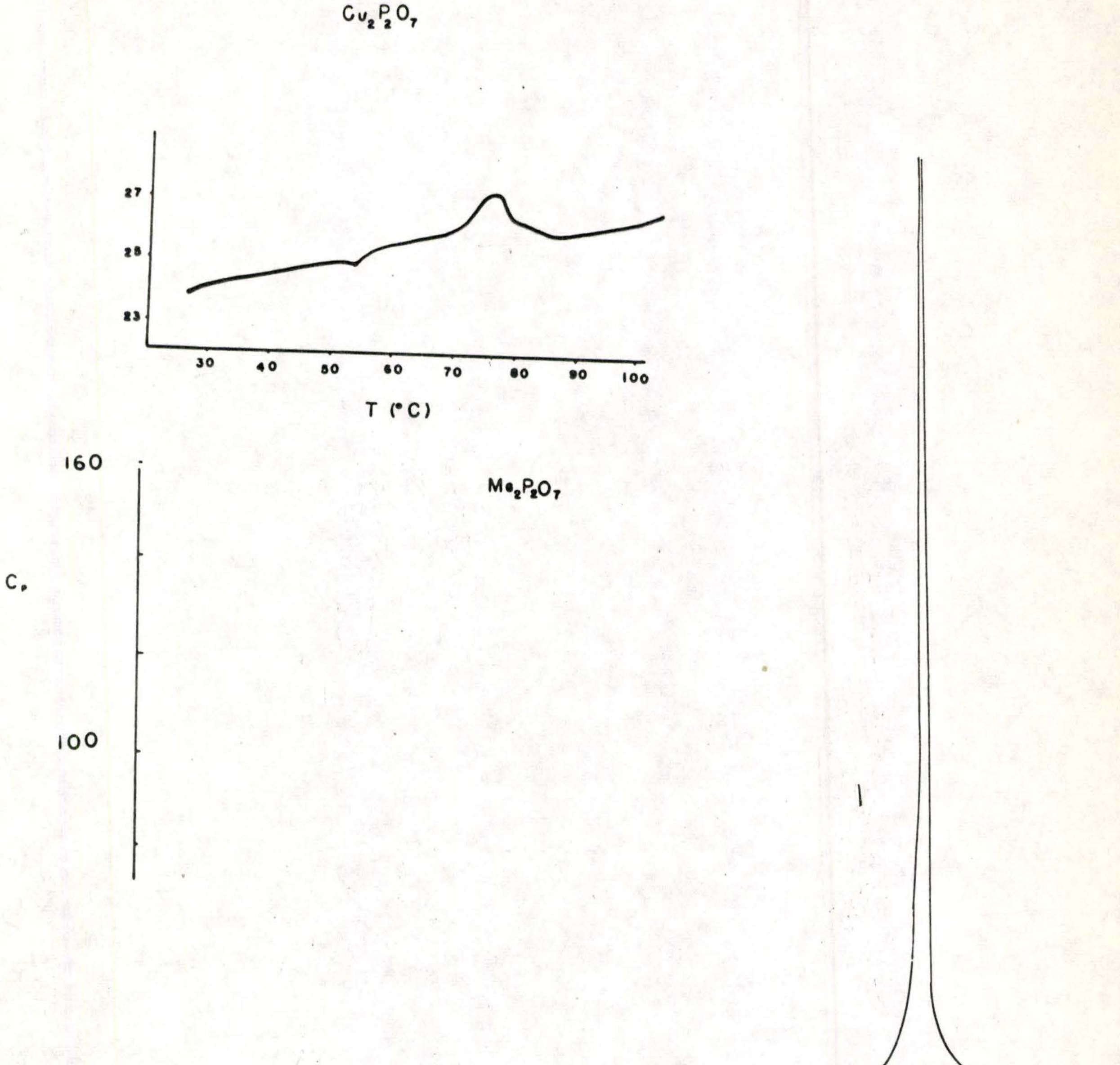

Figure 12

The specific heat at constant pressure of $Cu_2P_2O_7$ and $Mg_2P_2O_7$ in units of cal/mol-degree (From Melkvi et.al. 1967a and b)

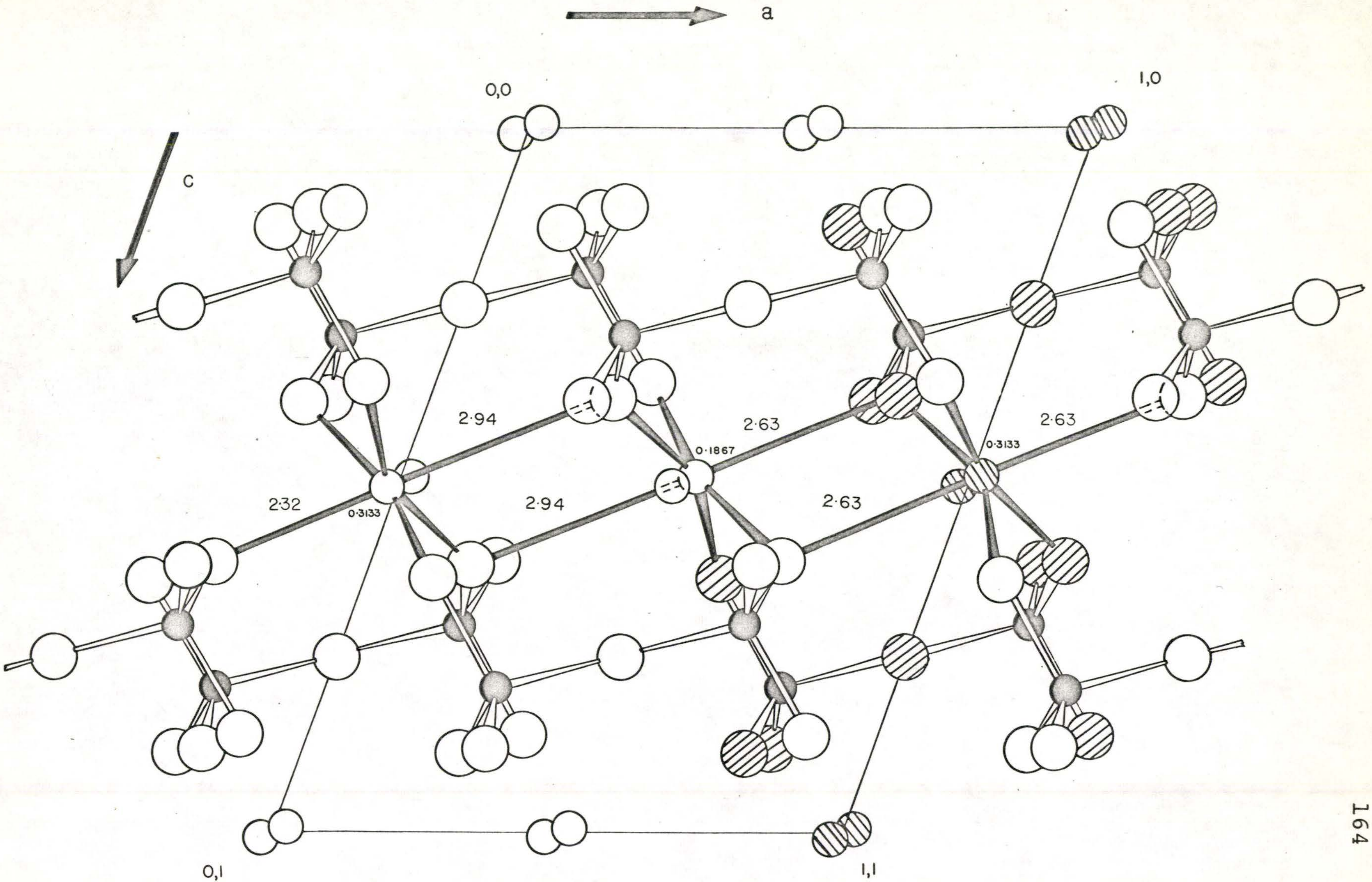

Figure 13

The crystal structure of α-$Cu_2P_2O_7$ in projection down the b axis. The shaded atoms belong to a disordered layer. The atoms are represented as in Figure 4.

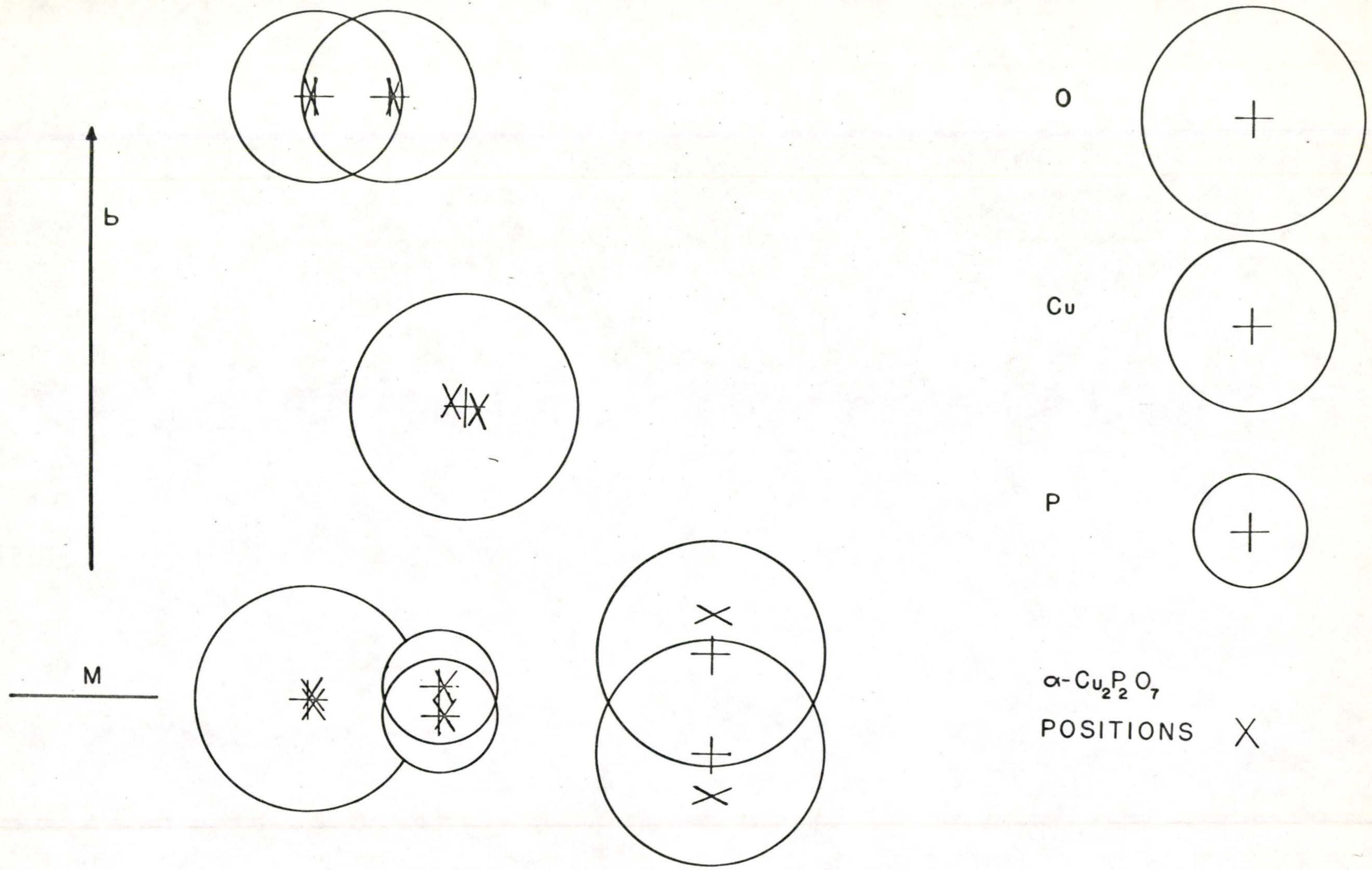

Figure 14

Comparison of the disordered model of β-$Cu_2P_2O_7$ with the crystal structure of α-$Cu_2P_2O_7$

CHAPTER 8: DISCUSSION

The small specific heat anomally, the absence of a volume discontinuity and the proposed interpretation of the diffuse streaks in $Cu_2P_2O_7$ are all indicative of a second order transformation. It would also appear that during the transformation the crystal has ordered regions of various sizes and therefore the transformation must then be classed as a non-homogeneous one. The change in space groups which accompanies the transformation are consistent with the restrictions imposed by Landau's criteria for a second order phase transformation. Since two phases coexist in $Mg_2P_2O_7$, the transformation must also be non-homogeneous. However the large specific heat anomally, the volume discontinuity, the e.p.r. and x-ray studies show that this transformation is diffuse first order. Here, Landau's criteria for a second order transformation, in terms of the relationship between the space groups of α and β phases, is violated. The e.p.r. experiments with Mn^{++} and Cu^{++} doped $Zn_2P_2O_7$ indicates that the transformation at 132°C is first order and is accompanied by a second order transformation extending to 155°C. The space group of the intermediate phase between 132°C and 155°C according to the e.p.r. results cannot be any of C2, Cm or C2/m but the Laue symmetry and extinctions give only these as the possible space group. This would suggest that the intermediate phase may be non-homogeneous but the e.p.r. results should be re-examined.

The obvious question must now be asked as to whether or not all the β phase structure are disordered as is the proposed structure of β-$Cu_2P_2O_7$. No evidence for diffuse streaks has been found in β-$Mg_2P_2O_7$, β-$Zn_2P_2O_7$ or $Mn_2P_2O_7$. Further, in order to be similar to β-$Cu_2P_2O_7$, the β phases of $Mg_2P_2O_7$ and $Zn_2P_2O_7$ would have to have a unit cell at some stage of their transformations which has the same relative dimensions and symmetry as α-$Cu_2P_2O_7$. It is not possible for either $Mg_2P_2O_7$ or $Zn_2P_2O_7$ to do this by adding additional symmetry operators to those of their space groups in the α form. Also, because of the large changes in bond lengths associated with the first order transformations in $Mg_2P_2O_7$ and $Zn_2P_2O_7$ their β structures cannot be constructed as averages of the α structures. However, the magnitude of the changes in bond length may not be as large as that indicated by a comparison of the room temperature and β structures since the α forms at the transformation temperature are not necessarily identical to the room temperature structure. All of the phase transformations involve the loss of a c glide plane which becomes a mirror plane in the β phase. Also, all of the structures isostructural to thortveitite which have been refined with anisotropic temperature factors show large anisotropic components associated with the central O1 atom of the anion. It appears quite probable then that the behaviour of the anion in these compounds is in some ways similar to that in β-$Cu_2P_2O_7$, but it cannot be stated whether their structures are disordered or undergoing extreme anharmonic thermal motion. The anion in β-$Cu_2P_2O_7$ may also begin to vibrate anharmonically as the temperature is raised beyond the transformation region. The existence of linear X-O-X groups in $X_2O_7^{-n}$ anions has been questioned by Liebau (1961).

The structure of the α-$Zn_2P_2O_7$ shows 2/3 of the cations with only five fold coordination. Lazarev, Tenisheva and Petrova (1965) investigated the infrared spectrum of α-$Zn_2P_2O_7$ and proposed that the cations were in octahedral environments as opposed to tetrahedral. They apparently did not consider the possibility of the five fold coordination. Paoletti and Ciampolini (1967) have recently studied the heat of formation of five coordinated complexes of the first transition series (Mn^{+2} - Zn^{+2}) compared with that of four and six coordinated compounds. They find that Zn^{+2} differs from the other members of the series in that five fold coordination appears slightly more energetically favorable than six coordination. Also the four coordinated $(ZnBr_4)^{-2}$ ion has approximately the same heat of formation as the six coordinated ion used in comparison. All of these results are referred to a zero heat of formation for Mn^{+2} with each coordination number. Zinc is also the only member of the series that is five coordinated as opposed to six coordinated in the elemental solid (Wells, 1962). A preference of zinc for lower coordinated sites has been noted in some recent x-ray studies of orthophosphates. β-$Zn_2(PO_4)_2$ (Stephens and Calvo, 1967a) shows a lower average cation oxygen coordination than does β'-$Mn_3(PO_4)_2$ or β'-$Cd_3(PO_4)_2$ (Stephens and Calvo, 1967b) which have similar structures to β-$Zn_3(PO_4)_2$. Also in γ-$Zn_3(PO_4)_2$ (Calvo, 1963) which has octahedrally and tetrahedrally coordinated cation sites, the luminescent wavelength suggests that Mn^{+2} ions substitute preferentially in the octahedral site although the correlation between luminescent wavelength and coordination number has been questioned by Calvo, Van Nest and Datars (1967). They studied the emission of Mn^{+2} in solid solutions in $Zn_2P_2O_7$ and found no marked change in the emission wavelength through the region of the phase transformations discussed earlier.

The difference in the length of the long M-$O3'$ bonds from the average length of the shorter equatorial bonds is significantly greater in β-$Cu_2P_2O_7$ than in the other isostructures of thortveitite. The lengthening of two trans bonds of an octahedrally ligated ion is referred to as a tetragonal distortion and is a relatively common occurrence in the case of Cu^{+2} cations (Pake, 1962). If the octahedron is otherwise regular this phenomenon may be explained by the "Jahn-Teller" effect (Ballhausen, 1962). The electronic states of an ion must be consistent with the symmetry of its ligands which is taken to be cubic. Under these conditions the ground state of $3d^9\ {}^2D_{5/2}$ Cu^{++} is a degenerate e_g state. A tetragonal distortion of the ligand positions removes the degeneracy of the ground state and the new ground state will be that of lowest energy arising from the former degenerate ground state. The difference in energy between the new ground state and the parent e_g state will depend on the magnitude of the tetragonal distortion. The position of the oxygen ligands will be altered from octahedral symmetry to a point where the difference between the energy gained from the removal of the degeneracy and the energy required to distort the cubic symmetry of the cation sites is a maximum. The symmetry of the Cu^{+2} site in either α-$Cu_2P_2O_7$ or β-$Cu_2P_2O_7$ cannot be described as tetragonally distorted from cubic and this analysis cannot be applied directly. However, we might speculate that the unusual length of the Cu-O3' bonds is related to the behaviour of the ground state of a Cu^{+2} ion in an octahedral environment. Further, the dependence of bond energy on the length of the trans Cu-O3' bonds may be relatively weak for long bond distances. The sum of the lengths of the trans bonds in α-$Cu_2P_2O_7$ is 5.26 A. This is roughly the same as the sum of the lengths of the two analagous cation-oxygen interatomic separations in α-$Mg_2P_2O_7$ and α-$Zn_2P_2O_7$ which become the two trans bonds of equal length in the β forms.

As was discussed earlier in Chapter 5 the elongated cation-oxygen bonds in the β phase of all these structures may be explained by a comparison with the structure of $PbSb_2O_6$. It would appear that $Cu_2P_2O_7$ accommodates the stress in the <u>a</u>-<u>c</u> direction by allowing one bond to increase in length to 2.322 A while the other, presumably much weaker, is 2.940 A long. In the other compounds only one bond is changed to accommodate the stress and this one is increased in length by over 1.0 A. It is not surprising then that the phase transformation in $Cu_2P_2O_7$ is somewhat unique.

The justification of the choice of space groups of α-$Cu_2P_2O_7$ and α-$Zn_2P_2O_7$ have been discussed earlier. It is now possible to discuss the choice of the space group of β-$Cu_2P_2O_7$. It is unlikely that the two fold axis of the α phase would be lost in transforming to the high temperature form and therefore the space group Cm is unlikely. Also the mechanism postulated for the phase transformation requires that the β phase have a mirror plane which is generated from the <u>c</u> glide plane. The space group C2/m is the only one which is consistent with Landau's criteria for the existence of a second order phase transformation.

The proposed mechanism of the phase transformation involves the motion of the central oxygen atom across the barrier of a multi-well potential. We may gain some further insight into the nature of the phase transformation by the following considerations. If a pyro ion $X_2O_7^{-n}$ with the staggered configuration is viewed down the length of the X-X vector, the oxygen atoms appear as a hexagonal arrangement about the X atoms. We now wish to consider the potential energy required to displace the central O1 atom from colinearity with the X-X vector as a function of the rotation angle about the X-X vector. This curve will have six minima corresponding to the six positions between the terminal oxygen atoms as they appear in projection. The environment of the anion in the structures of the "small cation" pyrocompounds causes two of these minima, which correspond to the direction of the b axis, to be deeper than the others. Further, in the low temperature structures of $Cu_2P_2O_7$ and $Mg_2P_2O_7$ one of these is slightly deeper than the other by some amount δ. α-$Zn_2P_2O_7$ may be more complicated because the displacement of the central O1 atom from colinearity with the P-P vector deviates significantly from the b direction. The energy δ may be considered as the "activation energy" of the transformation. As the temperature is raised δ may decrease slightly and when the contribution of the entropy term to the Gibbs free energy becomes sufficiently large near 71°C, the central O1 atom may cross to the second lowest energy minimum on the other side of the c glide plane. It should be understood that the motion of the O^1 atom involves the bending of the entire anion since it is bonded to the two tetrahedrally coordinated P atoms. The energy δ must still be finite up to

74°C where the Bragg peak disappears. Above this temperature neither minimum in the potential energy function is preferred and δ is small in comparison with the entropy contribution.

The photographs used to study the transformation show no hysteresis effects and since the crystal develops some long range order as the temperature is lowered, the non-zero value of δ between 71°C and 74°C must be a cooperative phenomenon and this implies some long range interaction between layers. The model of the phase transformation as has been presented is based only on the nature of the bonding between adjacent layers. The model is, in effect, a pseudo-one dimensional Ising model. Tobolsky,Kozak and Canter (1965) have discussed in detail the application of a one-dimensional Ising model in order to describe a phase transformation such as this.

It is instructive to compare the intensity profile of the streaks associated with the phase transformation of $Cu_2P_2O_7$ with those arising from growth disorder. If each layer has the probability α of going into the "wrong" position during the growth of a crystal, then the intensity profile of the reflections affected by the disorder is proportional to $\alpha/(\alpha^2 + \pi^2\xi^2)$ (Wilson, 1949). This is a Lorentzian curve centred about the point $\xi = 0$ which corresponds to the Bragg peak. In this case the streaks blend continuously into the Bragg peak and background. This is a manifestation of the breakdown of long range order which tends to produce diffuse scattering at small values of ξ since such values correspond to long interlayer distances in the real crystal. This is in marked contrast to the diffuse scattering in $Cu_2P_2O_7$ which remains distinct from the Bragg peak at all temperatures. This in turn is a manifestation of the loss of short range order in $Cu_2P_2O_7$.

The pyrophosphates of the alkaline earths Ba, Ca and Sr do not assume the thortveitite structure. Mg^{+2} is a member of the alkaline earths but it has the thortveitite structure, probably because it has a small ionic radius. The ionic radius of Cd^{+2} is larger than those of the cations belonging to thortveitite family of pyrophosphates and $Cd_2P_2O_7$ does not have the thortveitite structure (Au, 1966) while $Cd_2V_2O_7$ does (Au and Calvo, 1967).

The radii and radius ratios of M and X in $M_2X_2O_7$ are given in Table 21 for some compounds. The radii of P, As and Si are the covalent radii and are taken from Pauling (1960). The radius assigned to V is also the covalent radius and is taken from Bachmann and Barnes (1962). None of these radii are particularly accurate since they were obtained from several structural types and involve several assumptions, but they do show a definite trend. Except for $Ni_2As_2O_7$ and $Co_2As_2O_7$, these compounds assume the thortveitite structure if the ratio of the radius of M to the radius of X does not exceed roughly 0.85.

An increase in the cationic radius would decrease the magnitude of the perturbation from the idealized $PbSb_2O_6$ structure and the explanation for the limiting effect of the radius must be found elsewhere. The terminal oxygen atoms labelled O3 at one end of an anion are each bonded to one X atom and two M atoms whose octahedral arrangement of ligands share one edge formed by the O2 atoms. The maximum separation of the O3 atoms is limited by the size of the anion and their minimum separation is limited by the minimum separation of the cations. It is therefore evident that if the ratio of the radius of M to that of X exceeds some value the compound might find it energetically more favourable to adopt some other packing arrangement such as that of the alkaline earth pyrophosphates or $Cd_2P_2O_7$.

Table 22 shows the average P-O-P angles of all the pyrophosphate structures which have been studied to date and in which the P-O-P angles are not restricted by symmetry to be 180°. The $P_2O_7^{-4}$ groups are bent further from the linear configuration in the rare earth pyrophosphate $Na_4P_2O_7 \cdot 10H_2O$ and in the alkaline earth pyrophosphate $\beta\text{-}Ca_2P_2O_7$ than in the three "small cation" pyrophosphates whose cations are transition metal ions. This would suggest that the Na^+ and Ca^{+2} cations which are less electronegative than Zn^{+2}, Mg^{+2} or Cu^{+2} produce more charge delocalization which in turn causes the P-O-P angle to deviate further from 180°. However the P-O-P angle of $Cd_2P_2O_7$ should be similar to that of the transition metal compounds. The amount of bending of the P-O-P angle cannot then be predicted solely on the basis of charge delocalization and presumably such factors as the molecular packing significantly influence the character of the $P_2O_7^{-4}$ group.

TABLE 21

Radius ratios of pyro compounds, $M_2X_2O_7$ (see text for references)

M	Radius	X	Radius	Ratio	
Mg^{+2}	0.65	P	1.10	0.59	(thortveitite structure)
Mn^{+2}	0.82	P	1.10	0.75	(thortveitite structure)
Zn^{+2}	0.74	P	1.10	0.67	(thortveitite structure)
Ni^{+2}	0.68	P	1.10	0.62	(thortveitite structure)
Cu^{+2}	0.72	P	1.10	0.65	(thortveitite structure)
Ba^{+2}	1.35	P	1.10	1.23	
Ca^{+2}	0.99	P	1.10	0.90	
Sr^{+2}	1.13	P	1.10	1.03	
Cd^{+2}	0.97	P	1.10	0.88	
Cd^{+2}	0.97	V	1.20	0.81	(thortveitite structure)
Zn^{+2}	0.74	As	1.21	0.61	(thortveitite structure)
Mg^{+2}	0.65	As	1.21	0.54	(thortveitite structure)
Sc^{+3}	0.69	Si	1.17	0.59	(thortveitite structure)
Co^{+2}	0.72	As	1.21	0.59	
Ni^{+2}	0.68	As	1.21	0.56	

TABLE 22

P-O-P angles of some pyrocompounds

	Reference	P-O-P angle	Average
$Na_4P_2O_7 \cdot 10H_2O$	(a)	130°	130°
$Cd_2P_2O_7$	(b)	128°	128°
β-$Cu_2P_2O_7$	(c)	131° ,138°	134.5°
α-$Mg_2P_2O_7$	(d)	144°	144°
α-$Zn_2P_2O_7$		139°,137° ,150°	145°
α-$Cu_2P_2O_7$		156°	156°

(a) MacArthur and Beevers (1957)

(b) Au and Calvo (1967)

(c) Webb (1966)

(d) Calvo (1967d)

CHAPTER 9: CONCLUSION

The solid state phase transformations which occur in these compounds have been shown to be associated with the bent pyrophosphate anion and the c glide plane which is generated by this bent anion.

One half of the cations in the low temperature (α) form of $Mg_2P_2O_7$ are five coordinated and the other half are six coordinated as in the high temperature (β) form. Two-thirds of the cations in the α phase of $Zn_2P_2O_7$ are five coordinated and the remainder are six coordinated. The cations in the α phase of $Cu_2P_2O_7$ are bonded to four oxygen atoms with normal Cu-O interatomic separations and two other oxygen atoms are 2.322 A and 2,940 A from each cation. The phosphorus- oxygen distances in the "small cation" pyrophosphates which have been discussed previously show some variations because of the affects of the environment but they are nearly in agreement with the predictions of Cruickshank (1961). The phase transformation in $Cu_2P_2O_7$ indicates that the β form is disordered and the other high temperature forms, at least of $Mg_2P_2O_7$ and $Zn_2P_2O_7$, may be similar. This suggests that the anions in the structures isostructural to thortveitite may only appear linear either because of a statistical disordering or enhanced thermal motion across a multi well potential.

The order-disorder phenomenon in $Cu_2P_2O_7$ is one-dimensional and may be described as primarily a loss of short-range order although some long-range effects are implied by the behaviour of the Bragg peaks. In this respect it is quite uncommon since most one-dimensional disorders are related to growth defects and therefore are temperature independent.

The method used to refine the structure of the disordered model of β-$Cu_2P_2O_7$ is in essence the refinement of a rigid group with one least square variable defining the geometry of the group. This method should be applicable to any structure in which some of the atoms undergo enhanced thermal motion. If the root mean square displacement of an atom from its equilibrium position (due to thermal vibration) is of the same order of magnitude as the atomic radius, its time averaged electron density may be less at its center than at the point where it reverses the direction of its oscillatory motion. Its electron density distribution is no longer ellipsoidal and should not be approximated by an anisotropic thermal tensor.

In the light of the above results, a number of interesting questions may now be posed, most of which are, in fact, amenable to solution. It has been suggested that the structures of the low temperature forms of the "small cation" pyrophosphates near the phase transformation might be slightly different from their structures at room temperature. Also the structure of α-$Zn_2P_2O_7$ as it stands at the moment is not completely satisfactory. It should be possible to collect data suitable for these purposes as a function of temperature using a diffractometer and a variable temperature control device. If the intensity of each reflection were measured at a number of temperatures while the other experimental variables were held constant, the relative errors in the resultant structures should be sufficiently small to permit an analysis as to how the structure changes as a function of temperature even though the absolute errors may be much larger. This information would shed more light on the nature of the phase transformations. However, it may be necessary to collect data for the structure of α-$Zn_2P_2O_7$ at liquid nitrogen temperatures in order to surmount the correlation problems discussed previously.

A similar experimental arrangement could be used to investigate the structure of the intermediate phase of $Zn_2P_2O_7$ as a function of temperature. The results of such an analysis would be useful, not only to answer questions concerning the phase transformation, but to elucidate the relationship between the changes in electron density and changes in the e.p.r. parameters as measured by Chambers et. al. (1964).

The thortveitite structure and structures similar to thortveitite appear to occur quite commonly. It would be of interest to find the extent to which the structure does occur and the limiting factors which determine whether or not it is stable, since the radius ratio of M to X in $M_2X_2O_7$ has not proven to be a sufficient limiting condition. In particular the structures of $Co_2As_2O_7$ and $Ni_2As_2O_7$ should be investigated in order to determine, if possible, why they do not assume the thortveitite structure since their cations have small radii. Also, the resolution of the structures of the alkaline earth pyrophosphates, in particular, that of α-$Ca_2P_2O_7$ will help to elucidate the nature of a series of phase transformations which are quite different from those found in the "small cation" pyrophosphates.

There remain a number of questions concerning the phase transitions in the compounds studied here. The behaviour of the volume of the unit cell of $Zn_2P_2O_7$ in the transformation region is not known. Also the Cp curves of $Zn_2P_2O_7$ should be studied in detail. The diffuse streaks were only observed with crystals obtained from one "batch" of $Cu_2P_2O_7$ crystals. It is not unlikely that the behaviour of these streaks and the transformation temperature is dependent on the method of preparation of the crystals and the concentration of impurities in the crystals since entropy plays an important role in the transformation. Finally the treatment of one dimensional disordering mechanisms presented by Tobolsky et.al.(1965) should be applied in detail to the case of $Cu_2P_2O_7$.

APPENDIX A: GENERALIZED NON-LINEAR LEAST SQUARES ANALYSIS

Let S_i^o be a set of quantities which may be observed and measured. Let $S_i^c(\underline{p})$ be a member of a set of known functions of the vector $\underline{p}$ having n components p_j in a given basis. Then if the S_i^o can be measured accurately and $\underline{p}$ is accurately known, $S_i^o = S_i^c(\underline{p})$ exactly for all i. In practice, however, S_i^o will be measured with some error σ_i, but a sufficient number m of the quantities S_i^o can be measured such that the problem is overdetermined; that is $m >> n$. If approximate trial values are known for the components of $\underline{p}$ and the errors σ_i are such that S_i^o is normally distributed, then the best values of the components p_j are obtained by minimizing the quantity R defined in terms of $p_j + \Delta p_j$ where Δp_j is a small correction to be applied to the trial value p_j. R is then given by

$$R\ (\underline{p} + \Delta\underline{p}) = \sum_{i=1}^{m} \frac{1}{\sigma_i^2} \left| S_i^o - S_i^c(\underline{p} + \Delta\underline{p}) \right|^2$$

We must now find values of $\underline{\Delta p}$ such that $R(\underline{p} + \underline{\Delta p}) < R(\underline{p})$ We may first expand $S_i^c(\underline{p} + \underline{\Delta p})$ that is,

$$S_i^c(\underline{p} +\ \underline{p}) = Si^c(\underline{p}) + \sum_{j}^{n} \frac{\partial S_i^c(\underline{p})}{\partial \underline{p}_j} \Delta p_j + O(\underline{\Delta p})^2$$

We also define $D_i(\underline{p}) \equiv S_i^{\,o} - S_i^{\,c}(\underline{p})$ and drop terms of order greater than one in Δp. Then

$$R(\underline{p} + \underline{\Delta p}) = \sum_i^m \frac{1}{\sigma_i^{\,2}} \left| D_i(\underline{p}) - \sum_j^n \frac{\partial S_i^{\,c}(\underline{p})}{\partial p_j} \Delta p_j \right|^2$$

Now to find a minimum in R we set the variation of R with respect to Δp_j for all j equal to zero. If the components p_j are independent, we may write

$$\frac{\partial R(\underline{p} + \underline{\Delta p})}{\partial(\Delta p_k)} = 2 \sum_i^m \frac{1}{\sigma_i^2} \left| D_i(\underline{p}) - \sum_j^n \frac{\partial S_i^{\,c}(\underline{p})}{\partial p_j} \Delta p_j \right| \frac{\partial S_i^{\,c}(\underline{p})}{\partial p_k} = 0$$

In matrix form this equation becomes

$$\underline{\underline{B}}\ (\underline{\Delta p}) = \underline{A}$$

where

$$B_{jk} = \sum_i^m \frac{1}{\sigma_i^{\,2}} \frac{\partial S_i^{\,c}(\underline{p})}{\partial p_j} \frac{\partial S_i^{\,c}(\underline{p})}{\partial p_k}$$

and

$$A_k = \sum_i^m \frac{1}{\sigma_i^{\,2}} D_i(\underline{p}) \frac{\partial S_i^{\,c}(\underline{p})}{\partial p_k}$$

These are the "normal" equations of the least square refinement. In order to find the components of $\underline{\Delta p}$, $\underline{\underline{B}}^{-1}$ is determined and multiplied into $\underline{A}$. New trial parameters are obtained by adding $\underline{\Delta p}$ to $\underline{p}$ and the entire procedure may be repeated several times since the expansion is not exact. The standard deviation δ_j in p_j may be estimated from the matrix $\underline{\underline{B}}^{-1}$ That is

$$\delta_j = \left\{ \frac{B_{jj}^{-1}}{m-n} \sum_{i=1}^m \frac{1}{\sigma_i^{\,2}} D_i^2\ (\underline{p} + \underline{\Delta p}) \right\}^{1/2}$$

The interdependence or "correlation" C_{st} between the components s and t of $\underline{p}$ is given by

$$C_{st} = B^{-1}_{st} \, (B^{-1}_{ss} \, B^{-1}_{tt})^{-1/2}$$

The last two equations are derived by Hamilton (1964).

This procedure may be applied to the (i) analysis of a crystal structure in which case the $S_o{}^i$ and $S_c^i(\underline{p})$ are the magnitudes of the observed and calculated structure factors and the components of $\underline{p}$ are the configurational and thermal parameters defining the structure, or (ii) to the determination of the unit cell parameters in which case the $S_o{}^i$ and $S_c{}^i(\underline{p})$ are the Bragg angles.

The errors in the magnitude of the observed structure factors $|F_o(\underline{H})|$ are usually estimated according to the manner in which $I_o(\underline{H})$ is measured. However, it is not known how certain systematic errors contribute to $\sigma(\underline{H})$ and $(\frac{1}{\sigma(\underline{H})})^2$ may be replaced by a weight $\omega(\underline{H})$ which is then evaluated in one of four ways, one of which is to let $\omega(\underline{H})$ be $(\frac{1}{\sigma(\underline{H})})^2$. Since $\sigma(\underline{H})$ is usually proportional to $|F_o(\underline{H})|$ for most reflections, it may be set as a constant times $|F_o(\underline{H})|$ for all reflections. During the first few cycles of least squares, the phases (or signs if the structure is centric) of the weaker reflections are not well known and the stronger reflections are then the most useful in calculating $\underline{\Delta p}$. If all the $\omega(H)$ are set as unity then these stronger reflections are emphasized which may be necessary in order for the refinement to converge;

that is to insure $R(\underline{p} + \Delta\underline{p}) < R(\underline{p})$ The unknown errors are often a function of $|F_o(\underline{H})|$. Cruickshank et. al. (1961) have proposed that it is possible to account for these errors by insuring that the average value of

$$\omega(\underline{H})\,\big||F_o(\underline{H})| - |F_c(\underline{H})|\big|^2$$

is not a function of $|F_o(\underline{H})|$. This may be done by fitting a power series to a curve of the average value of $\big||F_o(\underline{H})| - |F_c(\underline{H})|\big|$ plotted against $|F_o(\underline{H})|$. If the coefficients of the power series are A, B, C and D then the weight is set as

$$\omega^{-1}(\underline{H}) = A + B\,|F_o(\underline{H})| + C|F_o(\underline{H})|^2 + D|F_o(\underline{H})|^3$$

APPENDIX B: COMPUTER PROGRAMS

The following is a list of the major programs used in this research.

1. FOTDIS (Fourier transforms of diffuse streaks; B. Robertson) . Used to calculate the $\alpha_n(T)$ curves from the profile of the diffuse streaks using the equations developed in Chapter 6.
2. DESLID (Debye-Scherrer line identication; B. Robertson) Used to identify the powder lines in order to calculate the unit cell parameters of α-$Cu_2P_2O_7$ and α-$Zn_2P_2O_7$ by comparison of observed and calculated line position and intensity.
3. DESLS (Debye-Scherrer least squares; B. Robertson) Used to find a least square fit of lattice parameters to observed Bragg angles with the procedure outlined in Appendix A.
4. DIC (Dead time corrections; B. Robertson) Corrects intensities measured with a diffractometer for dead time, filter attenuation, background, sweep rate and incident beam intensity.
5. PRELP (Precession "Lp"; A. K. Das and I. D. Brown) Applies "Lp" corrections to data obtained with a precession camera.

6. WEILP (Weissenberg "Lp"; A. K. Das and I. D. Brown) Applies "Lp" corrections to data obtained with a Weissenberg camera.
7. SCAB (Spherical and cylindrical absorption; B.Robertson) Applies absorption correction to $|F_o(\underline{H})|$ obtained from a crystal which is approximated by a sphere or cylinder.
8. MACFOU (McMaster Fourier; J. S. Rutherford) Calculates Patterson functions, generalized Patterson functions, Harker sections, electron density projections, generalized electron density projections, difference synthesis and non-axial projections in two or three dimensions.
9. MACLS (McMaster least squares; J. S. Stephens) Refines crystal structures using the method outlined in Appendix A with complex scattering curves and users weighting subroutine.
10. BAT (Bonds, angles and temperature factors; (I.D.Brown) Calculates bond lengths and directions, corrections for thermal effects, interatomic angles and principal axes of thermal ellipsoids.
11. CROOK (Cruickshank weighting curve; B. Robertson) Calculates the coefficients A, B, C and D as described in Appendix A.

BIBLIOGRAPHY

Anders, K. R., Fischer, K. and Gehring, W., Z. Anorg. Chem. 260, 331 (1949)

Atkinson, R. J. and Stager, C. V., Physics in Canada 22 (2) 44 (1966)

Au, P., Master's Thesis, McMaster University (1966)

Au, P. and Calvo, C. to be published, (1967)

Bachmann, H.G. and Barnes, W.H., Can. Mineralogist 7, 219 (1962)

Ballhausen, C.J., "Ligand Field Theory", McGraw-Hill, Toronto, (1962)

Buerger, M. J., "Crystal-structure Analysis", Wiley, N. Y. Pg. 105 (1960)

Busing, W. R. and Levy, H. A., Acta. Cryst. 17, 142 (1964)

Callen, H.B., "Thermodynamics", John Wiley and Son, N.Y. Ch. 9 (1960)

Calvo, C., J. Phys. Chem. Solids 24, 141 (1963)

Calvo, C., Can. J. Chem. 43, 436 (1965a)

Calvo, C., Can. J. Chem. 43, 1147 (1965b)

Calvo, C., Can. J. Chem. 43, 1139 (1965c)

Calvo, C., private communication, (1967a)

Calvo, C., private communication (1967b)

Calvo, C., private communication (1967c)

Calvo, C., Acta. Cryst. (in press),(1967d)

Calvo, C., Leung, J.S. and Datars, W.R., J. Chem. Phys. 46 796 (1967)

Calvo, C. and Neelakantan, to be published, (1967)

Calvo, C., Van Nest, J. P. and Datars, W. R., Materials Research Bulletin (in press), (1967)

Chambers, J. G., Datars, W. R. and Calvo, C., J. Chem. Phys. 41, 806 (1964)

Condon,E. A.and Odishaw, H. "Handbook of Physics", McGraw Hill, Toronto Pg (8) 108 (1958)

Corbridge, D.E.C., Acta. Cryst. 9, 308 (1956)

Corbridge, D.E.C., Acta Cryst. 10, 85 (1957)

Cruickshank, D.W.J., J. Chem. Soc., 5486 (1961)

Cruickshank, D.W.J., Pilling, D.E., Bujosa, A., Lowel, F.M. and Truter, M.R., "Computing Methods and the Phase Problem in X-ray Analysis", Pergamon Press, London, Pg. 45 (1961)

Cruickshank, D.W.J., Lynton, H. and Barclay, G.A., Acta. Cryst. 15, 491 (1962)

Datars, W. R. and Calvo, C., to be published (1967)

DeWolff, P.M., X-ray Powder Data File, A.S.T.M., Card 8-238/239 (1958)

Ehrenfest, Proc. Amsterdam Acad. Sci. 36, 153 (1933)

Goldschmidt, V. M., Nachr. Ges. Wiss. Göttingen, Math. Physik Klasse, 184 (1931)

Guggenheim, E. A. "Thermodynamics", North Holland, Amsterdam Pg 4 (1950)

Guinier, A., "X-ray Diffraction in Crystals", Freeman, San Francisco, (1963) Haas, C., Phys. Rev. 140, A863 (1965)

Hamilton, W.C., "Statistics in Physical Science", Ronald Press, N. Y. (1964)

Hamilton, W. C., Acta. Cryst. 18, 502 (1965)

Hoffman, C.W.W. and Mooney, R. W., J. Electrochem. Soc. 107 854 (1960)

"International Tables for X-ray Crystallography, Vol. I", Kynoch Press, Birmingham, England, (1962)

"International Tables for X-ray Crystallography , Vol. II", Kynoch Press Birmingham, England, (1959)

"International Tables for X-ray Crystallography , Vol. III", Kynoch Press, Birmingham England, (1967)

James, R. W., "Optical Principles of the Diffraction of X-rays", Bell, London, Ch. 1 (1962)

Katnack, F. L. and Hummel, F.A., J. Electrochem. Soc. 105, 125 (1955)

Landau, L. D., Physik. Z. Sovietunion 11, 26 (1937)

Landau, L. D. and Lifshitz, E.M.,"Statistical Physics" Pergamon Press, London, Ch. 14 (1962)

Lazarev, A.N., Kristallografiya 6, 125 (1961a)

Lazarev, A.N. and Tenisheva, T.F., Tr. Shestogo Soveshch po Eksperim i Tekn. Mineralog. i Petrogr., 319 (1961b)

Lazarev, A.N., Izv. Akad. Nauk, S.S.S.R. Otd. Khim. Nauk, 1314 (1962)

Lazarev, A.N., Izv. Akad. Nauk SSSR Ser. Khim. 60, 235 (1964a)

Lazarev, A.N., Izv. Akad. Nauk SSSR Ser. Khim. 60, 242 (1964b)

Lazarev, A.N. and Tenisheva, T.F., Izv. Akad. Nauk SSSR, Ser. Khim. 60, 403 (1964c)

Lazarev, A.N., Tenisheva, T.F. and Bonder, I.A., Izv. Akad. Nauk SSSR Neorgan. Materialy 1 (7), 1207 (1965)

Lazarev, A.N., Tenisheva, T.F. and Petrova, M.A., Izv. Akad. Nauk SSSR. Neorg. Materialy 1 (8) 1379 (1965)

Levi, G.R. and Peyronel, G., Z. Krist. 92, 190 (1935)

Liebau, F., Acta Cryst. 14, 1103 (1961)

Łukaszewicz, K., Roczniki Chemii 35, 31 (1961)

Łukaszewicz, K. and Smajkiewicz, Roczniki Chemii 35, 741 (1961)

Łukaszewicz, K. and Nagler, E., Roczniki Chemii 35, 1167 (1961)

Łukaszewicz, K., Bull. De L'Academic Polonaise Des Sciences XI 7, 361 (1963)

Łukaszewicz, K., "Bulletin of the Seventh Annual Congress and Symposium on Crystal Growth", A64 (1966)

Łukaszewicz, K., private communication, (1967a)

Łukaszewicz, K., private communication, (1967b)

MacArthur, D.M. and Beevers, C.A., Acta. Cryst. 10, 428 (1957)

Magnéli, A., Arkiv Kemi, Min.Geol. 15B, No. 3 (1941)

Mayer, J.E. and Streeter, S.F., J. Chem. Phys. 7, 1019 (1939)

McDonald, W.S. and Cruickshank, D.W.J., Acta.Cryst. 22, 43 (1967)

Melkvi, Z., Stager, C.V. and Calvo, C., private communication, (1967a)

Melkvi, Z., Stager, C.V. and Calvo, C., Can. J. Phys. 45, 83 (1967b)

Oetting, F.L. and McDonald, R.A., J. Phys. Chem. 67, 2737 (1963)

Pake, G.E., "Paramagnetic Resonance", Benjamin, N.Y. (1962)

Paoletti, P. and Ciampolini, M., Inorg. Chem. 6, 64 (1967)

Pauling, L., "The Nature of the Chemical Bond", Cornell University Press, Ithaca, N.Y. (1960)

Ramachandran, G.N., "Crystallography and Crystal Perfection". Academic Press, N.Y. (1963)

Ranby , P.W., Mash, D.H. and Henderson, S.T., Brit. J. Appl. Phys. Supplement 4, 518 (1955)

Robertson, B.E., Master's Thesis, McMaster University, (1965)

Robertson, B.E. and Calvo, C., Acta. Cryst., in press (1967a)

Robertson, B.E. and Calvo, C., Can. J. Chem., in press (1967b)

Roy, R., Middleswarth, E.T. and Hummel, F.A., Am. Mineral. 33, 458 (1948)

Sarver, J.F., Trans. Brit. Ceram. Soc. 65 (4), 191 (1966)

Scheringer, C., Acta. Cryst. 19, 504 (1965)

Schomaker, V. and Stevenson, D. P., JACS 63, 37 (1941)

Smoluchowski, Mayer and Weyl, "Phase Transformations in Solids", Wiley, N.Y., Ch. 1 (1951)

Stager, C.V. and Atkinson, R.J., private communication, (1967)

Stephens, J.S. and Calvo, C., Can. J. Chem., in press, (1967a)

Stephens, J.S. and Calvo, C., to be published (1967b)

Taylor, J.B. and Heyding, R.D., Can. J. Chem. 36, 597 (1958)

Tobolosky, A.V., Kozak, J.J. and Canter, N.H., Phys. Rev. 138, A651 (1965)

Van Wazer, "Phosphorous and its Compounds" Vol. I, Interscience N.Y.,(1958)

Webb, N.C., Acta. Cryst. 21, 942 (1966)

Wells, A.F., "Structural Inorganic Chemistry", Clarendon Press, Oxford, (1962) Wilson, A.J.C., "X-ray Optics", Methuen, London (1949)

Wooster, M.M., "Direct Methods in Crystallography", Clarendon Press, Oxford, (1961)

Zachariasen, W. H., Z. Kristallogr. 73, 1 (1930)